Climate Change Impact Assessment on the Khowai River Flow using HBV Model

by

Shovon Jubair

Roll No.: 0417162045

In partial fulfillment of the requirement for the degree of

MASTER OF ENGINEERING IN WATER RESOURCES ENGINEERING

Department of Water Resources Engineering

BANGLADESH UNIVERSITY OF ENGINEERING AND TECHNOLOGY

September 2021

CERTIFICATION OF APPROVAL

The thesis titled "Climate Change Impact Assessment on The Khowai River Flow Using HBV Model" submitted by Shovon Jubair, Roll No: 0417162045, Session: April 2017, has been accepted as satisfactory in partial fulfillment of the requirement for the degree of Master of Engineering in Water Resources Engineering on 22 September, 2021.

BOARD OF EXAMINERS

---   Chairman

Dr. Nasreen Jahan   (Supervisor)

Professor

Department of Water Resources Engineering

Bangladesh University of Engineering Technology

---   Member

Dr. Md. Mostafa Ali

Professor

Department of Water Resources Engineering

Bangladesh University of Engineering Technology

---   Member

Dr. Badal Mahalder

Assistant Professor

Department of Water Resources Engineering

Bangladesh University of Engineering Technology

DECLARATION

I, SHOVON JUBAIR, Roll no.: 0417162045, hereby declare that the work presented in this project entitled "Climate Change Impact Assessment on The Khowai River Flow Using HBV Model", being submitted to the Department of Water Resources Engineering, Bangladesh University of Engineering and Technology (BUET) for the degree of Master of Engineering, is the outcome of the original work done by me under the supervision of Dr. Nasreen Jahan, Professor, Department of Water Resources Engineering, Bangladesh University of Engineering and Technology (BUET). I have duly acknowledged all the sources of information which have been used in this project work. Neither this thesis nor any part of it has been submitted elsewhere for the award of any degree, diploma or other similar title or recognition from this or any other institution.

Shovon Jubair

(Signature of the Candidate)

Shovon Jubair

Roll No.: 0417162045

Department of Water Resources Engineering

Bangladesh University of Engineering and Technology

Dhaka.

ACKNOWLEDGEMENT

ABSTRACT

Water is one of the most indispensable resources on earth which is potentially useful for all living things. Consequential impacts of climate change are mediated through the changes in the water or hydrologic cycle due to the close connection between the climate and the atmosphere, hydrosphere, land surface and biosphere. Hydrologic models are being used in understanding the behavior of hydrologic systems of a watershed to make better predictions and to address the major challenges induced by climate change.

Khowai is one of the trans-boundary rivers that plays an important role in the fields of irrigation, transportation and flood events of the north-eastern region of Bangladesh. It also contributes to the flash flood hazard in this region damaging agricultural products of large areas. Anticipated climate change may exacerbate the current situation as climate change will have a profound impact on the availability and variability of fresh water throughout the world due to a change in rainfall pattern in response to the global warming. This response may vary from region to region. Hence assessing the impact of climate change on the streamflow of the Khowai river basin is very important for sustainable water resources management in this region.

In this study, HBV (Hydrologiska Byrans Vattenavdelning) hydrologic model has been set, calibrated and validated to assess the future flow of Khowai river and the suitability of two gridded datasets has been assessed in this regard. To test the datasets, three models have been set using three different datasets. Each model has been calibrated for 1980 to 2010 and validated for 2011 to 2019. In terms of Nash-Sutcliffe efficiency (NSE), ERA5 data driven model (NSE = 0.50 and 0.21) shows better result than NOAA data driven model (NSE = 0.49 and 0.19) in both calibration and validation, respectively. But, in the validation period (2011-2019), both ERA5 and NOAA show unsatisfactory results than the calibration results. For this reason, another model has been set using the average rainfall from the global gridded products (NOAA, ERA5) and measured precipitation of Habiganj station. This model shows better results for both calibration and validation periods and has been used for simulating future flow. For the calibration and validation period R^2 have been found to be 0.78 and 0.75 while NSE have been found to be 0.75 and 0.67, respectively.

Future precipitation, temperature and evaporation from the CANESM2 (The second-generation Canadian Earth System Model) climate model under RCP8.5 scenario and bias corrected by Quantile mapping method have been used to simulate future flow. Projections show an increase in precipitation by 7.69, 15.86 and 21.05%, in 2020-2040 (2020s), 2041-2070 (2050s) and 2071-2099 (2080s), respectively, from the baseline period (1980-2019) whereas temperature is expected to increase by 0.82, 1.46 and 2.41°C, in those periods, respectively. Evaporation is projected to increase in all future periods while actual evapotranspiration is projected to decrease as warmer environment may decrease vegetation coverage and transpiration due to water stress in the soil system which will reduce the overall actual ET in future.

The future (2020 to 2099) flow of the Khowai river has been simulated by the calibrated and validated model driven by bias corrected CANESM2 climate datasets. Analysis of monthly flow data indicates that wet months will be wetter while some dry months such as January, February and March will be drier with respect to the base period. Flow may decrease up to 61% (during February of 2020) while wet season flow may increase up to 50% (during July-August of 2070). Flow duration curve also indicates that at 1%-time, discharge may equal or exceed 117, 163, 184 and 192 m^3/sec during the base period (1980-2019), 2020s, 2050s and 2080s, respectively. Frequency analysis shows that discharge corresponding to 100-year return period may increase by 13, 25 and 48% during the 2020s, 2050s and 2080s, respectively.

This study may play a vital role in assessing the future flow of the Khowai river basin for the proper planning and water resources management in this basin. Furthermore, as Khowai river is a transboundary river, the results of this study can also be used for the development of an effective water sharing policy which will ensure that both countries (India and Bangladesh) can get enough water for the purpose of agriculture, livelihood, economic growth, and maintenance of ecology and biodiversity in this region in the coming decades.

Table of Contents

List of Figures

List of Tables

APPENDIX

List of Tables

List of Figures

1 INTRODUCTION

1.1 Background and Present State of the Problem

Bangladesh is the most downstream country in the Ganges-Brahmaputra-Meghna (GBM) basin and has at least 57 major transboundary rivers that enter Bangladesh from India and Myanmar (Mondal et al., 2018). These transboundary rivers affect Bangladesh largely as a huge amount of water and sediments that flow through Bangladesh are carried by these transboundary rivers (Mou and Jahan, 2021).

Khowai River is one of the transboundary rivers which originates in the eastern part of the Atharamura Hills of Tripura in India. The river leaves India at Khowai and enters Bangladesh at Ballah in Habiganj District. The river passes through the eastern part of Habiganj town and then it turns west to join the Kushiyara river near Adampur in Lakhai Upazila, Kishoreganj District. The Khowai river is approximately 166 km (103 mi) in length. This river is approximately 91 km in length in Bangladesh Territory. Tripura, the upstream part of the Khowai catchment, is characterized by hill ranges, valleys, and plains (Hossain T. , 1997).

The area of the Khowai catchment is 1325 square km (FFWC, 2006). There is no tidal effect and salinity intrusion in this basin as it is very far away from the sea. The majority of the catchment area lies in India.

Khowai river has a flashy flood regime and experiences frequent flooding, channel shifting, sediment deposition and scouring. Moreover, this river plays an important role in the North Eastern part of Bangladesh in the fields of agriculture, irrigation, transportation, flood and flash flood events, ecology and biodiversity maintenance especially in the Habiganj district. Flash Floods cause huge economic losses in this region by damaging property and agricultural products of large areas (Hossain T. , 1997). However, lack of rainfall data in the upper catchment of the river, outside of Bangladesh, has made the streamflow modelling challenging for this basin (FFWC, 2006). So, assessing the streamflow in the Khowai river basin, through the development of a hydrologic model, is very important for assessing the water balance for agriculture and

also for predicting floods in the north-eastern region of Bangladesh. Index map of the Khowai river and its basin is illustrated in Figure 1.1.
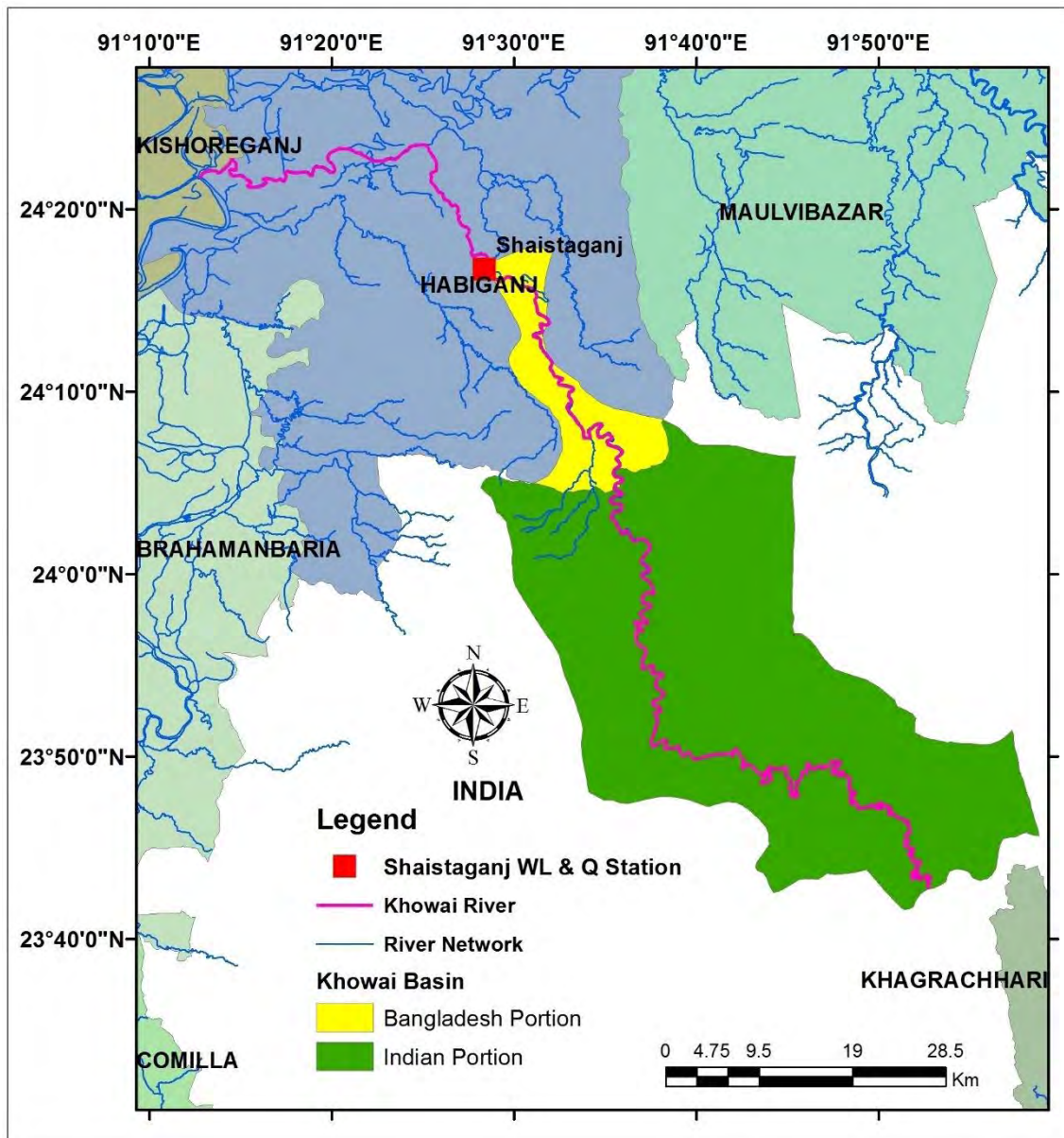
Figure 1.1: Index map - Khowai river and its basin

The Khowai river becomes disastrous during the rainy season (Debnath et al., 2017). Frequent flash floods in the Khowai river basin during the months of April-May damage the mature Boro rice of large area. This river passes through the towns of Chunarughat, Shaistaganj and Habiganj. The embankments often overtop during high floods and flood waters spill onto the floodplain (Deb, 2015).

In June 2017, residents of around 45 villages in Habiganj Sadar upazila became isolated due to flash flood triggered by heavy rain. Low lying areas in Khowai river basin were submerged during the period, and Aus paddy on thousands of hectares of land was also damaged due to the inundation. According to the locals, heavy downpour and water rolling down the hills caused breaches in different points of the Khowai River Protection Embankment (The Daily Star, 2017).

Figure 1.2: Flash Flood affected areas on the bank of the Khowai river in Habiganj Sadar (The Daily Star, 2017)

In May 2018, Habiganj experienced early flooding as the Khowai river crossed the danger level and some areas of the district including several roads went under water due to overflowing of the river. Moreover, continuous rainfall for several days triggered waterlogging in different places of the district town. Officials of Habiganj municipality admitted that rainwater cannot pass through the drains as those are too narrow and blocked due to indiscriminate dumping of wastes (The Daily Star, 2018).

Figure 1.3: Habiganj town encounters serious waterlogging due to days-long downpour, which also led to crossing of the Khowai river's danger mark (The Daily Star, 2018)

In June 2019, vast areas of several villages in Habiganj's Madhabpur upazila were inundated as water entered the areas through the collapsed embankment on the Sonai river due to flash flood triggered by heavy rain and storm surges. Vast tracts of croplands and vegetable fields in more than 30 villages have been submerged and fish in a number of ponds washed away due to the flash flood. Flash flood also caused waterlogging in different areas of Habiganj town and submerged many educational institutions, markets and residential areas. People of Habiganj town have long been suffering from waterlogging due to unplanned drainage system and illegal grabbing of the Khowai river (The Daily Star, 2019).

Figure 1.4: On rush of water from the hills in the Indian state of Tripura flooded a diversion road in Brahmanbaria's Bijoynagar upazila, disrupting vehicular movement on different regional roads (The Daily Star, 2019)

A calibrated and validated hydrologic model for the Khoai river can be very useful for flow forecasting based on forecasted climate data as well as to assess the effect of climate change on its flow and flood frequency.

1.2 Scope of the Study

Hydrological models play an important role to understand the watershed behavior and the interactions among hydrological variables in a quantitative way. Due to climatic changes and the increase of hydrologic extremes such as heavy precipitation events and droughts, which in recent years have been occurring more frequently and in greater severity worldwide, it is important to be able to credibly project hydrologic responses of river basins in order to adapt the water resources management of river basins. Among various elements of the hydrological cycle, possible quantitative changes to the future surface runoff of a river basin are important for water resources management: flood control, water quality, ecology, biodiversity, agriculture, etc. (Rahman, 2016).

This hydrological model will be extremely useful in the future for the evaluation of future streamflow and its temporal variation (seasonal flow volume), assessment of frequency and intensity of extreme events (flood events), evaluation of periodic variation of water availability due to the changes in the climate (significant air temperature warming), and to provide sufficient information for water resources management and planning and many more (Rahman, 2016). Choosing the right model for a catchment where hydrological responses are measured is difficult (Kirchner, 2006). Moreover, choosing a suitable model structure where the catchment is ungauged is even more challenging (Knoben et al., 2019).

This study conducts a systematic assessment of future streamflow under climate change in the data scarce Khowai river basin by using a semi-distributed, conceptual hydrological model HBV (Hydrologiska Byrans Vattenavdelning). HBV tend to have low data requirements and are less computationally intensive than spatially explicit models (Knoben et al., 2019). Also, the HBV model has already been used successfully in many mountainous and data scarce region (Normand et al., 2011). So far it has been successfully applied in over 90 countries for flow forecasting and climate change impact studies (Schreur, 2019).

Present study intends to set-up HBV hydrologic model to assess the effect of climate change on the streamflow of the Khowai river basin. Future changes in the frequency and the magnitude of annual maximum discharge will be assessed through frequency analysis of the future flow data of Shaistaganj station of the Khowai river.

1.3 Objectives of the Study

The specific objectives of the study are as follows:
i)   To set up, calibrate and validate the HBV hydrological model for the Khowai river basin.
ii) To simulate the future stream flow using the calibrated and validated model under RCP 8.5 climate scenario.
iii) To assess the future change in the frequency and magnitude of annual maximum discharge.

1.4 Possible Outcome

The possible outcomes of the study are:
i)   A flow simulating model for the khowai river basin,
ii) An assessment of the impact of climate change on the Khowai river flow.

These results will help the water resources engineers and policy makers to implement management strategies.

1.5 Organization of the Thesis

Chapter one

The first chapter of the thesis presents a general idea of the work. This chapter includes background of the study and present state of the problem, a brief description of the study area, scopes, objectives and possible outcome of the study.

Chapter two

The second chapter describes mainly literature review. This chapter includes necessity of catchment-scale hydrological modeling, the river system of Bangladesh, previous works

related to hydrological model: HBV-light. This chapter also includes previous studies on Meghna river basin and finally on Khowai River basin. A brief description on CORDEX is also presented in this chapter.

Chapter three

The third chapter consists of data sources and methodologies adopted in this research work. This chapter also provides a theoretical description of the hydrological model: HBV-light and the steps adopted for the setup of the model.

Chapter four

The fourth chapter includes the result and discussion. It includes results from calibration and validation of the model. The suitability of two global gridded datasets (NOAA vs ERA5) have been discussed in this chapter for modelling the streamflow of data-scarce Khowai river basin using HBV hydrologic model. The climate change impact assessment has also been discussed in this chapter.

Chapter five

The fifth chapter is the final chapter which concludes the thesis project along with some recommendations for further research and development.

2 LITERATURE REVIEW

2.1 The River System of Bangladesh

Bangladesh lies approximately between $20^030'$ and $26^040'$ north latitude and $88^003'$ and $92^040'$ east longitude. It is one of the biggest active deltas in the world with an area of about 1,48,560 sq.km. The country is under sub-tropical monsoon climate, annual average precipitation is 2,300 mm, varying from 1,200 mm in the north-west to over 5,000 mm in the north-east. India borders the country in west, north and most part of east. The Bay of Bengal is in the south, Myanmar borders part of the south-eastern area (Hossain, 2014).

Bangladesh is a riverine country. According to Bangladesh Water development board (BWDB), about 230 rivers currently flow in Bangladesh (during summer and winter). Old sources and history states about 700 to 800 rivers but most of them dried out due to lack of attention and pollution. About 17 rivers are on the verge of extinction and the 54 rivers flow directly from India and 3 from Myanmar. Total of 57 international rivers flow through Bangladesh. Sangu and Halda are the only two internal rivers originated and finished within Bangladesh. Surma is the longest river and Karnafuli is the swiftest. Jamuna is the widest river. There is an including tributaries flow through the country constituting a waterway of total length around 24,140 kilometers (15,000 mi). Most of the country's land is formed through silt brought by the rivers. The geography and culture of Bangladesh are influenced by the riverine delta system. Bangladesh lies in the biggest river delta of the world - the Ganges Delta system (Hossain, 2014).

Bangladesh has predominantly four major river systems (Hossain, 2014) –

1) the Brahmaputra,
2) the Ganges,
3) the Meghna, and
4) the Chittagong Region River system.

Meghna River System is one of the four major river systems of Bangladesh. It is the longest river (669 km) system in the country. It also drains one of the world's heaviest

rainfall areas (e.g., about 1,000 cm at Cherapunji, Meghalaya, India) (Hossain, 2014). Khowai is one of the rivers associated with the Meghna river system which is a tributary of the Kushiyara river.
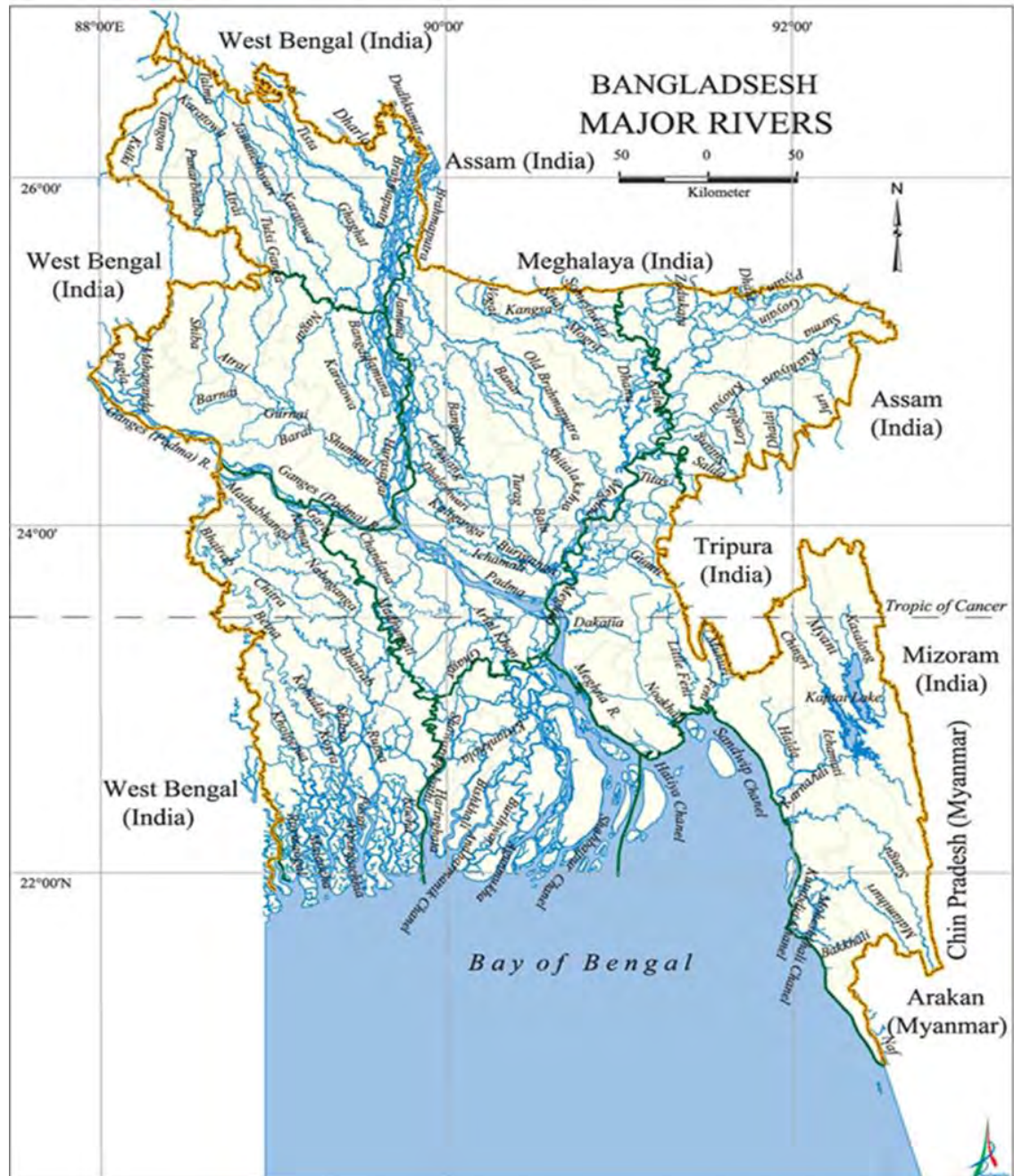
Figure 2.1: Major Rivers of Bangladesh. (Banglapedia)

2.2 A Brief History of Hydrological Modeling

A hydrologic model is a simplification of a real-world system (e.g., surface water, soil water, wetland, groundwater, estuary) that aids in understanding, predicting, and

managing water resources. Both the flow and quality of water are commonly studied using hydrologic models.

Depending on how a hydrological model represents different component processes of hydrological cycle, three types of models can be identified (Rahman, 2016):

    i)   empirical

    ii) conceptual and

    iii) physically based.

An empirical model is also termed metric or black-box model as it does not represent and so cannot explain internal hydrological processes of a catchment. Instead, such a model converts rainfall into runoff through a linear parametric equation (Rochester, 2010; Xu, 2002) or a transfer function (Mutlu et al., 2008; Rochester, 2010). The simplest empirical rainfall-runoff model is perhaps the single parametric runoff coefficient-based model. Runoff coefficient is the ratio of effective rainfall i.e., runoff to total rainfall falling over a catchment during a particular time period. In other words, runoff coefficient defines the water retention ability of a catchment (Giudice et al., 2012, 2014). Where detailed characteristics of a catchment are sparse such models may be used to estimate design flood peaks (Giudice et al., 2012, 2014). Example – ANN (Artificial Neural Network) (Rahman, 2016).

Conceptual models, also termed grey-box models, are generally recognized as superior to empirical rainfall-runoff models since they emulate the major component processes of hydrological cycle rather than lumping those processes empirically. In conceptual modelling, precipitation / snow melt water is cascaded through some linear storage reservoirs such as surface, soil, and groundwater. In conjunction with few physical properties of each storage reservoir, necessary parameters are incorporated to determine the water retention ability of each reservoir and to route / transfer water from one reservoir to another or from reservoir to channel. Most conceptual rainfall-runoff models maintain the conservation of mass law and use simpler physical expressions for water movement in the system (Xu, 2002). Moreover, in data scarce environments, conceptual model may be the better alternative to more physics-based approaches with their higher data demands (Rahman, 2016). Example – HBV Light.

Physically based rainfall-runoff models express major hydrological processes in the form of fundamental mathematical equations of conservation of mass, momentum, and energy (Freeze and Harlan, 1969; Valerity Y. Ivanov et al., 2004; Kavvas et al., 2004; Krysanova and Arnold, 2008; Meselhe et al., 2009). However, sometimes this definition of physics-based model is reduced to only laws of mass conservation. For instance, SWAT (Soil and Water Assessment Tools), one of the world's most frequently used catchment models, is often termed a physics-based model though it does not strictly consider the conservation of momentum and energy (Spruill et al., 2000). The major hydrological processes which are commonly used to identify a model if it is a physics-based are infiltration, evapotranspiration, overland and channel flows, and groundwater dynamics (Kampf and Burges, 2007). However, many physics-based models do not use the state-of-the-art one-dimensional (1D) Richard's soil water equation for estimating actual evapotranspiration as suggested by Kampf and Burges (2007). For example, MIKE SHE, one of the robust physics-based watershed models, estimates actual evapotranspiration based on empirical equation developed by Kristensen & Jensen (1975) (Rahman, 2016).

The early studies were often based on the relatively straightforward use of climate scenarios and conceptual hydrological models developed for other purposes such as hydrological forecasting and design. It was, however, soon realized that some components of the hydrological models can be questioned, if a changed climate is assumed. The most critical of these is the parameterization of evapotranspiration, which determines the response to increasing CO_2 concentrations and changed land-use. Despite the limitations in hydrological models, the main source of uncertainty related to water resources scenarios lies in the climate scenarios. Hydrologists demand a lot from the climate modelers in this respect. Recent studies have tried to address the issue by using several climate scenarios. Today the applied scientific literature on water resources is full of examples of climate change impact studies (Mou and Jahan, 2021).

2.3 Necessity of Catchment-Scale Hydrological Modeling

Globally the hydrological cycle experiences significant disturbances through the changes of its components (e.g., precipitation, evapotranspiration, river flows, soil water storage) in quantity, quality, space and time. Many nations and communities across the world have been experiencing intensified water related problems such as floods, drought and

associated water scarcity for the last few decades. Water related disasters killed more than 290,000 and affected more than 1.5 billion people worldwide during the period of 2000–2006 (UN Water, 2014a). About 1800 million people will suffer from water scarcity by 2025 (UN Water, 2014b). On one hand, increasing population pressure, unsustainable developmental activities and industrialization are together increasing pressure on the Earth's finite useable water resources. On the other hand, climate and land use changes have been found to be the dominant causes of frequent and intense flooding in many regions of the world (Rahman, 2016).

Sophocleous (2004) stated that water related problems are more visible at local scales (e.g., river catchment) than at the global scale. This is because the overall water turnover between Earth's atmosphere and land systems remains almost the same at the global scale but at more local scales this turnover varies in space and time. For this reason, catchment-scale water analysis has been one of the key approaches in the development of sustainable water management plans (Rahman, 2016).

Regional / local hydrologic models are generally calibrated and validated specifically to the site of interest. On the contrary, most global hydrologic models (GHM) are usually applied for impact studies with a global parameterization, which compromises the quality of local performance for assumed good performance globally, i.e., using a priori estimates of individual process parameters (e.g., Vörösmarty et al. 2000), or after calibration only for selected large catchments (e.g., Döll et al. 2003, Widén-Nilsson et al. 2007), or combinations of these approaches (e.g., Nijssen et al. 2001). It is impossible to achieve good performance at all locations and basins using GHM, so generally a regional or local hydrologic models will provide better performance than a GHM at the location for which a regional/ local hydrologic model has been tuned.

2.4   Previous Studies Using HBV Model

Hydrological models play an important role to understand the watershed behavior and the interactions among hydrological variables in a quantitative way. The HBV (Hydrologiska Byrans Vattenavdelning) model is a semi-distributed hydrologic model, named after the Hydrologiska Byrans Vattenavdelning unit at the Swedish Meteorological and Hydrological Institute (SMHI), where its development started in the 1970s. The version

HBV-light was developed at Uppsala University in 1993 using Microsoft Visual Basic. A new version of HBV model has recently been developed using Microsoft Visual Basic.net at the University of Zurich (Seibert and Vis, 2012). The HBV model has a long history since 1970 and this hydrological model has found applications in more than 90 countries (Schreur, 2019).

Bergström et al. (2001) performed a study on the climate change impacts on runoff in Sweden—assessments by global climate models, dynamical downscaling and hydrological modelling. The Swedish regional climate modelling program, SWECLIM, started in 1997 with the main goal being to produce regional climate change scenarios over the Nordic area on a time scale of 50 to 100 yrs. An additional goal is to produce water resources scenarios with a focus on hydropower production, dam safety, water supply and environmental aspects of water resources. The scenarios are produced by a combination of global climate models (GCMs), regional climate models and hydrological runoff models. The regional climate model is a modified version of the international HIRLAM forecast model and the hydrological model is the HBV model developed at the Swedish Meteorological and Hydrological Institute. Scenarios of river runoff had been simulated for 6 selected basins covering the major climate regions in Sweden (Bergström et al., 2001).

Linde et al. (2008) performed a study for the comparison of model performance of two rainfall-runoff models in the Rhine basin using different atmospheric forcing data sets. Due to the growing wish and necessity to simulate the possible effects of climate change on the discharge regime on large rivers such as the Rhine in Europe, there is a need for well performing hydrological models that can be applied in climate change scenario studies. There exists large variety in available models and there is an ongoing debate in research on rainfall-runoff modelling on whether or not physically based distributed models better represent observed discharges than conceptual lumped model approaches do. In addition, it is argued that Land Surface Models (LSMs) carry the potential to accurately estimate hydrological partitioning, because they solve the coupled water and energy balance. In this paper, the hydrological models HBV and VIC were compared for the Rhine basin by testing their performance in simulating discharge. Overall, the semi-distributed conceptual HBV model performed much better than the distributed land surface model VIC (Linde et al., 2008).

Normand et al. (2011) performed a study in which the HBV model has been used successfully to estimate runoff at Tapethok, Taplejung, in Eastern Nepal (2011), which is a mountainous and data-scarce region just like the Khowai river basin. As there was no discharge data available for this particular location, the model was first calibrated and validated for the bigger, gauged basins at Mulghat and Majithar. However due to its structure HBV showed difficulties in modelling low and high flows correctly at the same time. Therefore, two parameter sets were produced: one with focus on the model performance during low flows and the second one, on high flows. Those parameters were then applied to the basin at Tapethok. Generally, HBV was able to correctly simulate low flows except for some sharp peaks due to isolated precipitation events. However, pre-monsoon discharge was overestimated while the runoff of the monsoon season was most of the time underestimated (Normand et al., 2011).

Radchenko et al. (2014) conducted a study in the data scarce Ferghana Valley (Central Asia) for simulating water resource availability using HBV-light model. Glaciers and snowmelt supply the Naryn and Karadarya rivers, and about 70% of the water available for the irrigated agriculture in the Ferghana Valley. Nineteen smaller catchments contribute the remaining water mainly from annual precipitation. The latter will gain importance if glaciers retreat as predicted. Hydrological models can visualize such climate change impacts on water resources. However, poor data availability often hampers simulating the contributions of smaller catchments. This study tested several data pre-processing methods (gap filling, MODAWEC (MOnthly to DAily WEather Converter), lapse rate) and their effect on the performance of the HBV (Hydrologiska Byråns Vattenavdelning)-light model. Monte Carlo simulations were used to define parameter uncertainties and ensembles of behavioral model runs. Model performances were evaluated by constrained measures of goodness-of-fit criteria (cumulative bias, coefficient of determination, model efficiency coefficients (NSE)) for high flow and log-transformed flow. The developed data preprocessing arrangement can utilize data of relatively poor quality (only monthly means or daily data with gaps) but still provide model results with NSE between 0.50 and 0.88 (Radchenko et al., 2014).

Khorchani (2016) conducted a study to evaluate the land use/cover change impacts on hydrology of the Mellegue river sub-basin in the Upper Medjerda River Basin by using the semi-distributed HBV-Light hydrological model and remote sensing for two different

periods. ArcGIS was used to generate the land use-cover maps from Landsat TM (1984-1997) for the year 1988 and second land use / land cover map on 2003 was taken from the Regional Commissariat of Agricultural Development (CRDA) of Kef region (Khorchani, 2016).

Beck et al. (2016), studied Global-scale regionalization of hydrologic model parameters. The research shows current state-of-the-art models typically applied at continental to global scales (hereafter called macroscale) tend to use a priori parameters, resulting in suboptimal streamflow (Q) simulation. For the first time, a scheme for regionalization of model parameters at the global scale was developed. Data from a diverse set of 1787 small-to-medium sized catchments (10–10000 km^2) and the simple conceptual HBV model to set up and test the scheme. In this study, HBV was chosen because of its flexibility, computational efficiency, proven effectiveness under a wide range of climatic and physiographic conditions and successful application in many previous studies. Each catchment was calibrated against observed daily Q, after which 674 catchments with high calibration and validation scores, and thus presumably good-quality observed Q and forcing data, were selected to serve as donor catchments. The calibrated parameter sets for the donors were subsequently transferred to 0.58-degree grid cells with similar climatic and physiographic characteristics, resulting in parameter maps for HBV with global coverage. For each grid cell, the 10 most similar donor catchments, rather than the single most similar donor, and averaged the resulting simulated Q, which enhanced model performance. The 1113 catchments not used as donors were used to independently evaluate the scheme. The regionalized parameters outperformed spatially uniform (i.e., averaged calibrated) parameters for 79% of the evaluation catchments. Substantial improvements were evident for all major Koppen-Geiger climate types and even for evaluation catchments > 5000 km distant from the donors. The median improvement was about half of the performance increase achieved through calibration. HBV with regionalized parameters outperformed nine state-of-the-art macroscale models, suggesting these might also benefit from the new regionalization scheme (Beck et al., 2016).

Kuo et al. (2017) performed a study on the future streamflow patterns of three sub basins, i.e., East Holland, Beaver, and Pefferlaw River basins, located in the upstream of Lake Simcoe of Canada are assessed for 2021–2099. The individual set of parameters of a

conceptual hydrological model, HBV-light, were first calibrated for these three sub basins. The calibrated model was validated and further used to estimate the future streamflow driven by statistically downscaled projected precipitation and air temperature from the Pacific Climate Impacts Consortium under Representative Concentration Pathways 8.5 and 4.5 scenarios. The uncertainty of annual streamflow, hydrograph, flow duration curve (FDC), and flood frequency were evaluated. The results reveal that the annual stream flows of the Beaver and Pefferlaw River Basins (PRB) are projected to slightly increase in 2020–2099 while the annual stream flows of the East Holland River Basin (EHRB) are expected to be similar in 2020–2099. The monthly streamflow in winter is projected to increase but to decrease in spring across three sub basins. Based on the projected FDCs, daily streamflow of EHRB and PRB will likely increase by 2070–2099 (Kuo et al., 2017).

Sagor et al. (2017) simulated climate change impacts on the runoff processes of the Karnali River Basin of Nepal. Estimation of the variation of snowmelt contribution to streamflow in increased temperatures had been done in the research. The semi-distributed HBV rainfall-runoff model had been calibrated using hydro-meteorological data available from 1986 to 1997. The model simulated runoff based on precipitation, air temperature and potential evapotranspiration. The calibrated model was fed with the climatic projections developed using the PRECIS Regional Climate Model to estimate future (2040s) streamflow. The study indicated that the growing temperatures will generally result in wetter flow regime in the future (Shiwakoti, 2017).

Ali et al. (2018) performed a study on the projection of future streamflow of the Hunza River Basin, Karakoram Range (Pakistan) using HBV hydrological model. HBV-light model was used to evaluate the performance of the model in response to climate change in the snowy and glaciated catchment area of Hunza River Basin. The study aimed to understand the temporal variation of streamflow of Hunza River and its contribution to Indus River System (IRS). HBV model performed fairly well both during calibration and validation periods on daily time scale in the Hunza River Basin (Ali et al., 2018).

Ayalew (2019) tried to identify the best hydrological models in simulating the discharge in a comparative approach (SWAT vs HBV light) at Geba catchment and identifying of models which represent realistic simulation at sub basin scale. The various modelling

procedure (i.e., input data, sensitivity analysis, calibration, validation and uncertainty assessment) were employed to test the model's performance. These mentioned results depicted that both models are well reasonably simulated the discharge of Geba catchment and from uncertainty and identifiability of parameter applying HBV light model could be effective in simulation of runoff for sustainable water resources management in the watershed run off (Ayalew, 2019).

2.5   Previous Studies Using Other Models in The Meghna Basin and The Khowai Basin

Accurate streamflow simulation is crucial for water resources monitoring and management (Woldemeskel et al., 2013). Few past studies have employed hydrologic models for climate change impact assessment or flash flood forecasting in the north-eastern region of Bangladesh (IWFM, 2020). But only a few of them have so far been concentrated on the Khowai river. The majority of the Khowai catchment lies in India and flash flood of this region is triggered by the high intensity rainfall in the upstream Indian catchments located in the Tripura hills (FFWC, 2006). But the lack of rainfall data in the upper catchment of the river, outside of Bangladesh, has made the streamflow modelling challenging for this basin (IWFM, 2020).

Past studies reported that large scale/regional scale model generally compromises the quality of local performance at sub-basin scale therefore it is impossible to achieve good performance at all locations within a large basin using regional / large scale model (Krysanova et al., 2018). Therefore, individual model for khowai may provide better results for this basin instead of a regional model of Meghna basin or NE region.

Ullah (1989) performed a study on statistical characteristics of low flows of three rivers in Bangladesh. Analysis of low flow is essential for project involved with water supply, power generation, navigation, irrigation, pollution abatement, etc. In the study graphical relationships for low flow events had been derived for three selected rivers, namely Manu, Khowai and Ghagot, using both historic and synthetic stream flows (Ullah, 1989).

Hossain (1997) performed a study on aggradation and degradation of the Khowai River. Assessment of future sedimentation along the Khowai river was also carried out. The

reach extends from Ballah to the confluence of Khowai- Dhaleswari River and has an overall length of 87 km. The study revealed that there would be continued deposition of sediment indicating continued aggradation of the bed level along the study reach of the river (Hossain T. , 1997).

Flood Forecasting and Warning Center (2006) set up a rainfall-runoff model for the Khowai river basin but the results were also inconclusive. During the Main Project a rainfall-runoff model was set up for the Khowai basin. However, the available data on discharges at Remabagan, located at the Indian border had not been taken simultaneous with available rainfall data. Therefore, the calibration results were inconclusive, and the Flood Forecasting model was not extended to the Indian border at Remabagan (FFWC, 2006).

Past researchers have studied the geomorphological variables and bank erosion, channel migration of the Khowai River, and its impact on land use/land cover using Remote Sensing (RS) and Geographical Information System (GIS) (Majumdar et al., 2014). Majumdar and Das (2014) conducted a study to analyze the temporal change of the bank line of the Khowai River and to calculate the Bank Erosion Hazard Index (BEHI) of these vulnerable sites (Majumdar et al., 2014).

Rahman (2016) used SWAT model driven by limited observed rainfall to simulate the flow of Khowai basin but the results were also poor for both calibration and validation periods. The model produces unsatisfactory results due to lack of rainfall data of the upper catchment area. Also ignoring the effects of the upstream Chakmaghat Barrage on the catchment's hydrology might partly be responsible for the model's unrealistic water balance. But for Sheola station on the Kushiyara river during calibration (1990–2003) and validation (2004–2010) periods, the SWAT model showed good R^2 values of 0.81 and 0.90 respectively (Rahman, 2016).

Debnath et al. (2017) performed a study on channel migration and its impact on Khowai River of Tripura, North-East India. The study on bank erosion and channel migration of the present course of the Khowai River through the synclinal valley of Atharamura and Baramura Hill Ranges indicated that the area was under active erosion since long back. In the study, the rate of channel migration had been assessed and variation of sinuosity

index and radius of curvature had also been calculated. The work also documented land use changes in its surrounding flood plain area using supervised image classification. All the assessments of this study highlighted a significant message of immense vulnerability of Khowai River and also provided news about geomorphological instabilities of the study area (Debnath et al., 2017).

Mondol et al. (2018) used a multi-model approach to simulate the flood risks in the major rivers of Bangladesh due to increased rainfall and sea level under a high-end climate scenario. The models used include SWAT hydrological model for basin-scale rainfall-runoff modeling, HEC-RAS hydrodynamic model for flood routing, and Delft3D coastal model for sea level rise induced tidal forcing in the Bangladesh coast. These models together simulate flood hydrographs at different locations under climate change. The Ganges, Brahmaputra and Meghna rivers and their major distributaries and tributaries, the Bay of Bengal and the coastal region of Bangladesh were included in the different model setups. The models were calibrated and validated using observed water level and discharge data of BWDB and BIWTA for different years. It was found that the models could simulate the observed variation in flood hydrographs quite well. To assess the impact of climate change on flood, the flood hydrographs under the base condition and the high-end climatic condition were simulated and compared. The model simulated the flow data of Bhairab Bazar station for North-Eastern region (Mondal et al., 2018).

Narzis (2020) developed a semi-distributed hydrological model for the Meghna river basin using soil and water assessment tool SWAT to simulate the impact of changing climate (under RCP 4.5 and RCP 8.5) and upstream interventions on the hydrologic cycle of the basin area. The model was calibrated (2009-April, 2018) and validated (2000-2008) at the outlet station on the Kushiyara river near Sheola using the daily observed discharge and the SWAT model showed R^2 values of 0.68 and 0.71 respectively. The probable impact of the post-dam Barak River flow on the Surma-Kushiyara river system at Amalshid was analyzed by adding a reservoir / dam on the Barak River (Narzis, 2020).

Institute of Water and Flood Management (2020) had conducted a study on flash flood forecasting for the rivers in the northeast haor region of Bangladesh by coupling a number of open source-based models and tools. In that study, both HEC-HMS and HEC-RAS models were used. But the results were unsatisfactory for the Khowai river basin due to

the lack of reliable rainfall data in the upper catchment areas outside Bangladesh, lack of observations of discharge in the hydrodynamic model boundary, and lack of high-resolution bathymetry and topographic data (IWFM, 2020).

Mou (2021) performed a study applying HBV model for runoff simulation in khowai river basin in which the model calibration period was 2001 to 2007 and the validation period was 2008 – 2012. The whole catchment was divided into three elevation and three vegetation zones. For calibration period (2001-2007), the coefficient of determination was 0.71 (acceptable), whereas, for the validation period (2008 – 2012) the R^2 value was 0.39 (unsatisfactory) on monthly scale (Mou, 2021).

2.6   Climate Change Modeling for Hydrological Impact Assessment

Climate change impact studies are largely based on climatic projections simulated by climate models. Hydrological models are used to simulate the impact of climate change on the water cycle as well as to project future hydrological regimes. To drive such a model, reliable information on climatological variables (e.g., temperature, precipitation, or evapotranspiration) and on their distribution in space and time is required. This information can be provided by different climate models. Climate models use quantitative methods to simulate the interactions of the important drivers of climate including the atmosphere, oceans, land surface, and ice. They are used for a variety of purposes from the study of the dynamics of the climate system to projections of future climate. All climate models take account of incoming energy from the sun as short-wave electromagnetic radiation, chiefly visible and short-wave (near) infrared, as well as outgoing longwave (far) infrared electromagnetic (Narzis, 2020).

2.6.1   Climate change scenarios

There are several types of climate change scenarios. They range from scenarios that are devised arbitrarily based on expert judgment (arbitrary climate change scenarios) to scenarios based on past climate (analog climate change scenarios) to scenarios based on climate model output (Narzis, 2020).

2.6.1.1 Arbitrary climate change scenarios

Arbitrary climate change scenarios are changes in key variables selected to test the sensitivity of a system to possible changes in climate. These are often uniform annual changes in variables, such as temperature and precipitation. An example is combinations of 1°, 2°, and 4° increases in temperature combined with no change and increases and decreases of 10% and 20% in precipitation. Different changes can be assumed for different seasons. These scenarios are most useful for testing the sensitivity of systems to changes in individual variables and combined changes (Narzis, 2020).

2.6.1.2 Analogue climate change scenarios

Analogue, or past climates, can be created from historical instrumental records of climate or paleoclimate reconstructions. The instrumental record will often be a complete multi-decadal record of often daily or sub-daily weather observations. The advantage of these data is that they will be recorded at each observation station and thus could provide better information on the regional distribution of climate than many climate models. Their disadvantages include inaccuracies in the estimation of past climates, low temporal resolution (e.g., they may estimate seasonal or annual climates), and incomplete coverage (Narzis, 2020).

2.6.1.3 Climate model-based scenarios

Climate models are mathematical representations of the climate. Although there are many uncertainties with models such as climate models, they do enable us to simulate how global and regional climates may change as a result of anthropogenic influences on the climate. Models of both global and regional climate exist. Global climate models range from simple, one-dimensional models such as MAGICC, which is briefly described below, to more complex models such as general circulation models (GCMs). GCMs model the atmosphere and oceans, and interactions with land surfaces. The model on a regional scale, typically estimating the change in grid boxes that are approximately several hundred kilometers wide. GCMs, provide only an average change in climate for each grid box, even though real climates can vary quite considerably within several hundred kilometers (Narzis, 2020).

2.7   Emission Scenarios

Future greenhouse gas (GHG) emissions are the product of very complex dynamic systems, determined by driving forces such as demographic development, socio-economic development, and technological change. Their future evolution is highly uncertain. Scenarios are alternative images of how the future might unfold and are an appropriate tool with which to analyze how driving forces may influence future emission outcomes and to assess the associated uncertainties. They assist in climate change analysis, including climate modeling and the assessment of impacts, adaptation, and mitigation (Intergovernmental Panel on Climate Change, 2000).

2.7.1   The representative concentration pathways (RCPs)

Representative Concentration Pathway (RCP) is a greenhouse gas concentration (not emissions) trajectory adopted by the IPCC for its fifth Assessment Report (AR5) in 2014. It supersedes Special Report on Emissions Scenarios (SRES) projections published in 2000. It describes four different 21st-century pathways of greenhouse gas (GHG) emissions, atmospheric concentrations, air pollutant emissions, and land use. RCPs include a stringent mitigation scenario (RCP 2.6), two intermediate scenarios (RCP 4.5 and RCP 6.0), and one scenario with very high GHG emissions (RCP 8.5). The four RCPs, namely RCP2.6, RCP4.5, RCP6, and RCP8.5 are labeled after a possible range of radiative forcing values in the year 2100 (2.6, 4.5, 6.0, and 8.5 W/m^2, respectively). The newly developed RCP scenarios help the climate research community in several ways. They provide more detailed and better-standardized greenhouse gas concentration inputs for running climate models than those provided by any previous scenario sets. The RCP scenarios explicitly explore the impact of different climate policies to allow the cost-benefit evaluation of long-term climate goals. They also allow a more detailed exploration of the role of adaptation and further integration of scenario development across the different disciplines involved in climate research (Narzis, 2020).

2.7.1.1   RCP 2.6

This scenario might be described as the best case for limiting anthropogenic climate change. It requires a major turnaround in climate policies and a start to concerted action in the next few years in all countries, both developing and developed. Global CO_2 emissions peak by 2020 and decline to around zero by 2080. Concentrations in the atmosphere peak at around 440 ppm in midcentury and then start slowly declining. Global population peaks midcentury at just over 9 billion and global economic growth is high. Oil use declines but the use of other fossil fuel increases and is offset by the capture and storage of carbon dioxide. Biofuel use is high. Renewable energy (e.g., solar & wind) increases but remains low. Cropping area increases faster than current trends while the grassland area remains constant. Animal husbandry becomes more intensive. Forest vegetation continues to decline at current trends (Narzis, 2020).

2.7.1.2   RCP 4.5

Emissions peak around midcentury at around 50% higher than 2000 levels and then decline rapidly over 30 years and then stabilize at half of 2000 levels. CO_2 concentration continues on trend to about 520 ppm in 2070 and continues to increase but more slowly. Population and economic growth are moderate but slightly lower than under scenario RCP 2.6. Total energy consumption is slightly higher than RCP 2.6 while oil consumption is fairly constant through to 2100. Nuclear power and renewables play a greater role. Significantly, cropping and grassland area declines while reforestation increases the area of natural vegetation (Narzis, 2020).

2.7.1.3   RCP 6

In this scenario, emissions double by 2060 and then dramatically fall but remain well above current levels. CO_2 concentration continues increasing, though at a slower rate in the latter parts of the century, reaching 620 ppm by 2100. Population growth is slightly higher peaking at around 10 billion. This scenario assumes the lowest GDP growth of the four. Energy consumption increases to a peak in 2060 then declines and levels out to finish the century at levels similar to RCP2.6. Oil consumption remains high while biofuel

and nuclear play a smaller role than in the other 3 scenarios. The cropping area continues on the current trend, while the grassland area is rapidly reduced. Natural vegetation is similar to RCP 4.5 (Narzis, 2020).

2.7.1.4   RCP 8.5

This is the nightmare scenario in which emissions continue to increase rapidly through the early and mid-parts of the century. By 2100 annual emissions have stabilized at just under 30 gigatons of carbon compared to around 8 gigatons in 2000. Concentrations of CO_2 in the atmosphere accelerate and reach 950 ppm by 2100 and continue increasing for another 100 years. Population growth is high, reaching 12 billion by centuries end. This is at the high end of the UN projections. Economic growth is similar to RCP 6 but assumes much lower incomes and per capita growth in developing countries. This scenario is highly energy-intensive with total consumption continuing to grow throughout the century reaching well over 3 times current levels. Oil use grows rapidly until 2070 after which it drops even more quickly. Coal provides the bulk of a large increase in energy consumption. Land use continues current trends with the crop with grass areas increasing and forest area decreasing (Narzis, 2020).
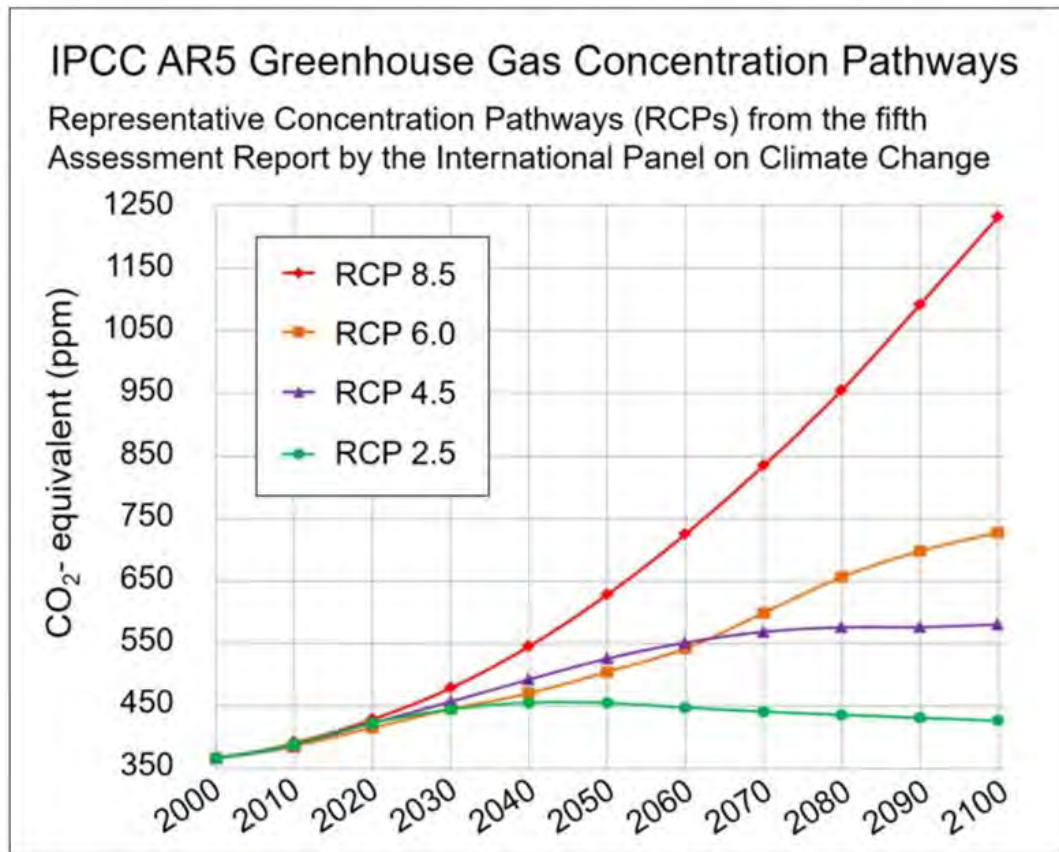
Figure 2.2: All forcing agents' atmospheric CO2-equivalent concentrations according to the four RCPs used by IPCC AR5 (Wikipedia, Representative Concentration Pathway, 2021)

The RCPs are an important development in climate research and provide a foundation for emissions mitigation and impact analysis. RCPs will facilitate the exchange of information among physical, biological, and social scientists. Researchers working on impacts, adaptation, and vulnerability will obtain model outputs sooner and have more time to complete their part of the AR5. Climate-model scenarios can also be developed without constraining future work on integrated assessments. As climate models improve, newer models can employ the same pathways, allowing modelers to isolate the effects of changes in the climate models themselves. The RCPs are supplemented with extensions (Extended Concentration Pathways, ECPs), which allow climate modeling experiments through to the year 2300. Development of the RCPs also brings together a diverse range of research communities that will help create fully integrated Earth-system models that include representation of the global economy and society, impacts and vulnerabilities (Narzis, 2020).

2.8   Regional Climate Model Data Portal-CORDEX

The Coordinated Regional Downscaling Experiment (CORDEX) program was recently established by the World Climate Research Program (WCRP) with the aim of developing an international coordinated framework to generate improved regional climate change projections world-wide for input into impact and adaptation studies, including input to the IPCC's Fifth Assessment Report (CCCR, 2021). The program consists of several subcomponents: development of a framework for evaluating downscaling methodologies, develop improved downscaling techniques, both statistical and dynamical; and promote interactions among global climate modelers, downscaling modelers, and assessment community who assess the impact of climate change on specific sectors using the downscaled data (Narzis, 2020).

2.8.1   CORDEX South Asia

The CORDEX South Asia program brings together researchers/scientists from the Climate Science and those involved in vulnerability, impacts and adaptation (VIA) research from the Asian region to interpret raw downscaled data for information on how climate processes over the continent may change, and to analyze how these changes may impact important sectors, such as health, agriculture and water security in multiple regions across the continent. The CORDEX South Asia activities are envisaged towards building capacity and expertise within the region to analyze, interpret and apply CORDEX results for decision making that are relevant to the knowledge needs of the South Asian region (CCCR, 2021).

CORDEX-South Asia is a partnership involving the Centre for Climate Change Research (CCCR) at the Indian Institute of Tropical Meteorology (IITM), the World Climate Research Program (WCRP), START, Swedish Meteorological Hydrological Institute (SMHI) and the University of Cape Town's Climate Systems Analysis Group (CSAG) (CCCR, 2021).

For the South Asian region, CORDEX presents an unprecedented opportunity to advance knowledge of regional climate responses to global climate change, and for these insights to feed into Working Groups One and Two of the IPCC Fifth Assessment Report as well

as to on-going climate adaptation and risk assessment research and policy planning in the region. The keys to success of this initiative in South Asia will be in developing a means for analysis and translation of CORDEX data in terms that are relevant to South Asia's knowledge needs, and in developing the internal capacity to perform the analyses and in doing so create expertise at regional levels in South Asia (CCCR, 2021).

2.8.2 Regional model: REGCM4 - a regional climate model system

The Regional Climate Model system RegCM, originally developed at the National Center for Atmospheric Research (NCAR), is maintained in the Earth System Physics (ESP) section of the ICTP. The first version of the model, RegCM1, was developed in 1989 and since then it has undergone major updates in 1993 (RegCM2), 1999 (RegCM2.5), 2006 (RegCM3) and most recently 2010 (RegCM4). The latest version of the model, RegCM4, is now fully supported by the ESP, while previous versions are no longer available. This version includes major upgrades in the structure of the code and its pre- and post-processors, along with the inclusion of some new physics parameterizations. The model is flexible, portable and easy to use. It can be applied to any region of the World, with grid spacing of up to about 10 km (hydrostatic limit), and for a wide range of studies, from process studies to paleoclimate and future climate simulation (International Center for theoretical physics, 2014).

The second-generation Canadian Earth System Model (CanESM2) is the fourth generation coupled global climate model developed by the Canadian Centre for Climate Modelling and Analysis (CCCma) of Environment and Climate Change Canada. CanESM2 represents the Canadian contribution to the IPCC Fifth Assessment Report (AR5) (Government of Canada, 2019). The second-generation Canadian Earth System Model (CanESM2) consists of the physical coupled atmosphere-ocean model CanCM4 coupled to a terrestrial carbon model (CTEM) and an ocean carbon model (CMOC) (Government of Canada, 2019).

Flash flood is a serious concern for the Khowai river basin. If future climate becomes warmer and wetter then it may increase the flooding risk of this region. Therefore, in this study, climate variables from CCCma-CanESM2 global climate model downscaled by REGCM4-4 RCM has been used as this dataset has showed an increase in temperature

and precipitation for the 21st century (wet and warm scenario) for south Asian region by few past researches (Khan and Koch, 2018) (Narzis, 2020). In addition, RCP 8.5 has been considered for future scenario as it represents extreme scenario.

3   METHODOLOGY

3.1   General

Hydrological modeling study which aims to derive scenarios of the future water situation in a river basin requires some basic data like digital elevation model, land use, weather data (precipitation, temperature, evaporation) and discharge data. The model development includes numerous amounts of preprocessing and post-processing that is quite challenging for the researchers. Assessment of the impact of future climate change and upstream barrage impact on the flow of any river basin using a hydrological model involves several steps. Steps followed in the present research can be described as the following:

Step 1-Data collection: This includes collection of the digital elevation model (DEM), land use pattern, climate data, and flow data.

Step 2-Data pre-processing: Digital elevation model within basin, land use pattern analysis, climate data analysis for missing value interpolation.

Step 3-Model setup: Model setup using HBV light hydrologic model, dividing the catchment in 20 elevation zones and 3 vegetation zones, weather data input.

Step 4-Calibration and validation of HBV model: Calibration and validation of the model, Sensitivity analysis of the model parameters, evaluation of the model performance.

Step 5-Selection of climate model and Scenarios: Selection of Regional Climate Model and scenario for climate change impact assessment.

Step 6-Bias correction of the future climate data set: Bias correction of the future precipitation, temperature and evaporation data.

Step 7-Simulation and analysis of future flow: Computation of future flow of the Khowai river basin based on using projected climate data for RCP 8.5 scenario and analyzing the impact of climate change on flow.

A flow chart of the methodology is given in Figure 3.1.
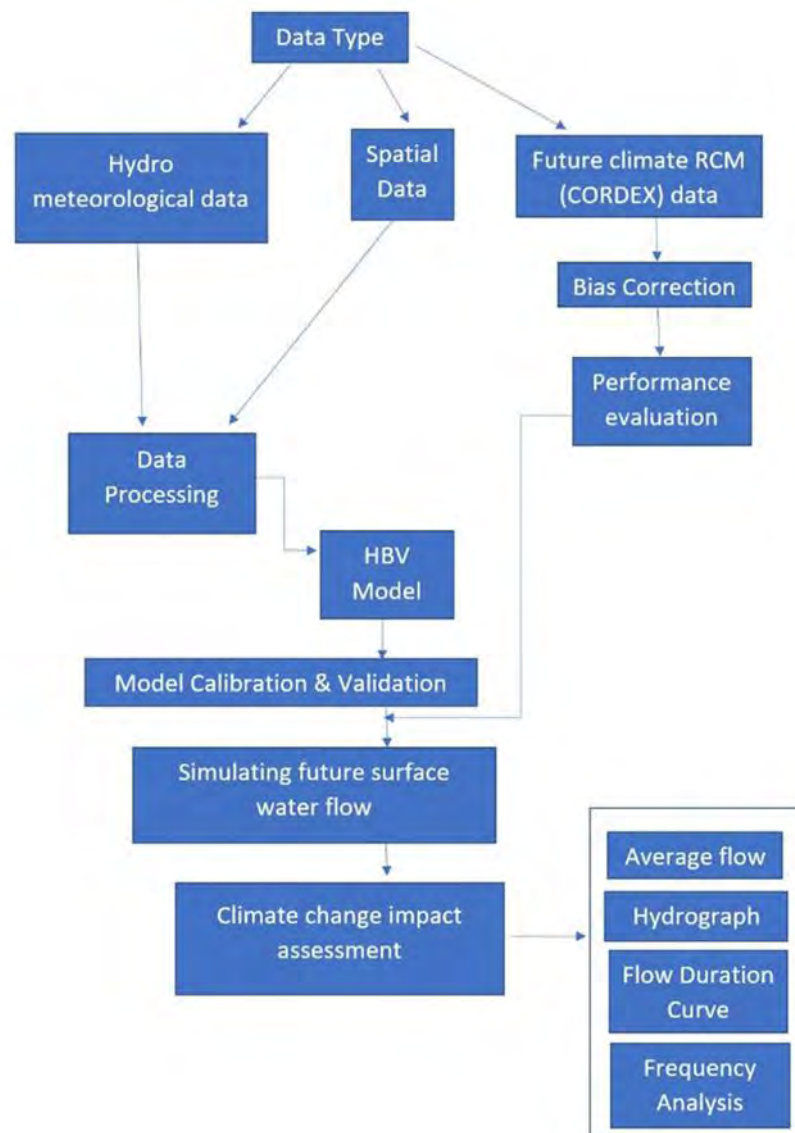
Figure 3.1: Flow chart of the methodology of this Thesis project

3.2 Data Collection

SRTM (Shuttle Radar Topography Mission) DEM (Digital Elevation Model) with a resolution of 30X30m was collected from USGS (United States Geological Survey) earth

explorer (USGS, 2019). Land Cover Map at 100m resolution was collected from the Copernicus – Global Land Cover Data (Copernicus, 2019). Precipitation, temperature, and evaporation data were collected from both ERA5 (Fifth Generation ECMWF - European Centre for Medium-Range Weather Forecasts Reanalysis) Land Hourly Dataset which is under the Copernicus Climate Change Service (C3S) and also from NOAA (National Oceanic and Atmospheric Administration) under NOAA Climate Prediction Center (CPC) Global Unified Gauge-Based Analysis. Precipitation, temperature and evaporation data of Habiganj were collected from BMD (Bangladesh Meteorological Department). Water Level and Discharge data at Shaistaganj station (SW 158.1, NTQ) were collected from BWDB (Bangladesh Water Development Board). Future data of precipitation, temperature and evaporation from 1979 to 2099 was collected from CORDEX (Coordinated Regional Climate Downscaling Experiment). A data collection summary and particulars of the future data is given in Table 3.1 and Table 3.2 respectively.

Figure 3.2: Shaistaganj Station (BWDB)

Table 3.1: Data collection summary

SL	Collected Data	Source	Resolution / interval	Duration
1	Digital Elevation Model (DEM)	SRTM (Shuttle Radar Topography Mission), USGS (United States Geological Survey) earth explorer	30m	2000 (acquisition), 2015 (updated)
2	Vegetation data	Copernicus – Global Land Cover Data	100m	2019
3	Reanalysis data of Precipitation, Temperature and Evaporation)	ERA5 (Fifth Generation ECMWF - European Centre for Medium-Range Weather Forecasts Reanalysis) (ECMWF, ERA5, 2019)	0.25 degree, Hourly	1979 – 2019
		NOAA (National Oceanic and Atmospheric Administration) Climate Prediction Centre (CPC) (NOAA, 2021)	0.5 degree, Daily	1979 – 2019
4	Precipitation, Temperature, Evaporation (Habiganj)	BMD	Daily	1979 – 2019
5	Future precipitation, Temperature and Evaporation	CORDEX (Coordinated Regional Climate Downscaling Experiment)	Daily	1979 – 2099
6	Water level and Discharge (Shaistaganj)	BWDB (Bangladesh Water Development Board)	Daily	1979 – 2019

Table 3.2: Particulars of CORDEX data download (CCCR, 2021)

SL	Subject	Answer	Remarks
1	Project	CORDEX	Coordinated Regional Downscaling Experiment
2	Domain	WAS 44	WAS means West Asia
3	Resolution	0.44 degree	
4	Institute	IITM	Indian Institute of Tropical Meteorology
5	RCM Model	RegCM4-4	Regional Climate Model latest version (2010)
6	Driving Model	RCP 8.5	worst case scenario
7	Experiment	CCCma-CanESM2	wet and warm scenario (selected in this study)

3.3 Data Pre-processing

3.3.1 Stream burning and watershed delineation

Stream burning has been performed using Khowai cross sections from IWM database, DEM (Digital Elevation Model) from USGS and stream network from Google Earth. Then watershed has been delineated using Shaistaganj station (SW 158.1, NTQ) as the outlet. The area of the Khowai River Basin has been calculated to be 1325.42 square kilometers. In Bangladesh portion, the Khowai basin's area is 139.82 square kilometers. In Indian portion, the Khowai basin's area is 1185.60 square kilometers.

3.3.2 Precipitation, temperature and evaporation data preparation

Precipitation, temperature and evaporation data from 1979 to 2019 had been collected from three different sources (Table 3.1).

With the purpose of putting daily data into the HBV Light Model, ERA5 hourly data had been processed into daily data for precipitation, temperature and evaporation.

A separate dataset for precipitation had been made by averaging ERA5, NOAA and BMD (Habiganj) precipitation datasets for further use. This dataset has been termed "**Average rainfall**" in the next sections of this report.

ERA5, NOAA and CORDEX future datasets are gridded data sets downloaded for an area near to the Khowai basin. By using Theissen polygon method in ArcGIS software, nearest gridded datasets from the basin are weighted averaged and prepared as ERA5, NOAA and CORDEX datasets (precipitation, temperature and evaporation). The details of the bias correction procedure for the CORDEX future datasets have been given in article 4.8.
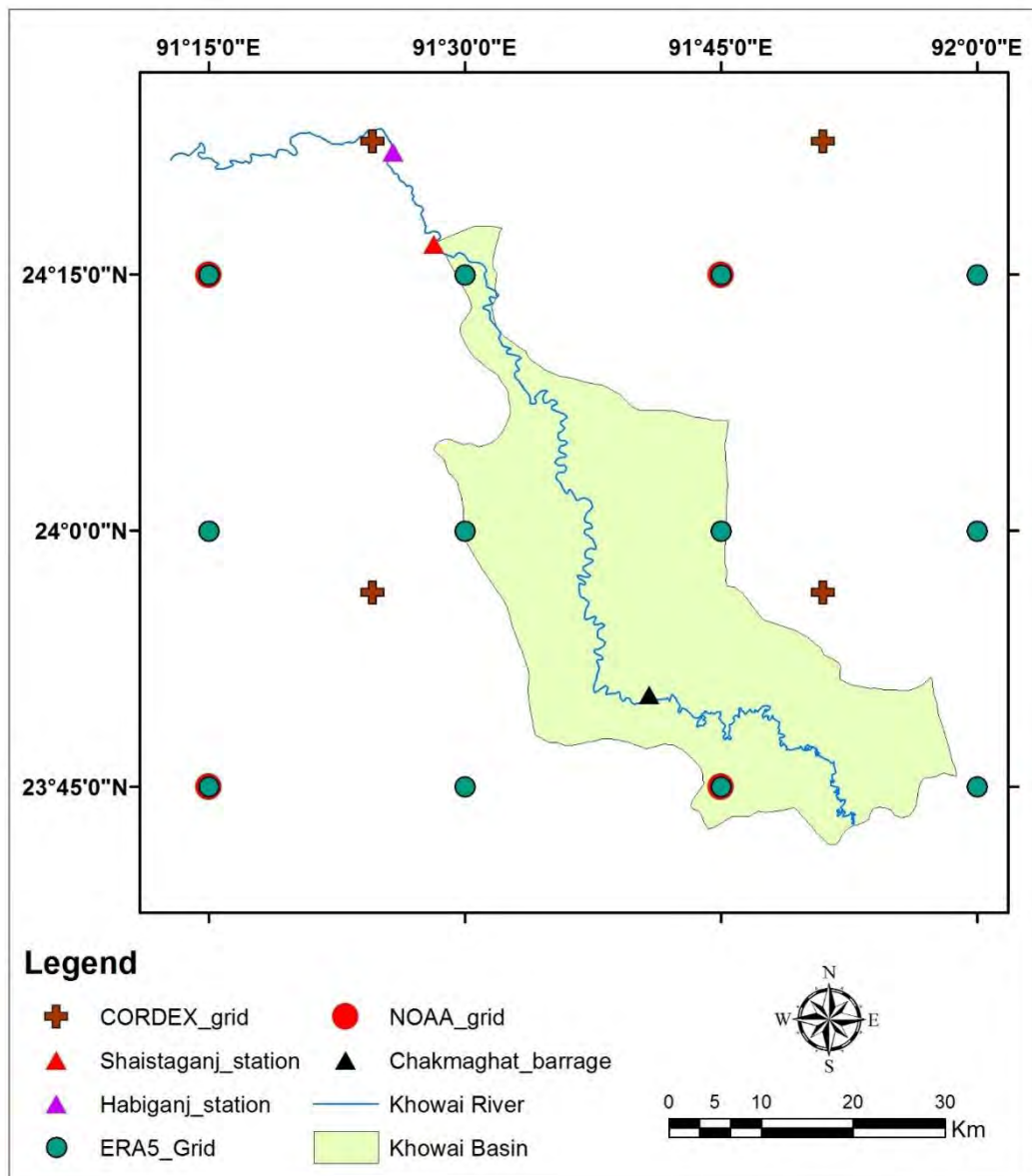
Figure 3.3: Location of climate data station

3.3.3 Discharge data preparation

Discharge data of Shaistaganj station collected from Bangladesh Water Development Board (BWDB) does not have regular interval. In case of missing water level data interpolation, NUM XL software oriented cubic spline method have been used. In case of missing discharge data interpolation, rating curve have been generated from water level.

3.3.3.1 Rating curve generation

Forty years (1979 – 2019) of discharge data and water level data of Shaistaganj station of BWDB had been distributed in 12 datasets according to month. From these 12 monthly distributed water level and discharge data of 40 years, 12 rating curve equations had been formed.

Rating curve equations analyzing 40 years water level and discharge data of Shaistaganj station of Bangladesh Water Development Board has been given in Appendix (Table A 1).

3.3.3.2 Missing values interpolation by NUM XL software

NUM XL software (NUMXL, 2021) works through Microsoft Excel in which the missing data is interpolated. More information can be found on www.numxl.com.
With the function generates as "interpolate" after it is installed in the PC, this function can generate four different data for the missing value in Microsoft Excel.

1. Forward
2. Backward
3. Linear
4. Cubic spline
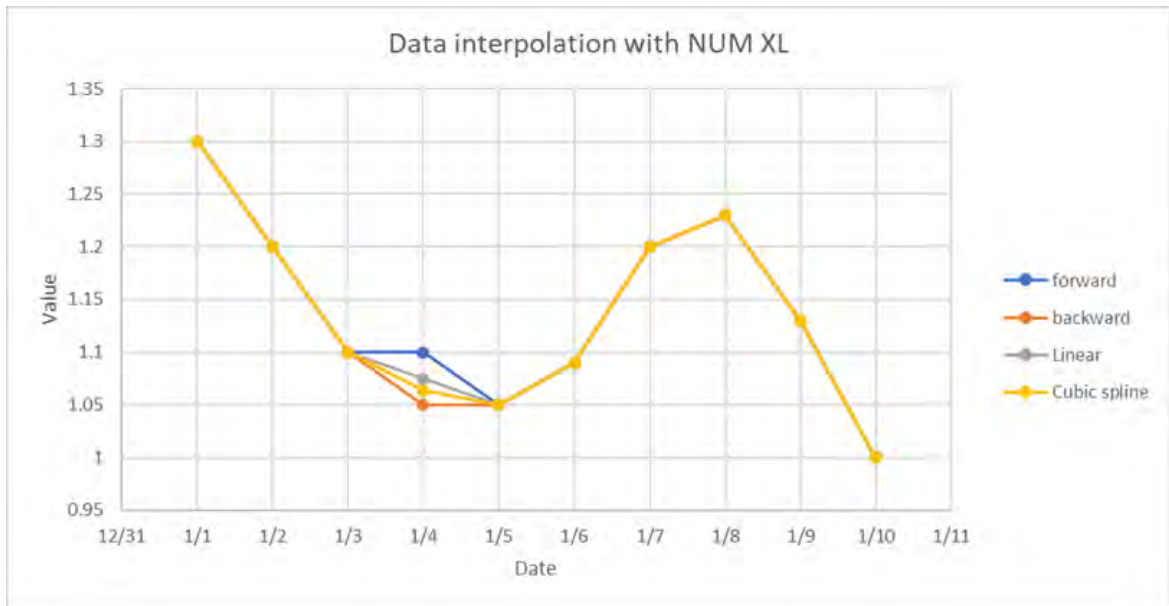
Figure 3.4: A simple data interpolation with NUM XL software

In this research, cubic spline method was applied for interpolating the missing water level value. From the water level data and the rating curve equations, the missing discharge has been generated.

3.4   Calibration and Validation of HBV Model

3.4.1   Description of HBV model

The full form of HBV is Hydrologiska Byrans Vattenavdelning. The HBV model is a semi-distributed hydrologic model, named after the Hydrologiska Byrans Vattenavdelning unit at the Swedish Meteorological and Hydrological Institute (SMHI), where its development started in the 1970s. The version HBV-light was developed at Uppsala University in 1993 using Microsoft Visual Basic. A new version of HBV model has recently been developed at the University of Zurich using Visual Basic.net (Seibert, 2005). This hydrological model has a long history and the model has found applications in more than 90 countries.

In general, The HBV model ...
- is a conceptual model for runoff simulation
- has a simple structure

- is semi-distributed, i.e., allows to divide the catchment into sub basins, elevation and vegetation zones

- is easy to understand, learn and apply

- has been applied to many catchments in Sweden and abroad

- provided good results in most applications

- has become a standard tool for runoff studies in the Nordic countries

- needs a moderate amount of input data

- can be run on a PC

In this study, HBV was chosen because of its flexibility, computational efficiency against data scarce catchments, proven effectiveness under a wide range of climatic and physiographic conditions and successful application in many previous studies.
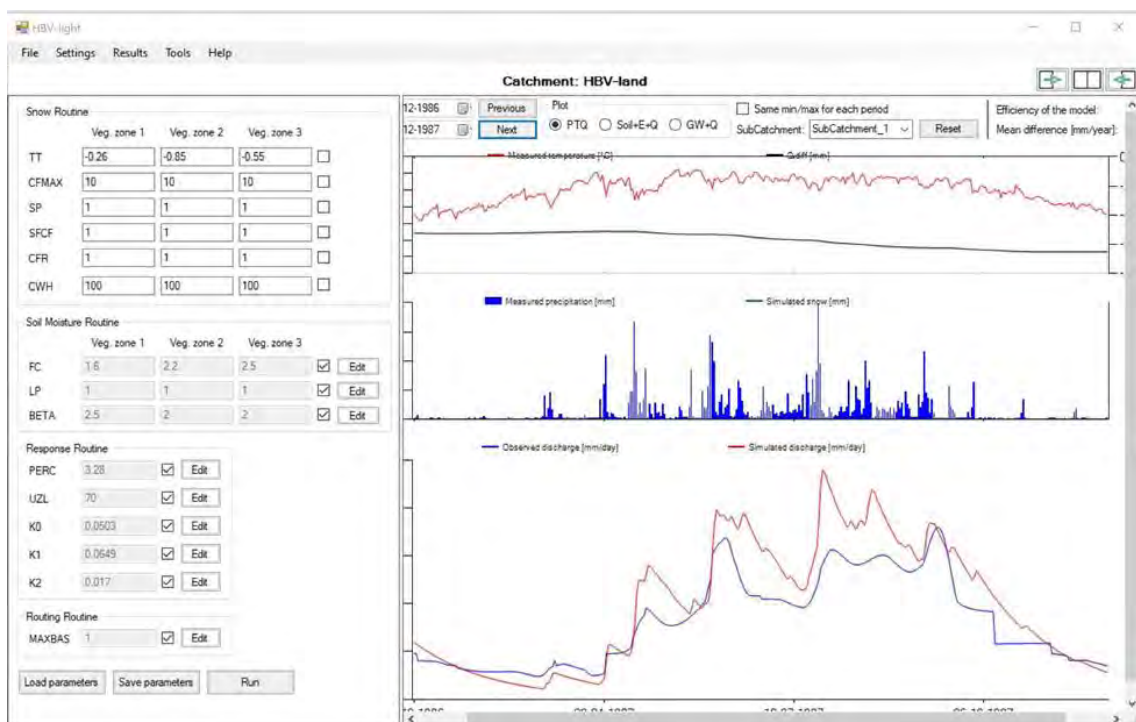
Figure 3.5: Main window of HBV Model

The HBV (Hydrologiska Byråns Vattenbalansavdelning) model (Bergström, 1976) is a rainfall-runoff model, which includes conceptual numerical descriptions of hydrological processes at the catchment scale. It is a user-friendly model. This model has been used successfully in 90 countries. The main idea behind the development of HBV-light was to provide an easy-to-use Windows-version for research and education (Seibert, 2005).

The general water balance can be described as in Equation 3.1 (Gendzh, 2015):

$$P - E - Q = d/dt\ [SP + SM + UZ + LZ + lakes] \quad \text{.........................} \quad \text{Equation 3.1}$$

Where:

P = precipitation

E = evapotranspiration

Q = runoff

SP = snow pack

SM = soil moisture

UZ = upper groundwater zone

LZ = lower groundwater zone

lakes = lake volume

3.4.2 General structure of HBV model

The selected HBV model consists of a snow routine, a soil moisture routine, runoff response routine, and a routing routine.

The **snow routine** of HBV uses a degree-day method to estimate snow accumulation and snowmelt processes.

The **soil moisture routine** of HBV is based on tank model, which control the contribution of precipitation to the runoff response and soil moisture storage.

Groundwater routine/response function routine: The model consists of two conceptual storages (tanks) that simultaneously redistribute the generated runoff in terms of quick and slow responses, respectively.

The total runoff response from both tanks is further transformed by a **routing routine**.

It has 5 stores and 15 parameters (TT, CFMAX, SP, SFCF, CFR, CWH, FC, LP, BETA, PERC, UZL, K0, K1, K2, MAXBAS) parameters. The model aims to represent:

- Snow accumulation, melt and refreezing;
- Infiltration and capillary flow and evaporation from soil moisture;
- A non-linear storage-runoff relationship from the upper runoff-generating zone;
- A linear storage-runoff relationship from the lower runoff-generating zone.
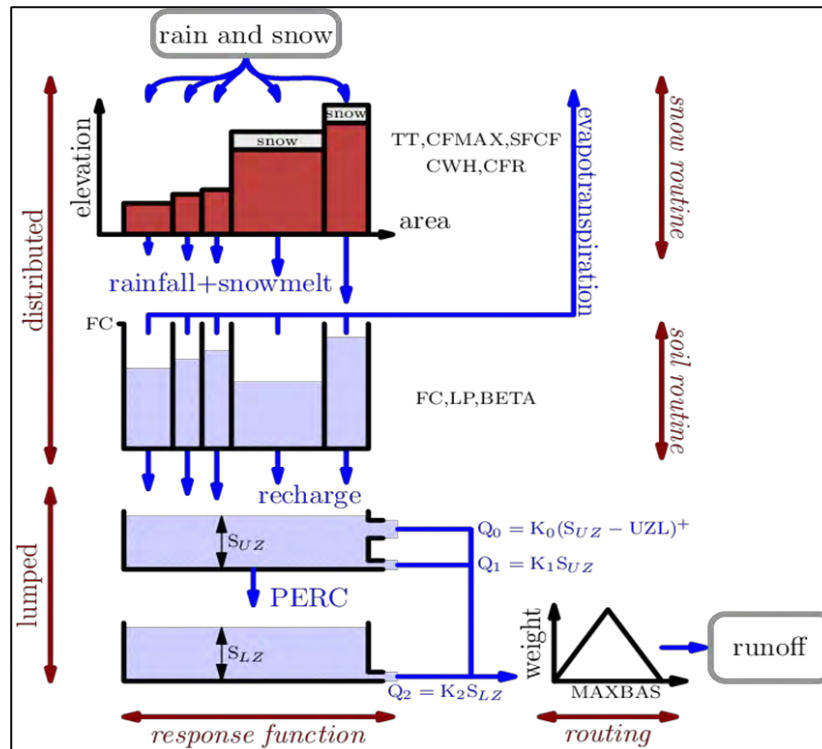
Figure 3.6: A Simplified Schematization of the HBV Light model

3.4.3   Model parameters

The model simulates daily discharge using daily rainfall, temperature and potential evaporation as input.

Precipitation is simulated to be either snow or rain depending on whether the temperature is above or below a threshold temperature, TT [°C]. All precipitation simulated to be snow, i.e., falling when the temperature is bellow TT, is multiplied by a snowfall correction factor, SFCF.

Melt = CFMAX (T(t) – TT)   Equation 3.2

Refreezing = CFR CFMAX (TT – T(t))   Equation 3.3

$$\frac{\text{recharge}}{P(t)} = \left(\frac{SM(t)}{FC}\right)^{Beta}$$ Equation 3.4

Snowmelt is calculated with the degree-day method (Equation 3.2). Meltwater and rainfall are retained within the snowpack until it exceeds a certain fraction, CWH, of the water equivalent of the snow. Liquid water within the snowpack refreezes according to Equation 3.3. Rainfall and snowmelt (P) are divided into water filling the soil box and

groundwater recharge depending on the relation between water content of the soil box (SM [mm]) and its largest value (FC [mm]) (Equation 3.4).

$$E_{act} = E_{pot} \min\left(\frac{SM(t)}{FC.LP}, 1\right)$$ <div style="float:right">Equation 3.5</div>

Actual evaporation from the soil box equals the potential evaporation if SM/FC is above LP. while a linear reduction is used when SM/FC is below LP (Equation 3.5).

Groundwater recharge is added to the upper groundwater box (SUZ [mm]).

$$Q_{GW}(t) = K_2 SLZ + K_1 SUZ + K_0 \max(SUZ - UZL, 0)$$ <div style="float:right">Equation 3.6</div>

$$Q_{sim}(t) = \sum_{i=1}^{MAXBAS} c(i)\, Q_{GW}(t-i+1)$$ <div style="float:right">Equation 3.7</div>

$$\text{Where, } c(i) = \int_{i=1}^{i} \frac{2}{MAXBAS} - \left| u - \frac{MAXBAS}{2} \right| \frac{4}{MAXBAS^2}\, du$$

PERC [mm d-1] defines the maximum percolation rate from the upper to the lower groundwater box (SLZ [mm]). Runoff from the groundwater boxes is computed as the sum of two or three linear outflow equations depending on whether SUZ is above a threshold value, UZL [mm], or not (Equation 3.6). This runoff is finally transformed by a triangular weighting function defined by the parameter MAXBAS (Equation 3.7) to give the simulated runoff [mm / d].

$$P(h) = P_0 \left(1 + (PCALT(h-h_0)/10000)\right)$$ <div style="float:right">Equation 3.8</div>

$$T(h) = T_0 - TCALT(h - h_0) / 100$$ <div style="float:right">Equation 3.9</div>

If different elevation zones are used the changes precipitation and temperature with elevation are calculated using the two parameters PCALT [%/100 m] and TCALT [ºC / 100 m] (Equation 3.8 and Equation 3.9).

$$E_{pot}(t) = (1 + C_{ET}(T(t) - T_M))\, E_{pot}, M$$ <div style="float:right">Equation 3.10</div>

But $0 \le E_{pot}(t) \le 2\, E_{pot}, M$

The long-term mean of the potential evaporation, Epot, M for a certain day of the year can be corrected to its value at day t, Epot(t), by using the deviations of the temperature, T(t), from its long-term mean, TM, and a correction factor, CET [°C-1] (Equation 3.10).

When each of the Snow Routine parameters (TT, CFMAX, SFCF, CFR and CWH), Response Function parameters (PERC, Alpha, UZL, K0, K1 and K2) and the CET

parameter were decreased, the efficiency of the model output increased. When each of the Soil Routine parameters (FC, LP and BETA) and the Routing Routine parameter (MAXBAS) was increased, the efficiency of the model output increased.

3.4.4 Description of four routines
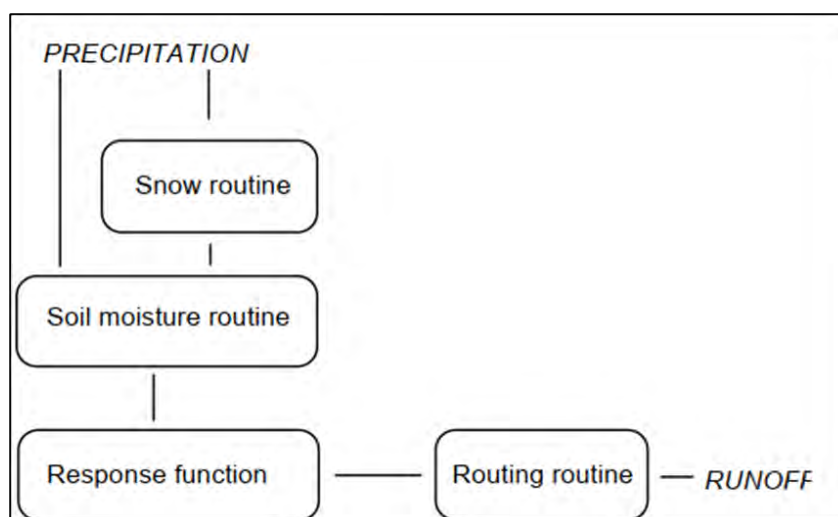
Figure 3.7: Schematic Structure of Four Routines of the HBV model

Table 3.3: Input and Output data for Four Routines

Sub Model	Input data	Output data
Snow routine	Precipitation, temperature	Snow pack, snow melt
Soil routine	Potential evaporation, precipitation, snowmelt	Actual evaporation, soil moisture, groundwater recharge
Response function	Groundwater recharge, potential evaporation	Runoff, groundwater level
Routing routine	Runoff	Simulated runoff

3.4.4.1 Snow routine

According to the HBV light User's Manual (Seibert, 2005),

CFMAX= degree-day factor (mm $^{\circ}C^{-1}$ day^{-1})

CFR = refreezing coefficient

TT = threshold temperature ($^{\circ}C$)

1. Accumulation of precipitation as snow if temperature<TT (TT is normally close to 0 °C)

2. Melt of snow starts if temperatures are above TT calculated with a simple degree-day method.

   meltwater = CFMAX (T-TT) (mm day^{-1})

   CFMAX varies normally between 1.5 and 4 mm °C-1 day-1 (in Sweden), with lower values for forested areas. As approximation the values 2 and 3.5 can be used for CFMAX in forested and open landscape respectively.

3. The snow pack retains melt water until the amount exceeds a certain portion (CWH, usually 0.1) of the water equivalent of the snow pack. When temperatures decrease below TT this melt water refreezes again.

   refreezing meltwater = CFRCFMAX (TT-T)

   (CFR 0.05)

NOTE:

a) All precipitation that is simulated to be snow is multiplied by a correction factor, SFCF.

b) These calculations are carried out separately for each elevation and vegetation zone.

3.4.4.2 Soil moisture routine

According to the HBV light User's Manual (Seibert, 2005),

FC = maximum soil moisture storage (mm)

LP = soil moisture value above which ETact reaches ETpot (mm)

BETA = parameter that determines the relative contribution to runoff from rain or snowmelt

NOTE: FC is a model parameter and not necessarily equal to measured values of 'field capacity'.

3.4.4.3 Response routine

According to the HBV light User's Manual (Seibert, 2005),

Simple linear reservoir:

The model of a single linear reservoir is a simple description of a catchment where the runoff Q(t) at time t is supposed to be proportional to the water storage S(t).
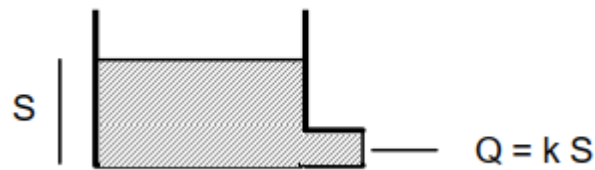
Figure 3.8: Simple linear reservoir

Q(t) = k. S(t)

Here,

S = storage (mm)

Q = outflow (mm day^{-1})

t = time (day)

k = storage (or recession) coefficient (day^{-1})

(A realization of a single linear reservoir is a box with porous outlet)

The water balance of the catchment is

P(t) = E(t) + Q(t) + d. S(t) / dt

Recharge	= input from soil routine (mm day-1)
SUZ	= storage in upper zone (mm)
SLZ	= storage in lower zone (mm)
UZL	= threshold parameter (mm)
PERC	= max. percolation to lower zone (mm day-1)
Ki	= Recession coefficient (day-1)
Qi	= runoff component (mm day-1)

NOTE:

- SUZ has no upper limit

- Q2 can never exceed PERC SLZ can never exceed PERC/K_2
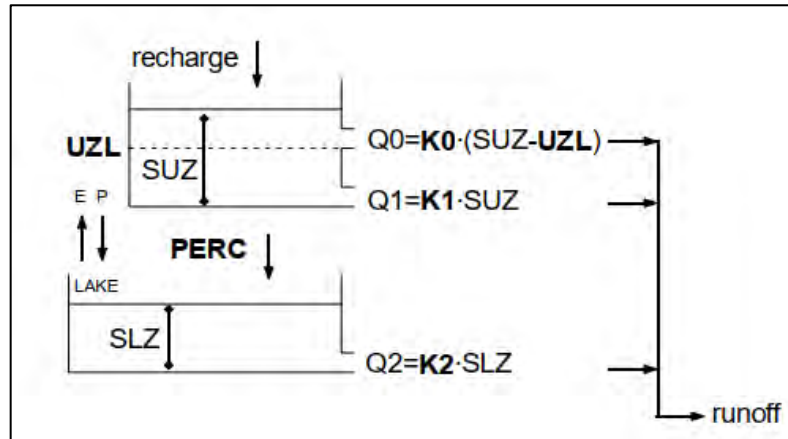
Figure 3.9: Response Function

3.4.4.4 Routing routine

According to the HBV light User's Manual (Seibert, 2005),

Transformation function:

The generated runoff of one-time step is distributed on the following days using one free parameter, MAXBAS, which determines the base in an equilateral triangular weighting function.
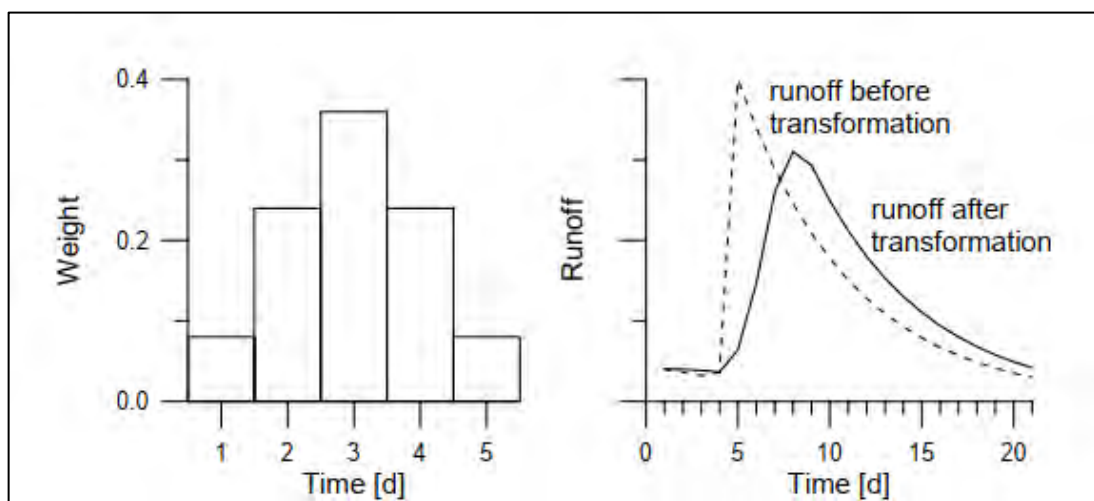
Figure 3.10: Example for a transformation with MAXBAS=5

3.4.5   Input climate data

The PTQ-file contains time series of precipitation [mm/Δt], temperature [ºC] and discharge [mm/Δt]. If the catchment consists of more than one sub catchment, a distinct set has to be specified for each of the sub catchments. Time series can be on a daily basis, hourly basis, or any other time interval, as long as the time interval remains constant over the time series.

The evaporation-file contains values for the potential evaporation [mm/Δt]. This could be either one set of values which will be applied to all sub catchment, or one set per sub catchment.

3.4.5.1   Precipitation

According to the HBV light User's Manual (Seibert, 2005),
The areal average precipitation P $_{area}$ is calculated as weighted mean of precipitation stations in and around the catchment.

$$P_{area} = \sum C_i P_i$$

The weight C_i of station can be determined subjectively or by Thiessen Polygons or by the Isohyetal or the Hypsometric method

The catchment can be divided into different elevation zones. For each zone the precipitation will be corrected according to the its increase with elevation above sea level (usually 10-20% per 100 m, parameter PCALT).

3.4.5.2   Temperature

According to the HBV light User's Manual (Seibert, 2005), Temperature data is needed in catchments with snow and is calculated as weighted mean of stations in and around the catchment. When different elevation zones are used temperature will be corrected for elevation above sea level with usually -0.6ºC per 100 m (parameter TCALT).

3.4.5.3 Potential evaporation

According to the HBV light User's Manual (Seibert, 2005),

Estimates of the potential evaporation may be provided by calculations using, for instance, the Penman formula or measurements by evaporimeters. Normally monthly mean values are assumed to be sufficient. The long-term mean evaporation can be corrected by using the deviations of the temperature from its long-term mean.

$$E_{pot}(t) = (1 + C_{ET}(T(t) - T_M)) E_{pot,M}$$

(But $0 \leq E_{pot}(t) \leq 2 E_{pot,M}$)

$E_{pot}(t)$ potential evaporation at day t (mm d^{-1})

C_{ET} = correction factor (^{0}C^{-1})

$T(t)$ = temperature at day t (^{0}C)

T_M = long term mean temperature for this day of the year (^{0}C)

$E_{pot,M}$ = long term mean evaporation for this day of the year (mm d^{-1})

3.4.6 Model setup

After the processing of discharge, water level, precipitation, temperature, evaporation data as well as digital elevation model and land use data collection, now it is time for the simulation using HBV Light.

3.4.6.1 Model settings

Then clicking settings in the menu bar - model settings button, Model Settings window pops up. Model settings was done selecting the following options given in the following Figure 3.11.
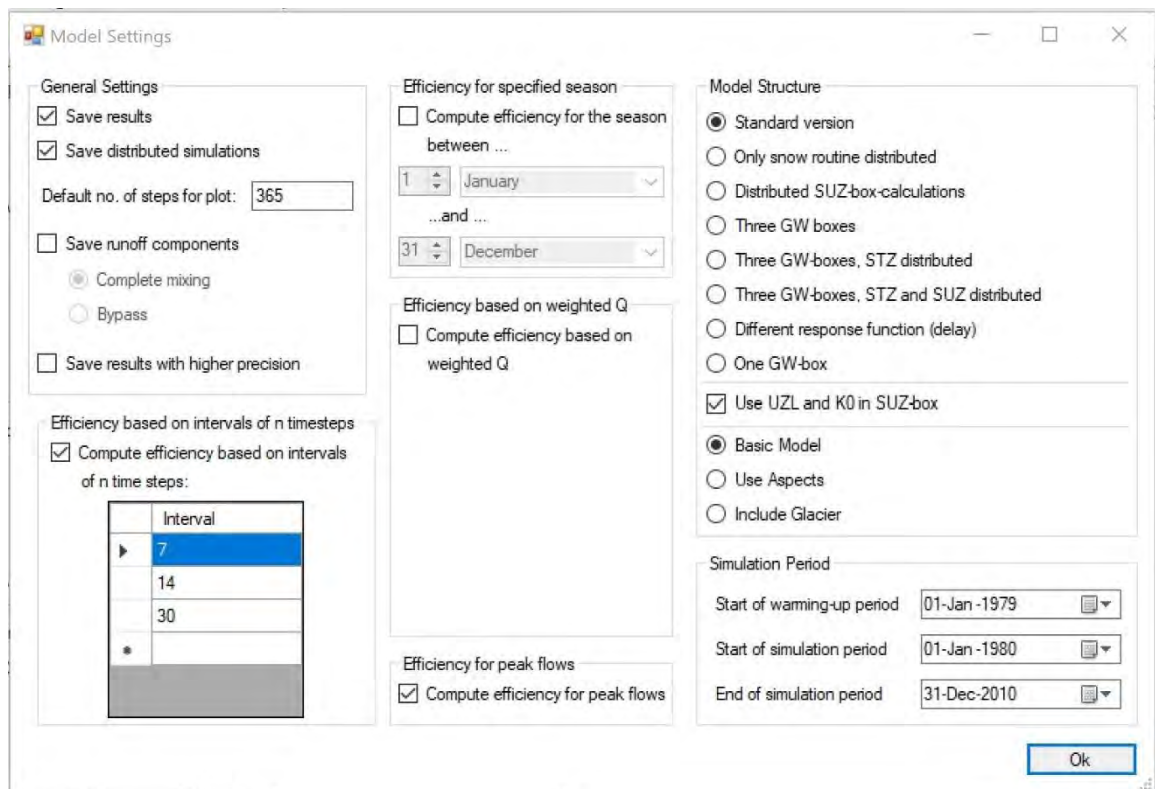
Figure 3.11: Model settings

3.4.6.2 Catchment settings

The whole catchment is divided into 20 elevation zones and 3 vegetation zones. Elevation zone wise vegetation zones distribution ratio sum area should be equal to 1. If not, the model will not run.

3.4.6.3 Calibration and validation of HBV model

Calibration is the process where we look at parameters that closely simulate the behavior of the basin (Madsen et al., 2002). It consists of adjusting numerical values assigned to the model parameters to reproduce the best observed response (Khorchani N. , 2016). This process can be used manually by trial-and-error method, or automatically by an optimization process in looking at the optimum value of a given criterion to enhance consistency between the observed and simulated discharge response of the basin for a certain period of time (Madsen et al., 2002).

Once the hydrological model is calibrated for a given time period, then the model's ability to simulate the discharge for another time period is checked in the validation step.

In this study, the HBV model has been calibrated for the Khowai catchment for the period 01-01-1980 to 31-12-2010. The first year of the simulation period is treated as a warm-up period for HBV Light model (Bergström 1976, 1992; Seibert and Vis 2012) because the model initial conditions are unknown. One year of warm-up is generally sufficient to spin-up a conceptual hydrologic model such as HBV. Therefore, only the first-year simulation was discarded for analysis. The model is validated for the period 01-01-2011 to 31-12-2019. The performance of the calibrated model has been evaluated by comparing the observed discharge and the simulated discharge values and also based on the values of Goodness of Fit functions.

Three types of simulation can be done in HBV to optimize the model parameters:

- Monte Carlo simulations
- Batch simulations
- GAP simulation (Genetic Algorithm and Powell optimization).

Monte Carlo simulations and GAP simulation can be used to run a large number of simulations based on randomly selected parameter sets (within user-defined parameter boundaries) and for automatic calibration of the model. In this research only Monte Carlo simulation has been considered and the parameters' ranges (Table 3.4) have been obtained from Beck et al. (2016), Wawrzyniak et al. (2017) and Melsen and Guse (2021).

Table 3.4: Maximum and minimum of parameters for the Monte Carlo Run for HBV Land (the parameters' ranges have been obtained from Beck et al. (2016), Wawrzyniak et al. (2017) and Melsen and Guse (2021))

Routine	Parameter	Explanation	Min	Max	Unit
SNOW ROUTINE	TT	Threshold temperature	-1.5	0	°C
	CFMAX	Degree-day factor	1	10	mm °C^{-1} d^{-1}
	SFCF	Snowfall correction factor	0.4	1.0	
	CWH	Water holding capacity	0.0	0.2	
	CFR	Refreezing coefficient	0.0	0.1	
SOIL ROUTINE	FC	Maximum of SM (storage in soil box)	1	1000	mm
	LP	Threshold for reduction of evaporation (SM/FC)	0.3	1.0	
	BETA	Shape coefficient	1	7	
	CET	Correction factor for potential evaporation	0.0	0.3	°C^{-1}
RESPONSE ROUTINE	K0	Recession coefficient (upper box)	0.001	0.4	d^{-1}
	K1	Recession coefficient (upper box)	0.001	0.18	d^{-1}
	K2	Recession coefficient (lower box)	0.0001	0.50	d^{-1}
	PERC	Maximal flow from upper to lower box	0	10	mm d^{-1}
	UZL	Threshold parameter	0	100	mm
ROUTING ROUTINE	MAXBAS	Routing, length of weighting function	1	7	d

After Monte Carlo Simulation, a Multi.txt file would be created in the Results folder. This file is opened in Excel and the parameter values corresponding to maximum coefficient of efficiency (Reff) are considered as the optimized parameter set and are selected for calibration.

In this study, the suitability of two global gridded datasets (NOAA and ERA5) have been assessed in modelling the streamflow of data-scarce Khowai river basin (Table 3.5) as no measured data is available for the major portion of the basin lying in India. Measured precipitation is available only at the Habiganj BMD station. So, it could be possible to correct the ERA5 or NOAA data for only Habiganj area if there was any bias by comparing them with the observed. But it was not possible to evaluate whether there is any bias in ERA5 or NOAA data for Indian part of the basin as we do not have any measured data from India. It would be inaccurate to assume that NOAA or ERA5 data of Indian portion have bias without any evidence and it may produce uncertainty if we correct the precipitation data of Indian part based on the bias observed for the Habiganj station as the amount and nature of bias (positive or negative) varies from region to region. As it was not possible to evaluate if there is any bias for all part of the basin except Habiganj, this study did not employ any correction or adjustment to the ERA5 or NOAA data.

Another dataset termed as "Merged dataset" has been prepared by averaging ERA5, NOAA and Habiganj (BWDB) precipitation datasets and have been used in the trial-3. But the temperature and evaporation dataset were taken from the ERA5 dataset in trial 3 as ERA5's resolution is better. The description of three trials is given in Table 3.5. The HBV model was calibrated for each dataset individually and the model that produced the highest Reff has been used for climate change impact assessment.

Table 3.5: Description of three trials in terms of applying datasets in the model

Trials	Acronym of the trial	Precipitation data source	Temperature data source	Evaporation data source
Trial 1	ERA5	ERA5	ERA5	ERA5
Trial 2	NOAA	NOAA	NOAA	NOAA
Trial 3	Merged	Average of ERA5, NOAA and measured precipitation from Habiganj BMD station	ERA5	ERA5

3.5 Evaluation Criteria Based on Goodness of Fit Functions

Evaluation criteria based on Goodness of Fit Functions are as follows (Seibert, 2005):

Table 3.6: Goodness of Fit Functions

RMSE	Root Mean Square Error
R^2	Coefficient of Determination
Reff / NSE	Coefficient of Efficiency/ Nash-Sutcliffe Efficiency
PBIAS	Percent Bias

Coefficient of determination (R^2) describes the proportion of the variance in measured data explained by the model. R^2 ranges from 0 to 1, with higher values indicating less error variance, and typically values greater than 0.5 are considered acceptable.

The Nash-Sutcliffe efficiency (NSE) is a normalized statistic that determines the relative magnitude of the residual variance compared to the measured data variance. NSE ranges between $-\infty$ and 1.0 (1 inclusive), with NSE as 1 being the optimal value. Values between 0.0 and 1.0 are generally viewed as acceptable levels of performance, whereas values <0.0 indicates that the mean observed value is a better predictor than the simulated value, which indicates unacceptable performance. For optimizing the model parameters while calibration, NSE value has been considered until the final acceptable model appears.

Table 3.7: Criteria for Evaluating Model Performance (Carlos et al., 2021)

Parameter	Very Good Range	Good Range	Acceptable Range	Unsatisfactory Range
R^2	0.75-1.00	0.60-0.75	0.50-0.60	<0.5
NSE	0.75-1.00	0.60-0.75	0.5-0.6	<0.5
PBIAS	0 - ±10	±10 - ±15	±15 - ±25	> ±25

3.6 Bias Correction of The Future Climate Data Set

In this study two bias correction methods have been tested such as Linear Scaling and Quantile based mapping.

3.6.1 Linear scaling method

Climate model outputs often suffer from biases. To overcome these bias, future rainfall, temperature and evaporation data from CORDEX CANESM2 model were bias-corrected based on average rainfall, ERA5 temperature and evaporation using the linear scaling (LS) method of bias correction. Linear scaling method computes a ratio of observed dataset (In this study, merged rainfall, ERA5 temperature and evaporation) and corresponding raw data from CORDEX for the historic period. Then, the future data is corrected by multiplying the future data with this ratio (Narzis, 2020).

Bias-corrected climate data = Raw data from climate model × C.F.

Where, Correction factor (C.F.) for month i = $\dfrac{\text{Mean of observed data for month i}}{\text{Mean of raw data from climate model for month i}}$

3.6.2 The quantile mapping method

The quantile mapping method (Haibin Li, Justin Sheffield, Eric F. Wood, 2010) [Panofskyand Brier, 1968] maps the distribution of monthly climate model variables (precipitation and temperature) onto that of gridded observed data. The method is a relatively simple approach that has been successfully used in hydrologic and many other climate impact studies [e.g., Cayan et al., 2008; Hayhoe et al., 2004; Maurer and Hidalgo, 2008]. For a climate variable x, the method can be written as

$$\tilde{x}_{\text{m-p.adjst.}} = F_{o-c}^{-1}\left(F_{m-c}\left(x_{m-p}\right)\right) \qquad \text{Equation 3.11}$$

where F is the Cumulative distribution factor (CDF) of either the observations (o) or model (m) for a historic training period or current climate (c) or future projection period (p). Basically, to bias correct model values for a future period, we first find the corresponding percentile values for these future projection points in the CDF of the model for the training period and then locate the observed values for the same CDF values of the observations. These are the model values after bias correction.

3.7   Simulation and Analysis of Future Change of Flow

Using the bias corrected climate data and calibrated HBV model future flow has been simulated. The future change of flow has been analyzed in three different future periods (2020 – 2040, 2041-2070, 2071-2099) in terms of mean, median and different percentiles. Besides those, change in flow will also be assessed in terms of flow duration curves and frequency analysis.

3.7.1   Flow duration curve

The flow-duration curve is a cumulative frequency curve that shows the percent of time specified discharges were equaled or exceeded during a given period. It combines in one curve the flow characteristics of a stream throughout the range of discharge, without regard to the sequence of occurrence. If the period upon which the curve is based represents the long-term flow of a stream, the curve may be used to predict the distribution of future flows for water- power, water-supply, and pollution studies (Searcy, 1959). In this study, flow duration curves for different periods such as base period (1980 to 2019), 2020 -2040, 2041-2070, 2071-2099 have been compared.

3.7.2   Frequency analysis

Flood frequency analysis is a technique used by hydrologists to predict flow values corresponding to specific return periods or probabilities along a river. In this study, the best frequency distribution is chosen from the existing statistical distributions such as Gumbel, Normal, Log-normal, Exponential, Weibull, Pearson and Log-Pearson. After choosing the probability distribution that best fits the annual maxima data, flood frequency curves are plotted. These graphs are then used to estimate the design flow values corresponding to specific return periods which can be used for hydrologic planning purposes. Flood frequency plays a vital role in providing estimates of recurrence of floods which is used in designing structures such as dams, bridges, culverts, levees, highways, sewage disposal plants, waterworks and industrial buildings. In order to evaluate the optimum design specification for hydraulic structures, and to prevent over-designing or under designing, it is imperative to apply statistical tools to create flood frequency estimates (Saksena, 2017).

4 RESULTS AND DISCUSSION

4.1 General

In the first segment of this chapter, results from data preprocessing such as watershed delineation, land use mapping, rating curve analysis have been presented. Later, the results of calibration and validation of the HBV model has been discussed. The HBV model has been calibrated separately for three different input dataset such as ERA5, NOAA and a merged dataset. The model that showed best performance in calibration and validation has been used for analyzing the impact of climate change. The results from bias correction of CANESM climate data has also been discussed in this chapter. In the last part of this chapter, future flow has been computed from calibrated model using the bias corrected data. An analysis on future change in flow duration curve and extreme flow have also been presented in this chapter.

4.2 Watershed Delineation

From the SRTM digital elevation model, the mosaic DEM has been generated by ArcGIS software. After computing flow direction, flow accumulation, snap pour point etc. in the hydrology tab, the Khowai watershed with outlet at the Shaistaganj station was delineated. The area of the Khowai basin from ArcGIS is 1325.42 which matches with Consolidation and Strengthening of Flood Forecasting and Warning Services, final report (FFWC, 2006). The digital elevation model (DEM) within the delineated Khowai basin is shown in Figure 4.1.
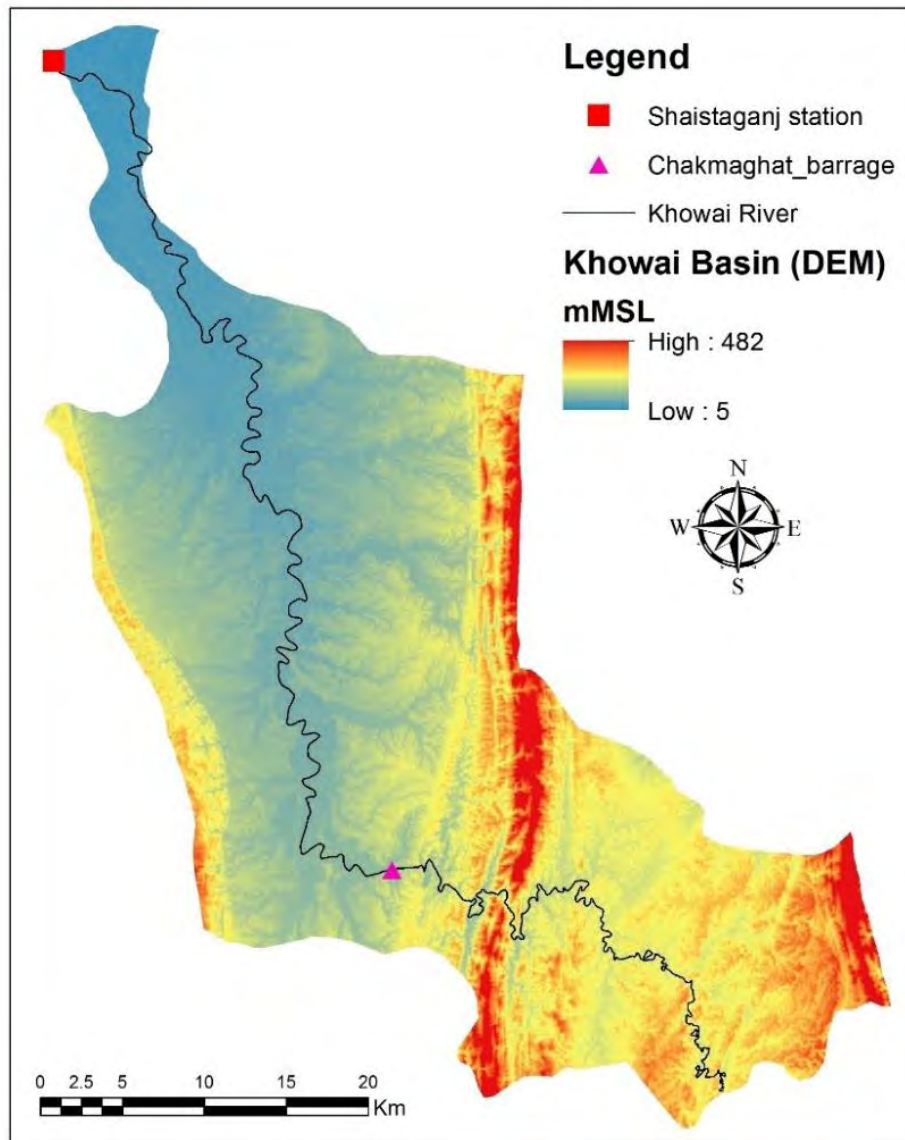
Figure 4.1: Extracted Digital Elevation Model (DEM)

4.3 Elevation Wise Zone Distribution

The extracted digital elevation model (Figure 4.1) is divided into 20 elevation zones for further use in HBV model. Elevation wise zone distribution is given in Figure A 1 and Table A 2 (Appendix).

4.4 Land Use Data Processing

Land use data was downloaded from Copernicus – land cover data. Downloaded land use data has been processed and divided into three vegetation zone. Twenty elevation zones were then distributed into three vegetation zones. The results have been compared with Debnath et al. (2017).

The land use map has been shown in Figure 4.2 and elevation wise distribution of the land use area has been shown in Appendix (Table A 3).

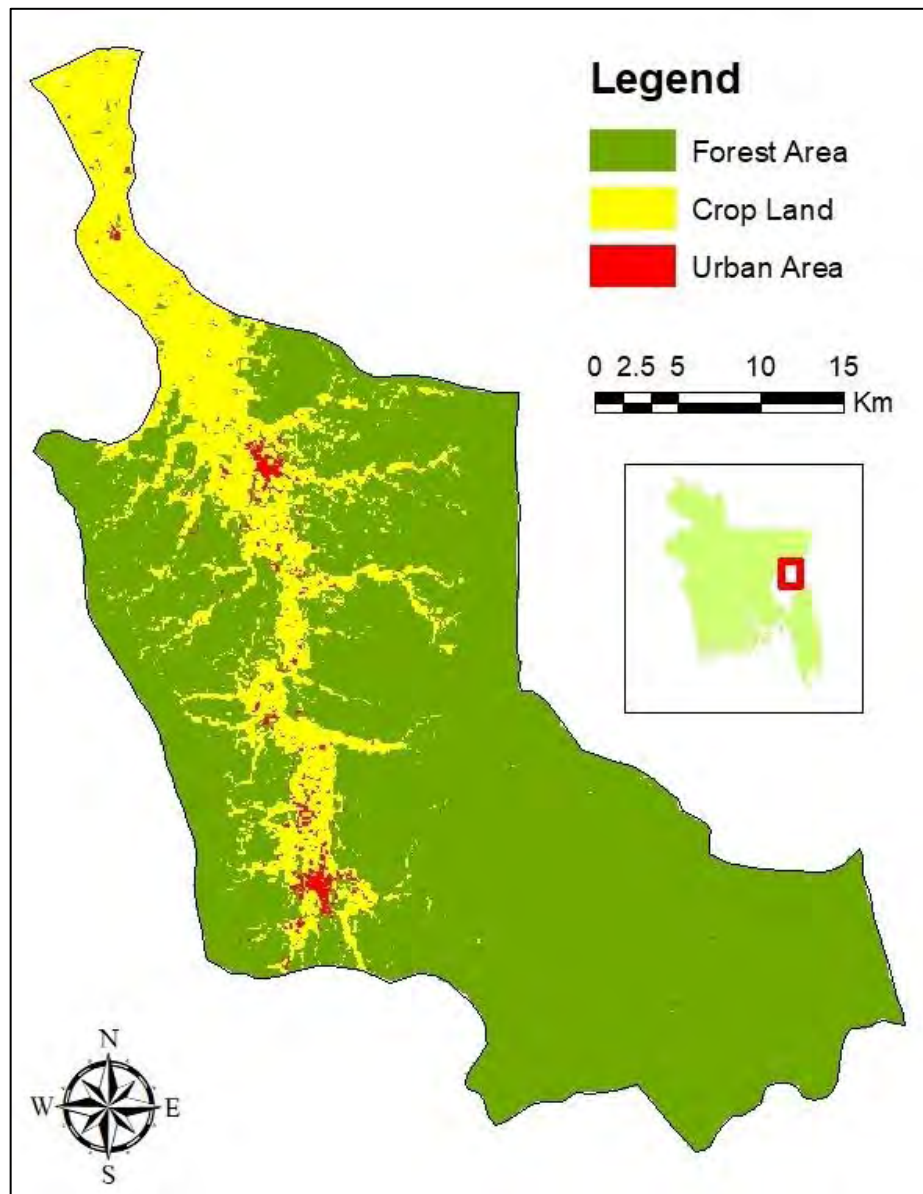Figure 4.2: Land use map

4.5   Filling Gaps in Discharge Data

Discharge data (Deb, 2015 and Rahman, 2016) of Shaistaganj station from 1979 to 2019 has been collected from BWDB for this research (Figure 4.5). The water level of Shaistaganj station is shown in Figure 4.3. Figure 4.4 shows the Shaistaganj (BWDB) station's rating curve formed from WL and the original discharge. From the time series

of discharge data (Figure 4.5), it has been found that after the chakmaghat barrage came into operation in 2015, the low flow did not decrease rather increased.

This gaps in the discharge data have been filled by rating curve generated from the WL and Q data of Shaistaganj station. If there is missing data in the WL, then the missing values have been interpolated by NUM XL software cubic spline method. This gap-filled discharge dataset has been used in calibration and validation of the HBV model.
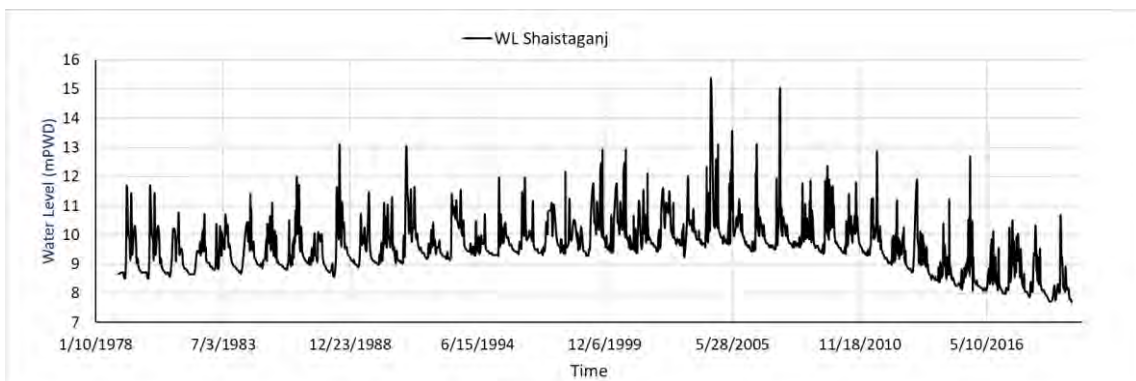

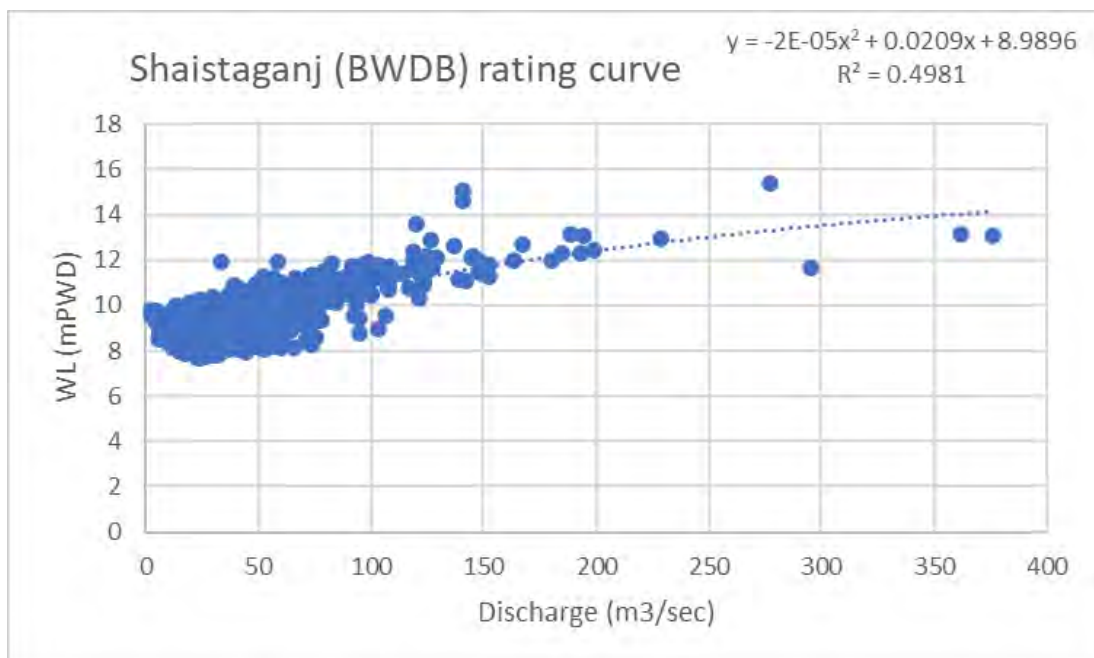Figure 4.3: Water Level Hydrograph of Shaistaganj (BWDB) Station

Figure 4.4: Rating curve plot for a period of 1980 to 2019 using Shaistaganj station's Water level and original Discharge
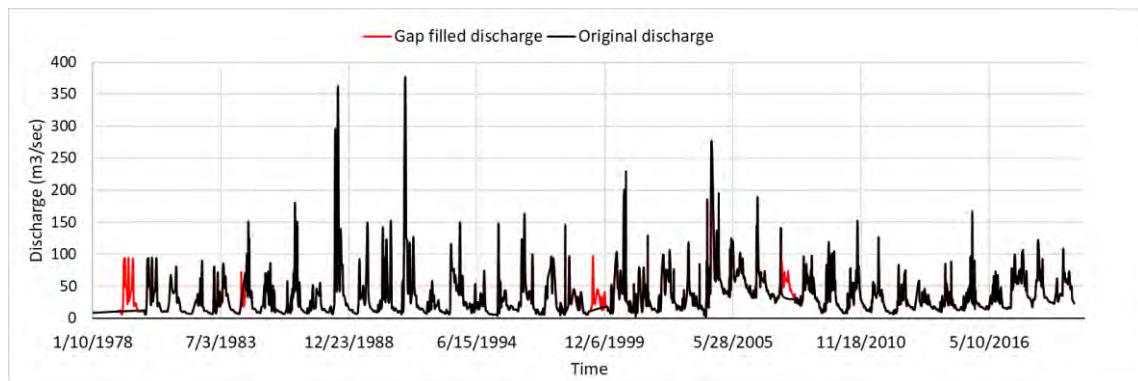
Figure 4.5: Original and gap-filled discharge of Shaistaganj station of the Khowai river

4.6 Model Calibration and Validation

In this section, the suitability of two global gridded datasets (NOAA and ERA5) and a merged dataset, as described in Table 3.5, has been assessed in modelling the streamflow of data-scarce Khowai river basin using HBV hydrologic model. In this study, the HBV model has been calibrated for the Khowai catchment for the period 01-01-1980 to 31-12-2010 (where the warm-up period is from 01-01-1979 to 31-12-1979). While the model is validated for the period 01-01-2011 to 31-12-2019.

4.6.1 Results from calibration and validation with ERA5 datasets (trial 1)

In this trial, ERA5 precipitation, temperature and evaporation datasets (Table 3.1) from 1979 to 2019 have been used. A plot between observed and simulated discharge data using this ERA5 datasets is shown in Figure 4.6. The coefficient of determination (R^2) based on the observed and simulated discharge for the calibration period is 0.51 and for the validation period is 0.44. The Nash-Sutcliff coefficient (NSE) for the calibration and the validation period are 0.38 and 0.08 respectively (Table 4.1). It has been noticed that the ERA5 data driven model could not simulate the high peaks quite accurately in several years. A large difference is found for 2004. However, the model could simulate the low flow quite efficiently. The PBIAS for the calibration and validation period are 5.23 and -2.35 respectively.
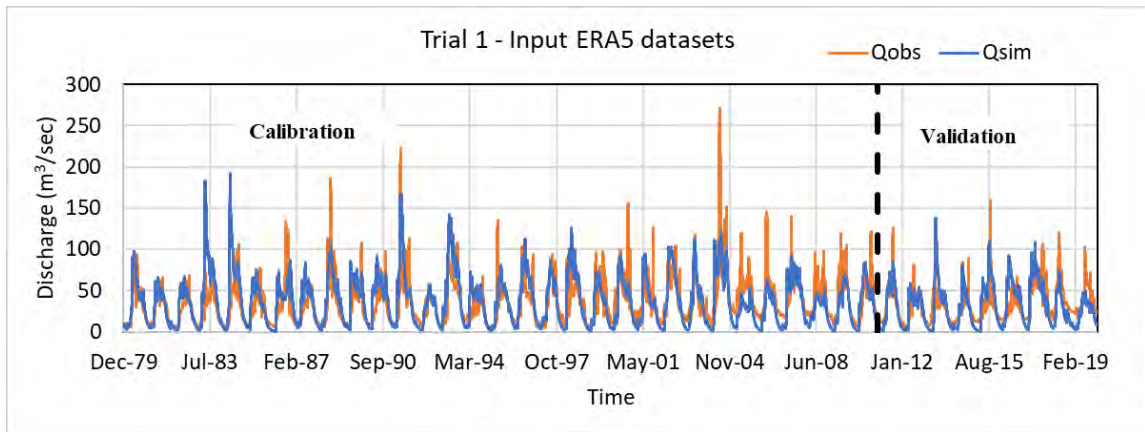
Figure 4.6: Results from calibration and Validation with ERA5 datasets (Trial 1)

4.6.2 Results from calibration and validation with NOAA datasets (trial 2)

In Trial 2, precipitation, temperature and evaporation datasets downloaded from NOAA CPC (Table 3.1) from 1979 to 2019 have been used as input. A plot between observed and simulated discharge data using this NOAA datasets in this trial is shown in Figure 4.7. The coefficient of determination (R^2) for the observed and simulated discharge for the calibration and the validation period are 0.48 and 0.40, respectively (Figure 4.7). The NSE for the calibration and the validation period are 0.37 and 0.06, respectively (Table 4.1). The NOAA data driven model also underestimated the peaks for most of the years. The errors in the model output were large for the large flood events such as for the events of 1988 and 2004.
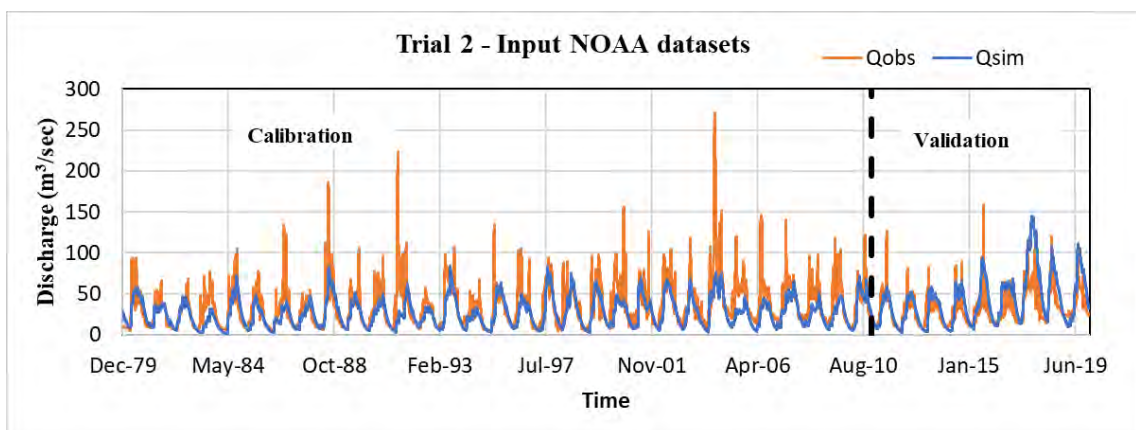

Figure 4.7: Results from calibration and Validation with NOAA datasets (Trial 2)

4.6.3 Results from calibration and validation with merged datasets (trial 3)

In this trial, average rainfall of NOAA, ERA5 and Habiganj (BWDB) has been used. For, temperature and evaporation ERA5 datasets (Table 3.1) have been used because temperature and evaporation from both NOAA and ERA5 datasets are close but ERA5 has better resolution. A plot between observed and simulated discharge data from this trial is shown in Figure 4.8. The coefficient of determination (R^2) for the observed and simulated discharge for the calibration and validation period are 0.67 and 0.63, respectively on daily time scale (Table 4.1). The Nash-Sutcliff coefficient (NSE) for the calibration and the validation period are 0.65 and 0.56 respectively (Table 4.1). The PBIAS for the calibration and the validation period are 1.30 and -14.35 respectively (Table 4.1). The model driven by the average data showed better performance than the model driven by the NOAA or ERA5 datasets. This model could simulate the peaks more accurately than the previous two trials for most of the years with some exceptions. However, the peak of 2004 could not be predicted accurately. The reason behind this can be the inability of the precipitation data sets (Appendix - Figure A 2) to capture the high rainfall of 2004.
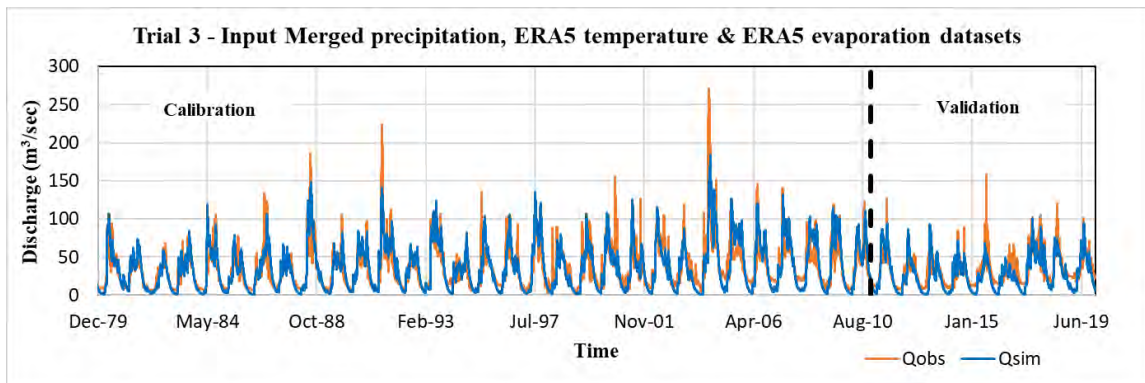

Figure 4.8: Results from calibration and Validation with merged datasets (Trial 3)

4.6.4 Comparison of the ERA5 and NOAA gridded datasets and merged dataset

In each trial (Trial 1, 2 and 3), different parameter sets have been found from the Monte Carlo simulation. The optimal parameter set for each trial is presented in Appendix (Table A 4).

Table 4.1: Comparison of the ERA5 (trial 1), NOAA (trial 2) and merged dataset (trial 3) driven models' output for the calibration and the validation periods

Period	Goodness of fitness functions	Trials					
		Trial 1		Trial 2		Trial 3	
		ERA5	Evaluation	NOAA	Evaluation	Merged	Evaluation
Calibration (1980-2010)	R²	0.51	Acceptable	0.48	Not satisfactory	0.67	Good
	NSE	0.38	Not satisfactory	0.37	Not satisfactory	0.65	Good
	PBIAS	5.23	Good	-24.59	Acceptable	1.30	Very Good
Validation (2011-2019)	R²	0.44	Not satisfactory	0.40	Not satisfactory	0.63	Good
	NSE	0.08	Not satisfactory	0.06	Not satisfactory	0.56	Acceptable
	PBIAS	-2.35	Very Good	26.54	Not satisfactory	-14.35	Good
Whole Period (1980-2019)	R²	0.50	Acceptable	0.41	Not satisfactory	0.66	Good
	NSE	0.34	Not satisfactory	0.33	Not satisfactory	0.64	Acceptable
	PBIAS	3.02	Very Good	-13.66	Good	-2.38	Very Good

Table 4.1 shows a comparison among the models driven by different datasets. Table 4.1 indicates that ERA5 shows better result than NOAA in both calibration and validation. But in the validation period (2011-2019), both ERA5 and NOAA show worse results than the calibration results. For this reason, another trial (trial 3) has been done using average rainfall (average of NOAA, ERA5 & Habiganj) which shows better results for all three periods (calibration, validation & whole period). Therefore, the model obtained from trial 3 will be used to assess the impact of climate change on the Khowai river flow. The optimal parameter set of the final selected model has been shown in Appendix (Table A 5).

Table 4.2: The results on monthly scale for final selected "merged dataset" used model

Evaluation for	Period		R^2	Remarks	NSE	Remarks	PBIAS	Remarks
	From	To						
Whole data set	1979	2019	0.77	Very Good	0.74	Good	-2.38	Very good
Calibration	1980	2010	0.78	Very Good	0.75	Very Good	1.30	Very good
Validation	2011	2019	0.75	Very Good	0.67	Good	-14.35	Good

Rahman (2016) used the SWAT model to simulate the discharge of Shaistaganj station in which calibration period was 1990-2003 and validation period was 2004-2010. The SWAT model produces unsatisfactory results for the Shaistaganj station for both calibration (NSE = 0.43, PBIAS = -37.88%, R^2 = 0.60) and validation (NSE = 0.05, PBIAS = 17.84%, R^2 = 0.43) periods in case of mean monthly analysis (Rahman, 2016). So, it can be said that the HBV model results from calibration and validation is better than that of Rahman (2016).

IWFM (2020) set-up a hydrologic model to forecast flash flood in the north-easter region of Bangladesh. They reported that due to insufficient observations of discharge, it was not possible to accurately calibrate and validate hydrologic (HEC-HMS) and hydraulic models (HEC-RAS). Lack of observations of rainfall in the upper catchment areas outside Bangladesh also made their research challenging. Because transboundary collaborations on sharing observed data from the rainfall stations inside India is very limited (IWFM, 2020). Shaistaganj station was not analyzed in this research. However, the results were acceptable to good for the two other near-by rivers such as Korangi and Sutang which also belong to the Tripura basin like the Khowai river. The R^2 were 0.75 and 0.71 for the calibration period and 0.68 to 0.52 for the validation period, respectively.

4.7 Model Parameter Uncertainty Analysis

In a hydrological modeling context, the optimized parameter set is obtained by running the hydrological model multiple times using different parameter sets, generated using, for

instance, Monte-Carlo procedures, Bayesian methods or evolutionary algorithms. The sensitivity of a parameter is obtained by plotting the values of model goodness against the different values of the parameter. For a well-defined parameter the goodness statistics decreases clearly as parameter values deviate from some optimal value. If, on the other hand, good simulations could be achieved using parameter values over a wide range, this parameter is not well-defined.

HBV-light allows many model runs with randomly generated parameter sets using the "Monte Carlo Runs" tool. Optimum parameters and parameter uncertainty is estimated by allowing single or multiple (up to all) parameters to vary within the limit mentioned in the Table 3.4. After Monte Carlo Simulation, a Multi.txt file would be created in the Results folder. This file is opened in Excel and the parameter values corresponding to maximum Nash-Sutcliffe value (Reff) is selected as final parameter set (Appendix – Table A 5). If there are too many solutions / combinations to get the required objective function value, it may lead to the problem of equifinality and large uncertainty. While well-defined behavioral parameters lead to more certainty and confidence in the solution. While model calibration, two most sensitive parameters have been found – K2 (baseflow parameter from response routine variable) and MAXBAS (routing parameter). Varying K2 from 0.005 to 0.04, it has been noticed that NSE varies from 0.33 to 0.64 (Figure 4.9). Varying MAXBAS from 1 to 7, it has been noticed that NSE decreases from 0.64 to 0.58 (Figure 4.10).
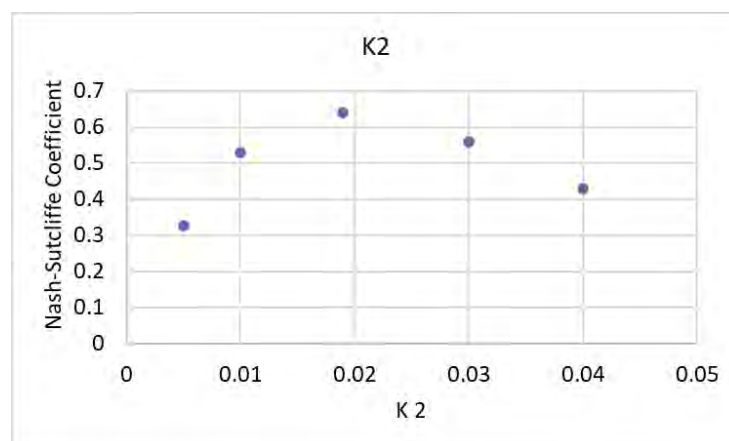

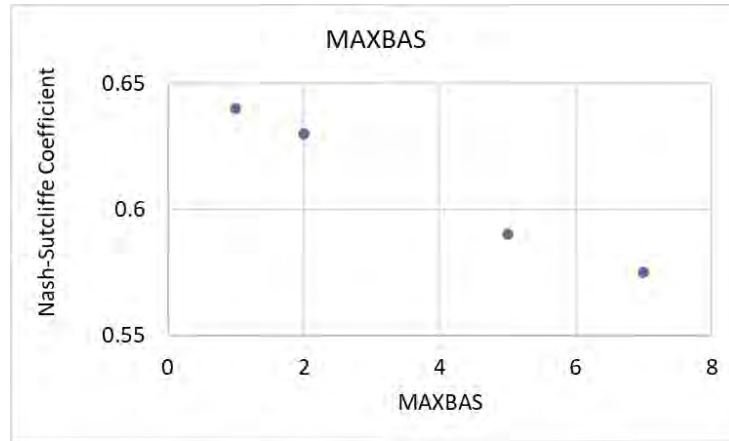Figure 4.9: Sensitivity analysis – K2 (from response routine)

Figure 4.10: Sensitivity analysis – MAXBAS (from routing routine)

4.8 Bias Correction of The Future Climate Data Set

4.8.1 Linear scaling method

Climate model outputs often suffer from biases. To overcome these bias, future rainfall, temperature and evaporation data from CORDEX CANESM2 model were corrected for bias based on merged rainfall, ERA5 temperature and evaporation using the linear scaling (LS) bias correction method.

The plot of bias corrected CORDEX rainfall and merged rainfall (average of ERA5, NOAA, Habiganj) is given in Figure 4.11. The plots of bias corrected CORDEX temperature and evaporation vs ERA5 temperature and evaporation are given in Figure 4.12 and Figure 4.13, respectively.

Table 4.3: Comparison of Linear Scaling and Quantile Mapping

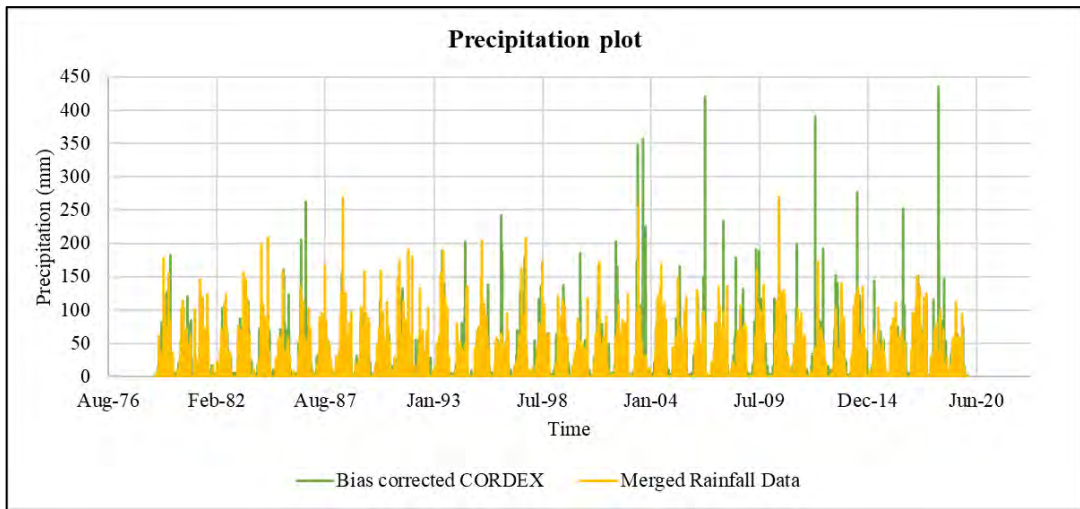| Variable	RMSE before bias correction	RMSE after bias correction	
		Linear Scaling	Quantile Mapping
Precipitation	20.70	20.11	15.49
Temperature	3.52	2.77	2.59
Evaporation	1.43	1.45	1.11

Figure 4.11: Bias corrected CORDEX rainfall using linear scaling method
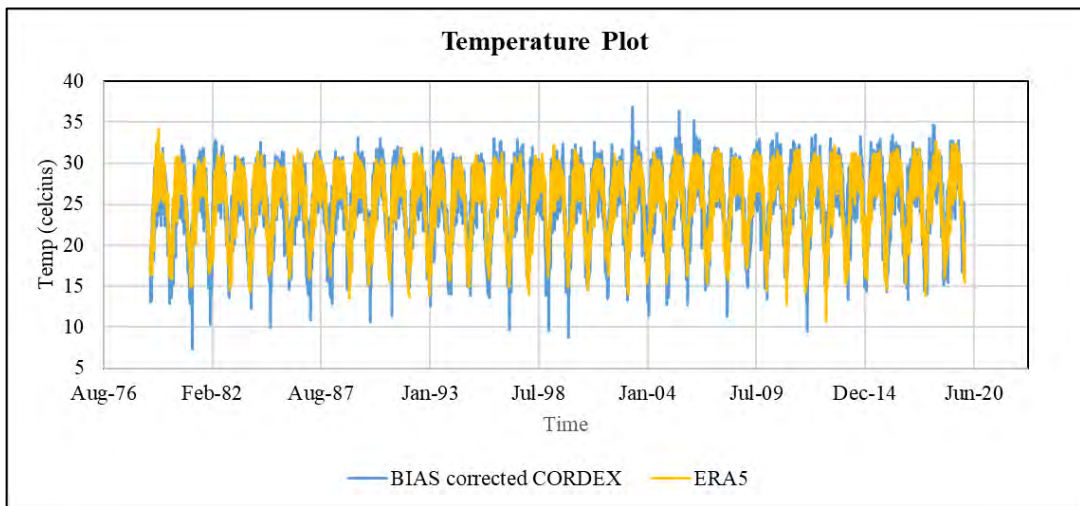

Figure 4.12: Bias corrected CORDEX temperature using linear scaling method
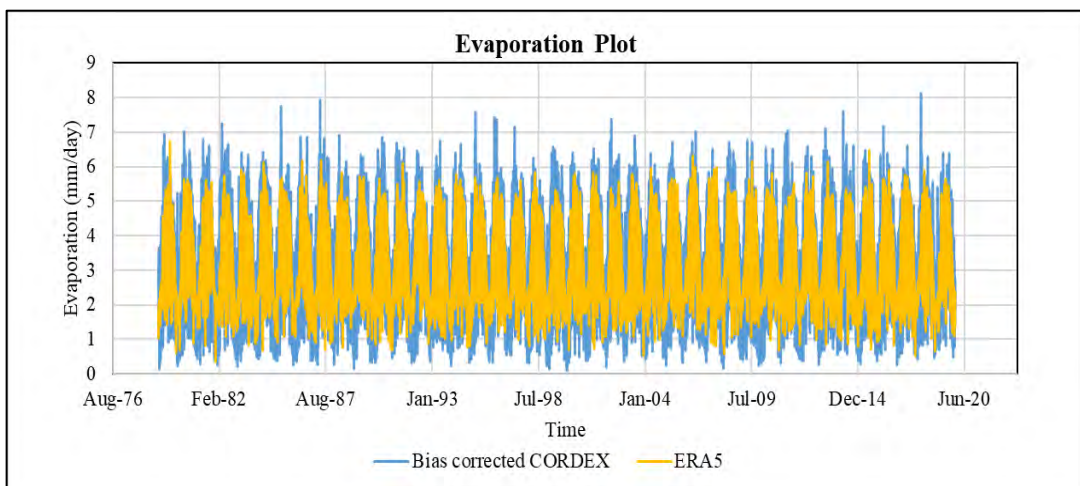
Figure 4.13: Bias corrected CORDEX evaporation using linear scaling method

65

Figure 4.11 to Figure 4.13 clearly show linear scaling method could not remove the bias efficiently and it either underestimated or over-estimated the observed data therefore, another bias correction method called quantile mapping has been employed.

4.8.2   The quantile mapping method

The results from the quantile mapping bias correction for the precipitation data is shown in Figure 4.14 and Figure 4.15. Figure 4.14 shows that the CDF of observed data and bias corrected data match very well.

Figure 4.14: Cumulative distribution function for observed (merged precipitation), biased and bias corrected precipitation (mm/day) data

Figure 4.15: Comparison of observed (merged) precipitation with biased and bias corrected (Quantile Mapping) CANESM precipitation for the historic period

The results from the quantile mapping bias correction for the temperature data is shown in Figure 4.16 and Figure 4.17. Figure 4.16 shows that the CDF of observed data and bias corrected temperature data match very well.
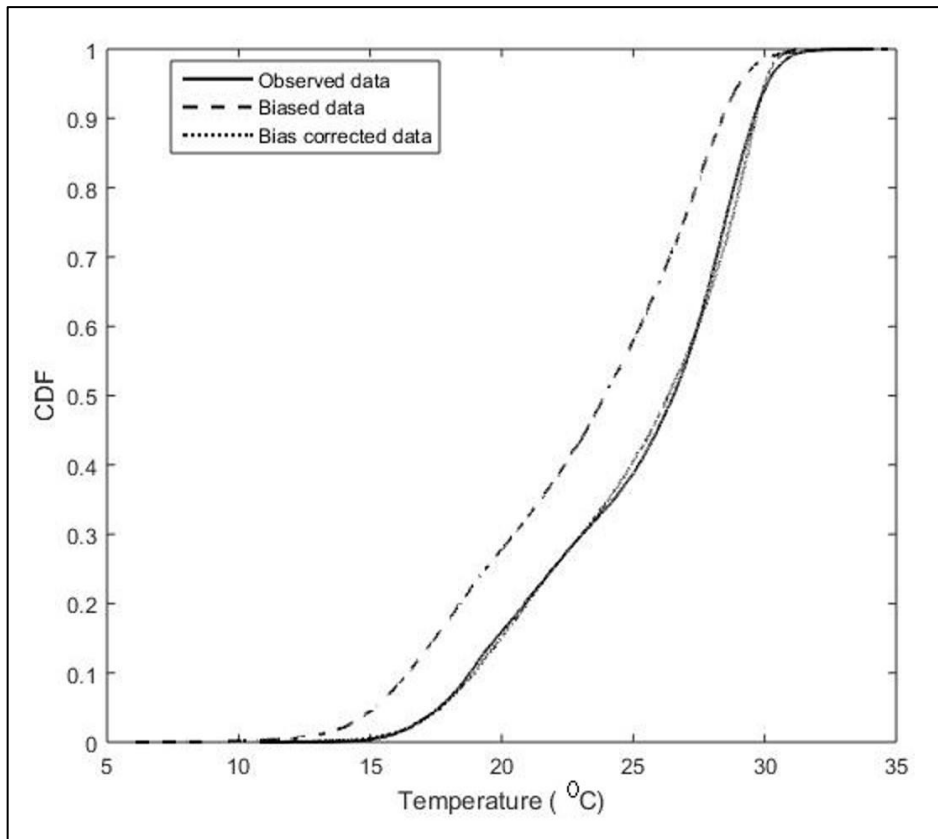
Figure 4.16: Cumulative distribution function for observed (ERA5), biased and bias corrected temperature (^{0}C)

Figure 4.17: Comparison of observed (merged) temperature with biased and bias corrected (Quantile Mapping) CANESM temperature for the historic period

The results from the quantile mapping bias correction for the evaporation data is shown in Figure 4.18 and Figure 4.19. Figure 4.18 shows that the CDF of bias corrected evaporation data follows the CDF of observed data very closely.
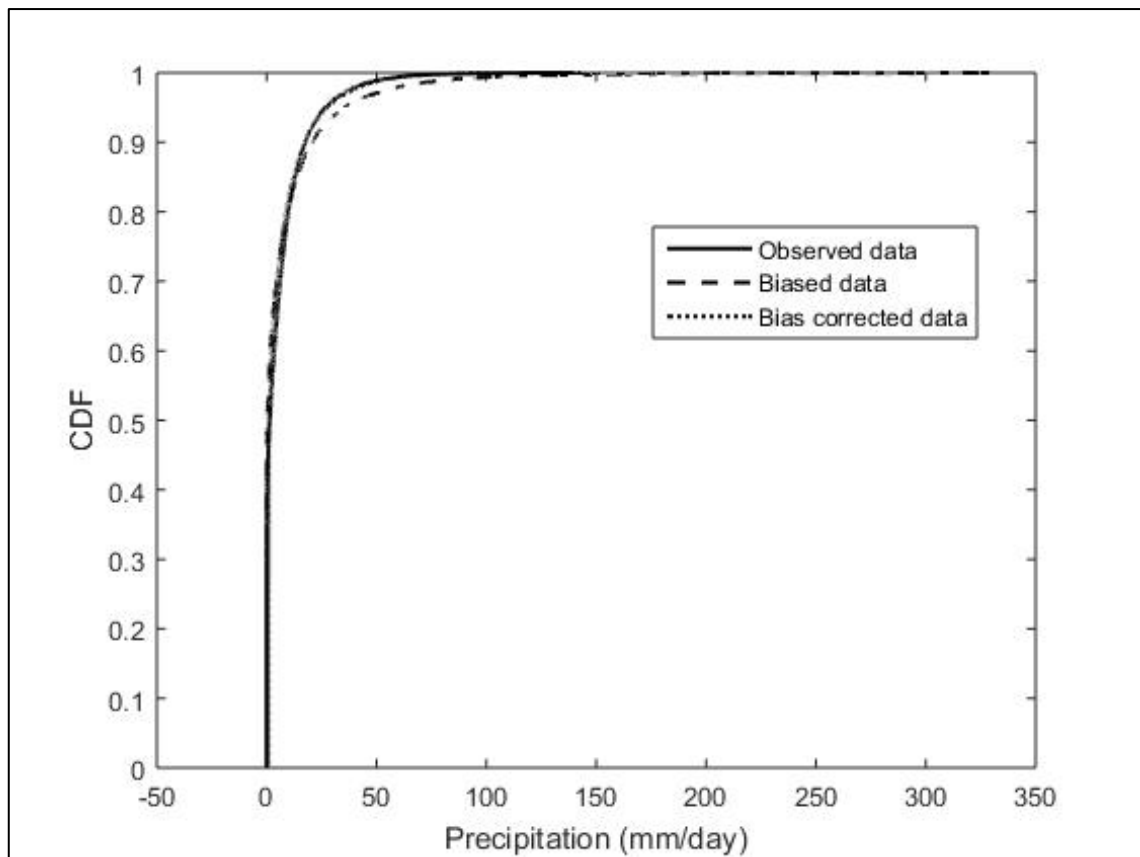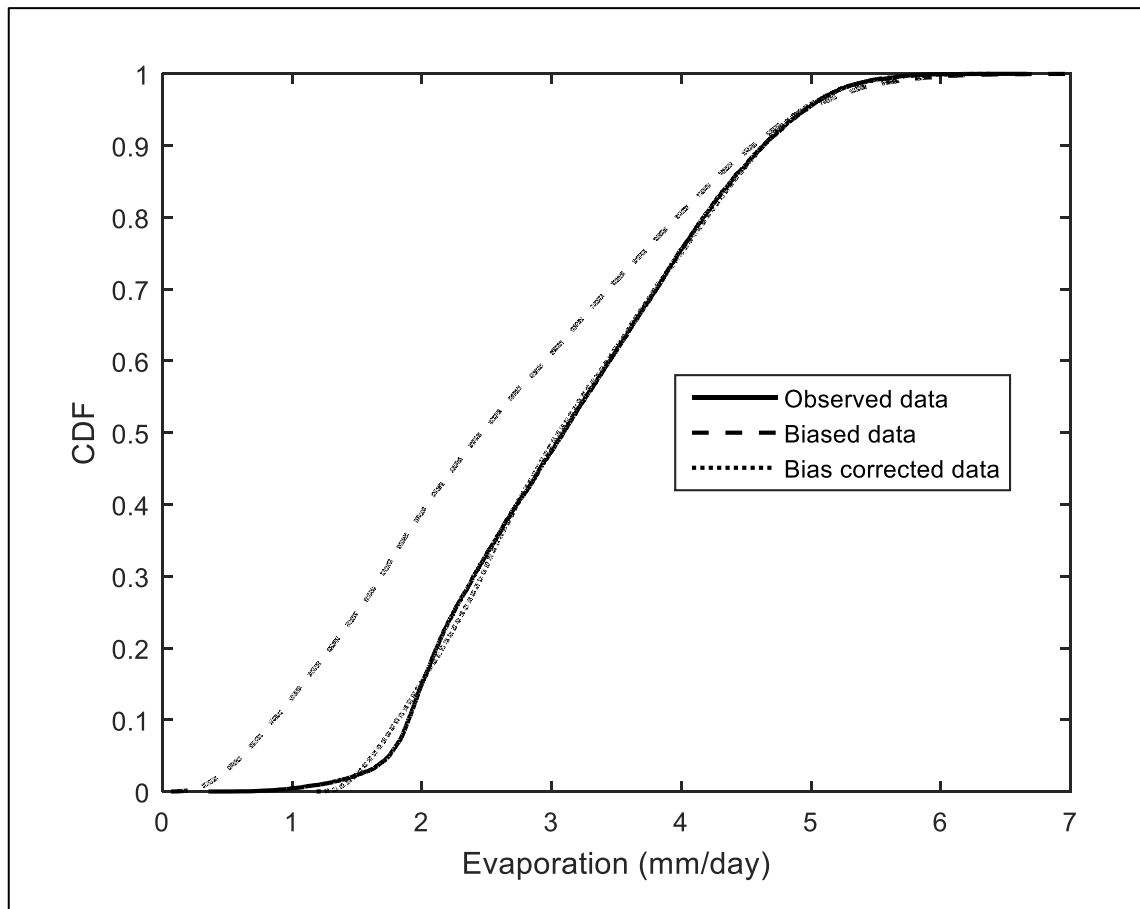

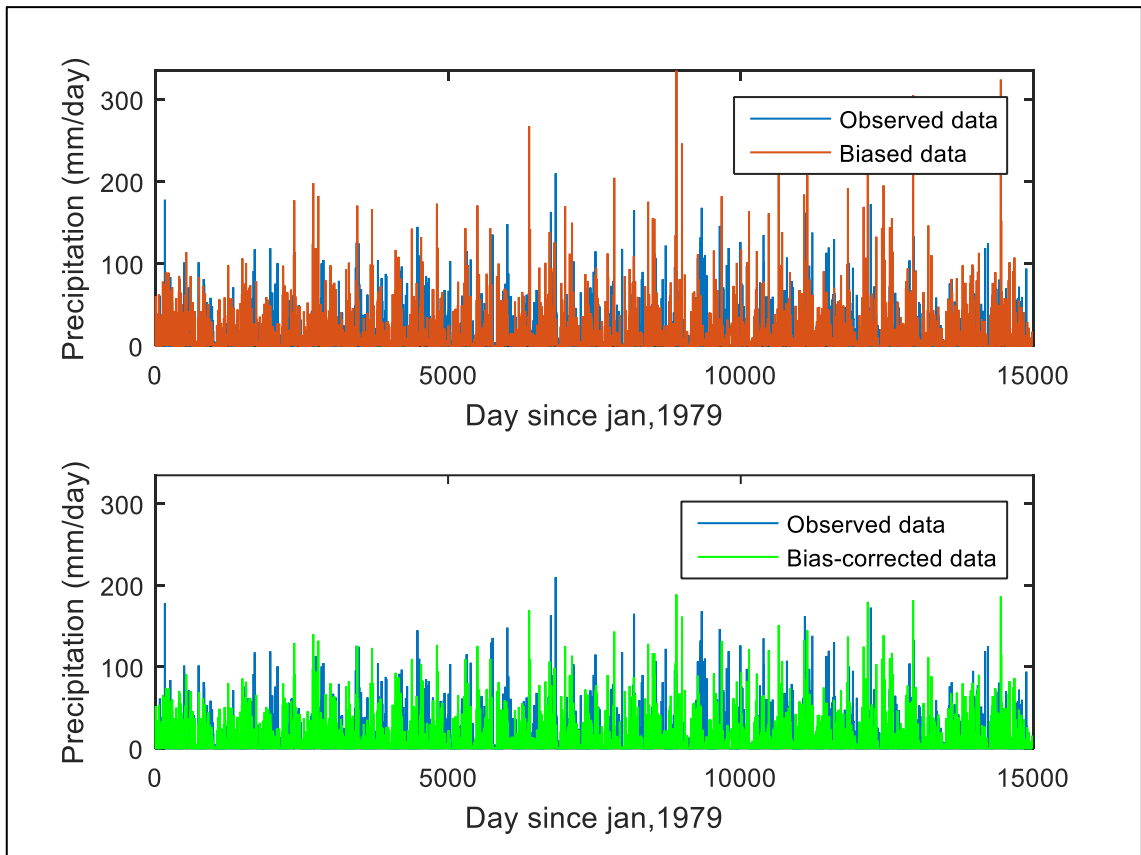Figure 4.18: Cumulative distribution function for observed (ERA5), biased and bias corrected evaporation (mm/day) data
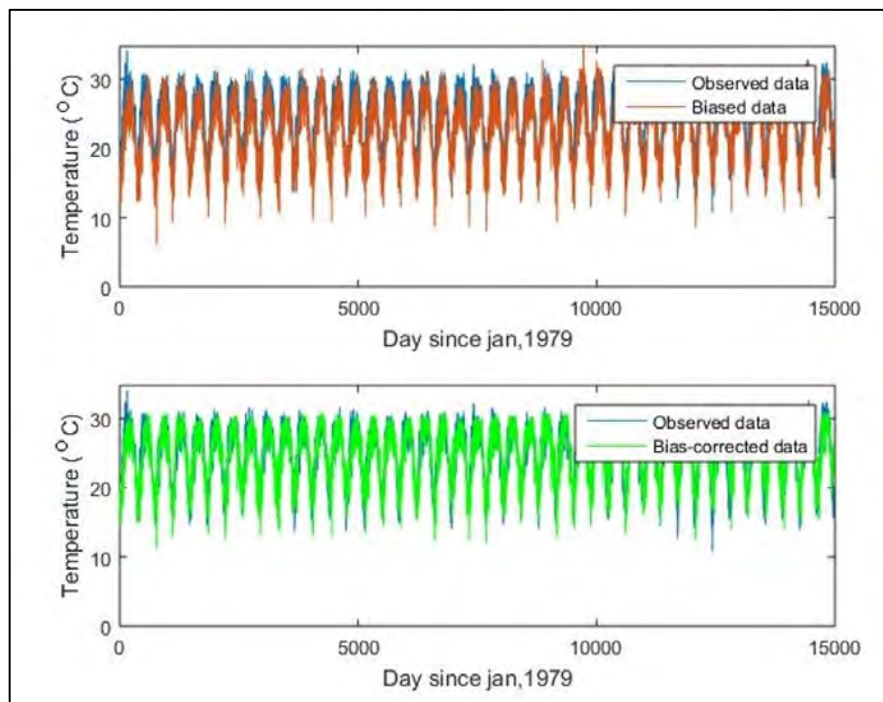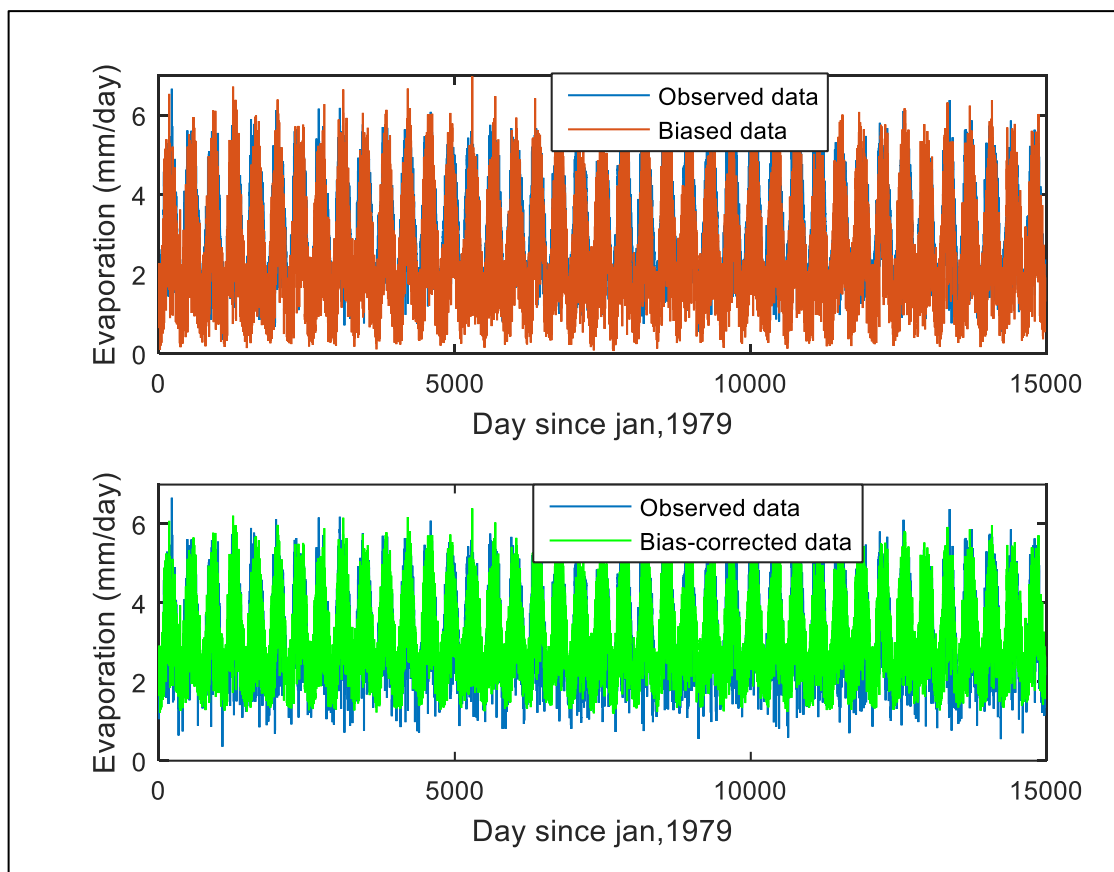
Figure 4.19: Comparison of observed (merged) evaporation with biased and bias corrected (Quantile Mapping) CANESM evaporation for the historic period

As quantile mapping could correct the bias more efficiently (Table 4.3) with respect to the merged rainfall, ERA5 temperature and evaporation, this approach will be used to correct the future climate dataset. Later the corrected datasets will be used to simulate the future flow using the calibrated HBV model.

4.9   Climate Change Impact Assessment

4.9.1   Change in precipitation, temperature and evaporation due to climate change

Bias-corrected precipitation time series of 1980 to 2099 (Figure 4.20) shows an increasing trend. In the base period (1980-2019), the peak does not exceed 300 mm/day once, but in future period (2020-2099), the peak crosses 350 mm/day 8 times. So, the precipitation intensity shows an upward trend.
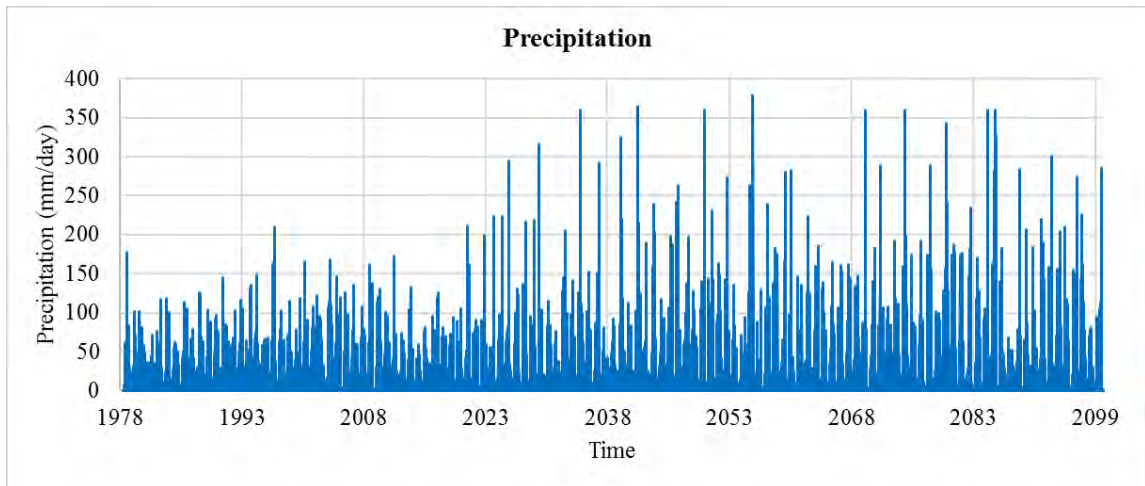
Figure 4.20: Precipitation time series (1980 – 2099)
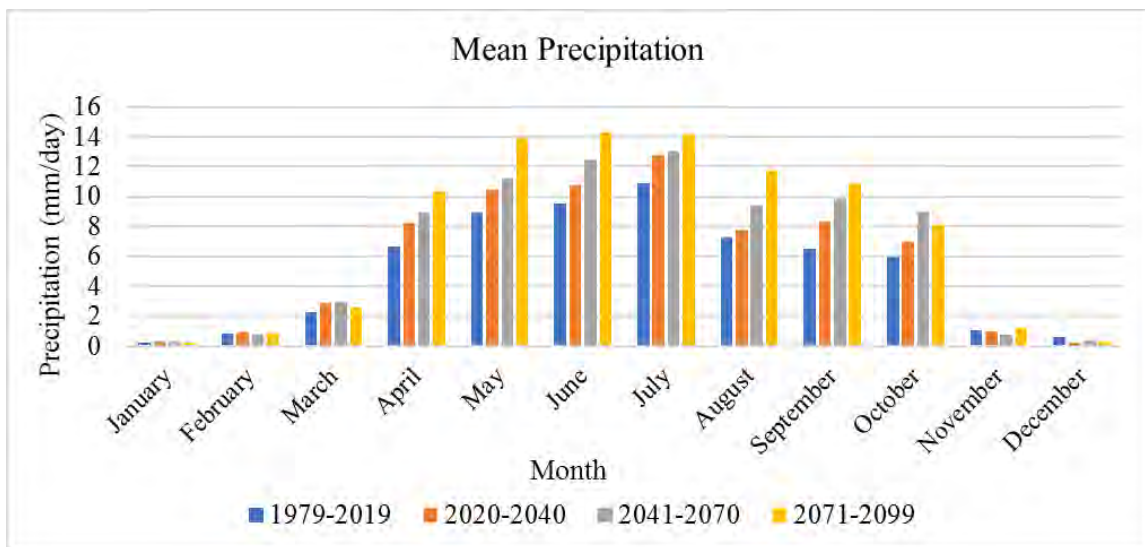
Figure 4.21: Monthly variation of observed and projected precipitation over different time periods.

Increase in mean precipitation from baseline have been found to be 7.69, 15.86 and 21.05 percent for 2020-2040, 2041-2070 and 2071-2099, respectively. The maximum daily precipitation for periods 1980-2019, 2020-2040, 2041-2070 and 2071-2099 are 270, 325.22, 379.17 and 356.29 mm/day respectively.

The trend in temperature rises from 1980 to 2099 has been shown in Figure 4.22. From this figure, it can be said that the mean temperature increases from 1980 to 2099 by almost 3^0C.
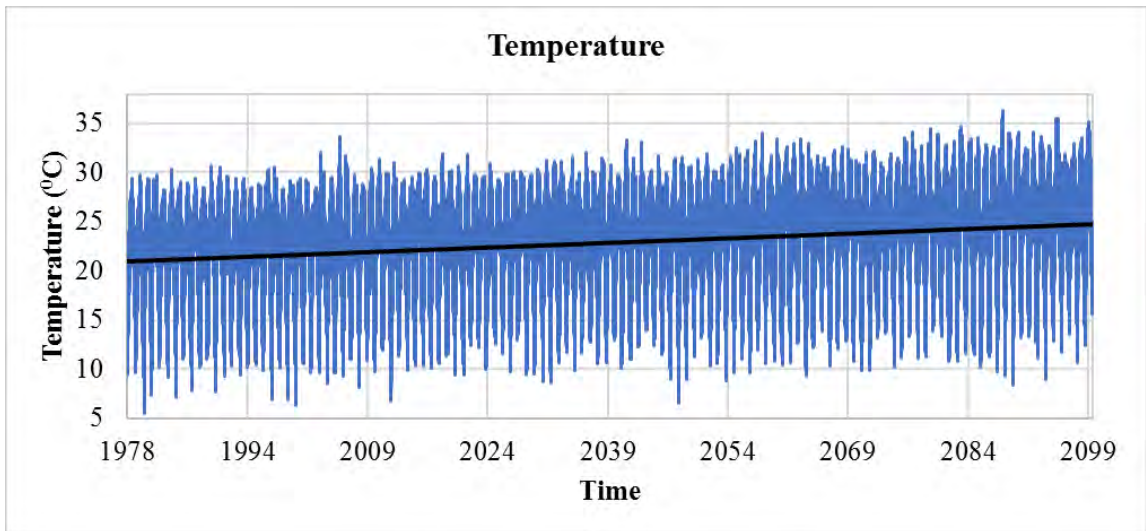
Figure 4.22: Temperature time series (1980-2099)

Figure 4.23: Boxplots of observed and projected temperature for different time periods

Table 4.4: Temperature (daily) change analysis

Temperature (^{0}C)	1980 - 2019	2020 - 2040	2041 – 2070	2071 – 2099	Whole future period (2020 - 2099)
Minimum	6.08	8.73	6.63	8.41	6.63
Median	23.95	24.15	25.77	26.97	25.89
Maximum	34.78	34.80	35.65	36.30	36.30
Mean	23.10	23.92	24.56	25.51	24.74
Mean change		0.82	1.46	2.41	1.64
Change (%) from the baseline period		3.55	6.11	9.80	6.42
Upper whisker	34.78	34.80	35.65	36.30	36.30
Lower whisker	8.12	8.73	6.63	8.41	6.63
skewness	Negative	Negative	Negative	Negative	Negative

From Table 4.4, increase of mean temperature from baseline (1980-2019) for 2020-2040, 2041-2070 and 2071-2099 have been found to be 0.82, 1.46 and 2.41 degree Celsius, respectively and 3.55%, 6.11% and 9.80% respectively.
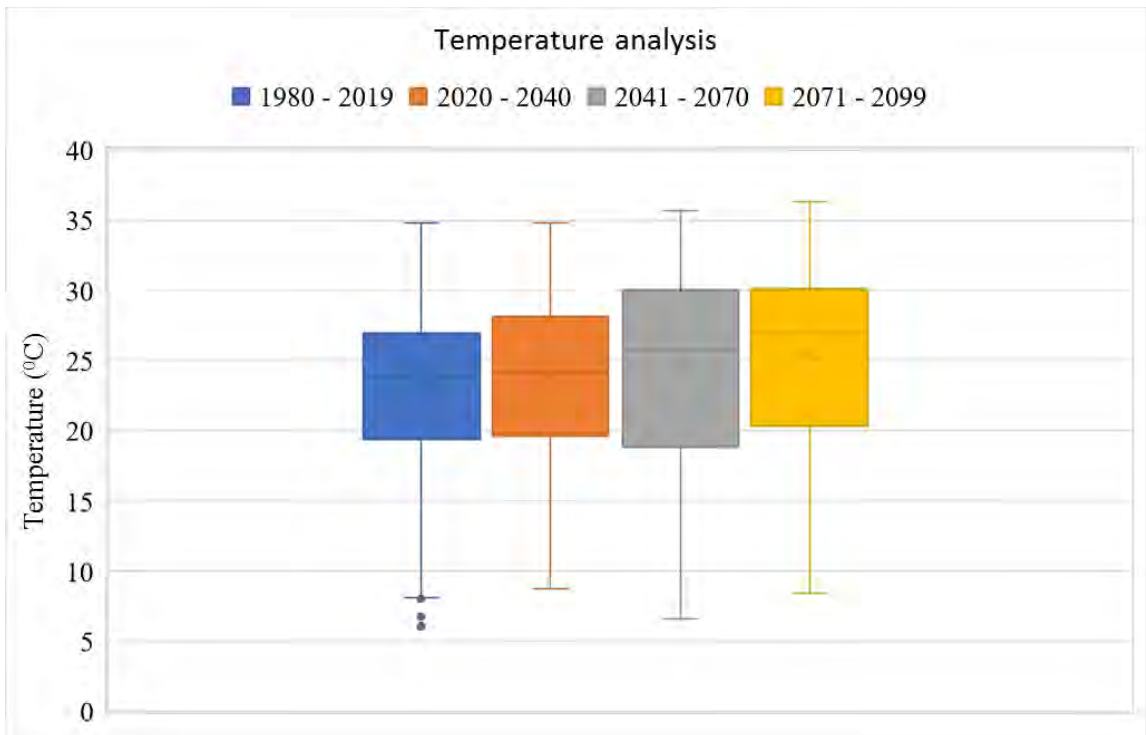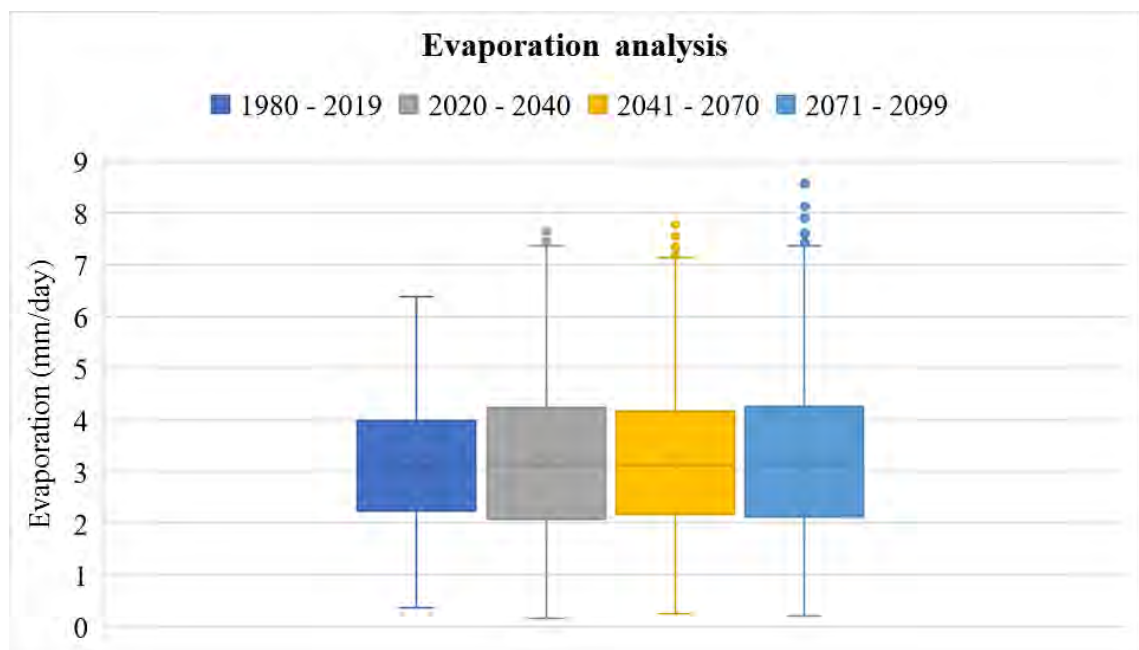

Figure 4.24: Boxplots of observed and projected evaporation for different time periods

Table 4.5: Evaporation (daily) change analysis

Evaporation (mm/day)	baseline observed (1980 - 2019)	2020 - 2040	2041 - 2070	2071 - 2099
Minimum	0.354	0.159	0.240	0.200
Median	3.089	3.124	3.108	3.138
Maximum	6.376	7.649	7.888	8.567
Mean	3.165	3.187	3.221	3.250
Mean change		0.022	0.056	0.084
Change (%) from the baseline period		0.695	1.755	2.662
Upper whisker	6.571	7.484	7.290	7.470
Lower whisker	0.354	0.159	0.240	0.200
skewness	positive	positive	positive	positive

Increase of mean evaporation from baseline for 2020-2040, 2041-2070 and 2071-2099 have been found to be 0.022, 0.056 and 0.084 mm/day respectively. Evaporation is projected to increase by 0.695%, 1.755%, 2.662% in 2020-2040, 2041-2070 and 2071-2099, respectively. The median value is also projected to increase.

Month wise mean daily AET and PET plots are given in Figure 4.25 and Figure 4.26 respectively. From the plots, it can be mentioned that monthly PET will not increase much in future for the monsoon and post-monsoon months. But in 2071-2099, although the rainfall increases from the base period (1980-2019), the actual evaporation decreases in the pre-monsoon to monsoon and increases in the post-monsoon period and dry period.

Figure 4.25: Monthly variation of observed and projected actual evapotranspiration (AET) for different time periods.

Figure 4.26: Monthly variation of observed and projected potential evapotranspiration (PET)

Changes of evapotranspiration in response to climate change have been widely studied at regional and continental scales. Climate factors affecting evapotranspiration include three independent factors: Demand, supply, and energy. Demand depends on air temperature and win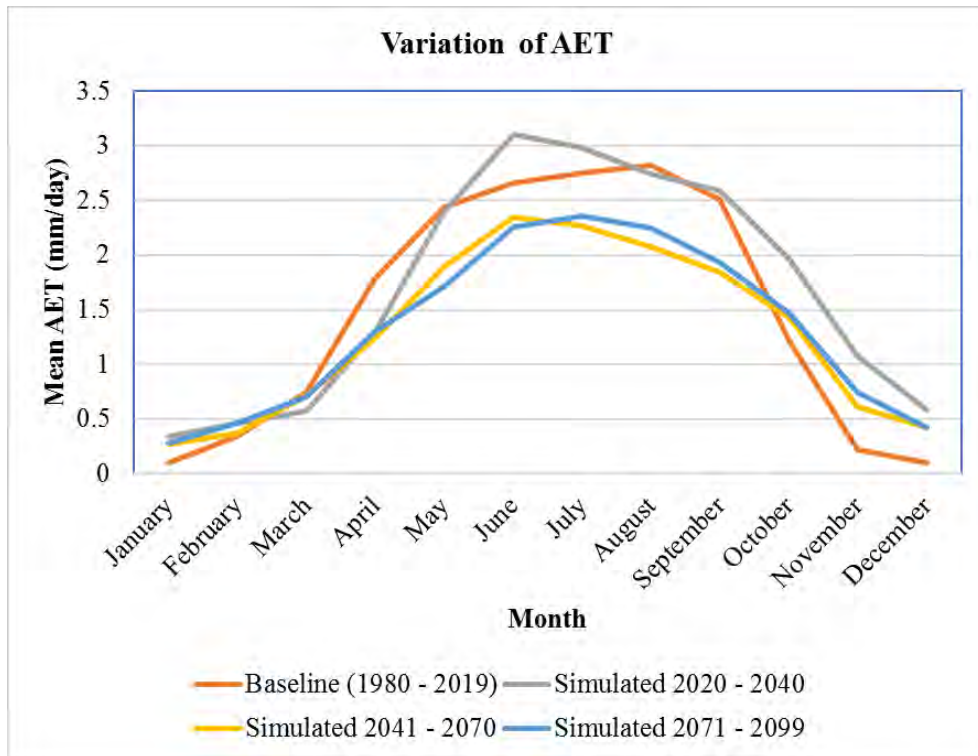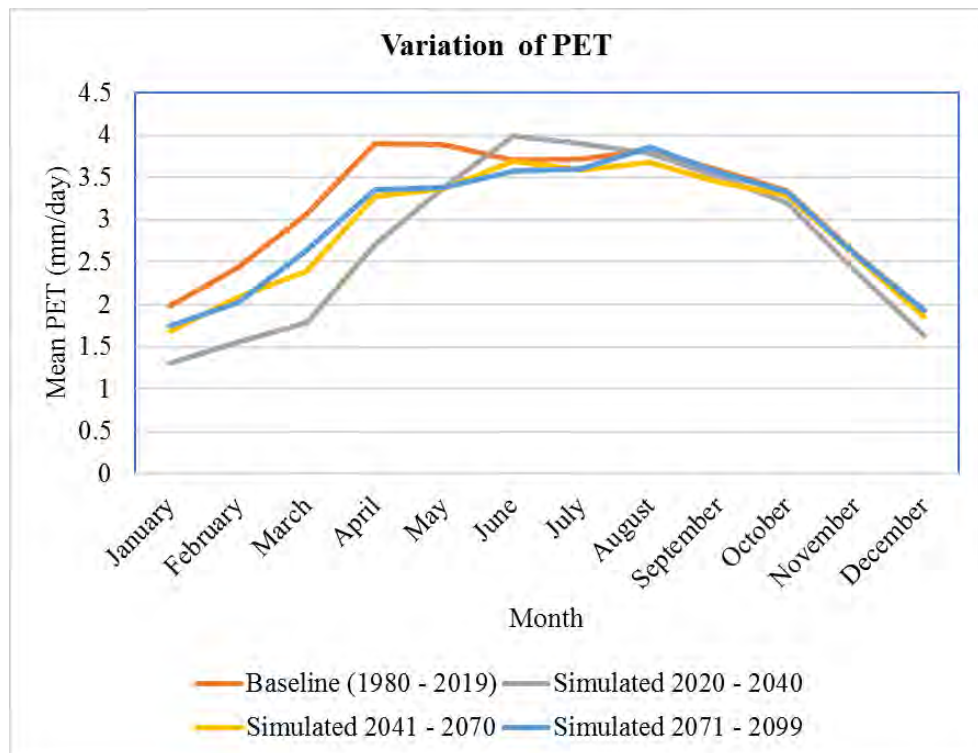d speed, while supply and energy are determined by precipitation and solar radiation, respectively (Xiuliang and Bai, 2018). Murray et al. (2012) in their study, used a dynamic global vegetation model, showed that a warmer environment decreases vegetation coverage and transpiration due to water stress in the soil system which reduces overall actual ET. Kirschbaum and McMillan (2018) reported reductions in daily transpiration rates over the twenty-first century that became stronger under higher atmospheric CO_2 concentrations. They found that the effect of CO_2-induced reduction of stomatal conductance would have a stronger transpiration-depressing effect than the stimulatory effect of future warming (Kirschbaum, M.U.F. and McMillan, A.M.S., 2018). Alfi et al. (2014), in their research shows that in the recent decades, the average evapotranspiration in Bangladesh has reduced from January to April. However, from July to December, ET shows slight increase in recent decades. Spatial Analysis has revealed that ET_0 has reduced more in the western part than in the eastern part of the country. The south eastern region of Bangladesh shows a notable decrease of ET_0 (Alfi et al., 2014). In this study we also noticed decrease in AET in some months. As for example, it is noticed that in 2071-2099, the actual evaporation decreases in the pre-monsoon to monsoon and increases in the post-monsoon period and dry period.

4.9.2 Future flow simulation

The calibrated and validated model obtained from Trial 3 has been used to simulate the discharge of Shaistaganj station for 2020 to 2099 using the bias corrected CANESM climate data as input. The simulated discharge hydrograph from 2020 to 2099 is shown in Figure 4.27.
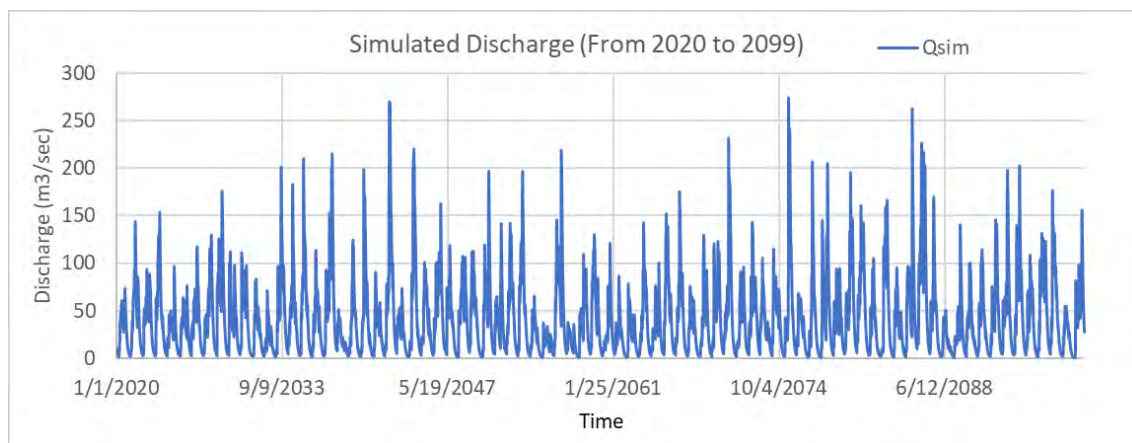
Figure 4.27: Simulated discharge hydrograph from 2020 to 2099 for Shaistaganj Station of BWDB

The highest discharge value in the simulated period from 2020 to 2099, is 273.96 m³/sec will occur on 19/07/2075 (as per model simulation). From the above figure, it can be mentioned that the daily discharge at Shaistaganj station will cross 250 m³/sec three times from 2020 to 2099.

4.9.3 Analysis of future change of flow

The change of flow has been analyzed in three different future periods (2020 – 2040, 2041-2070, 2071-2099). The boxplots showing month-wise mean daily flow for four different periods (base line 1980-2019, 2020-2040, 2041-2070 and 2071-2099) have been given in from Figure 4.28 to Figure 4.39. The overall change of daily flow analysis for a period from 1980 to 2099 has been given in Table 4.6. Month wise mean daily discharge hydrograph for different periods is shown in Figure 4.40.

From Figure 4.28 to Figure 4.30 for January, February and March it can be seen that both highest and lowest flow is decreasing in the future periods with respect to the base period (1980-2019). From April to December (Figure 4.31 to Figure 4.39), the highest flow increases for all the future periods compared to the base period. For August to December (Figure 4.35 to Figure 4.39), the lowest flow decreases for all the future periods compared to the base period.
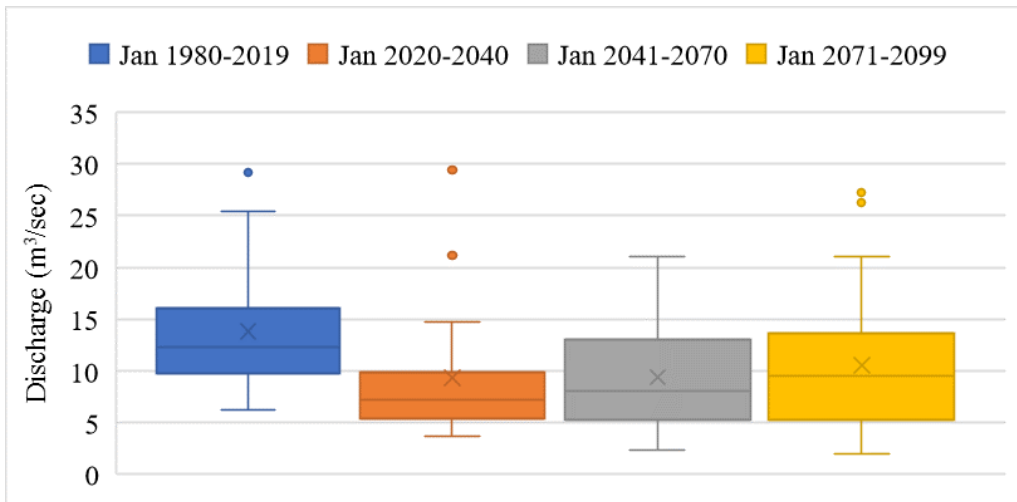
Figure 4.28: Boxplot of month-wise mean daily flow for January
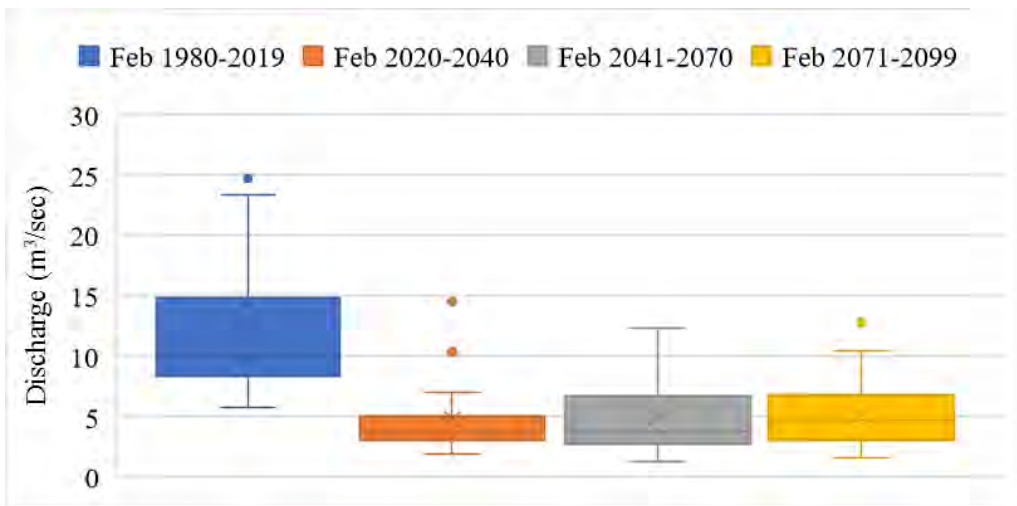
Figure 4.29: Boxplot of month-wise mean daily flow for February
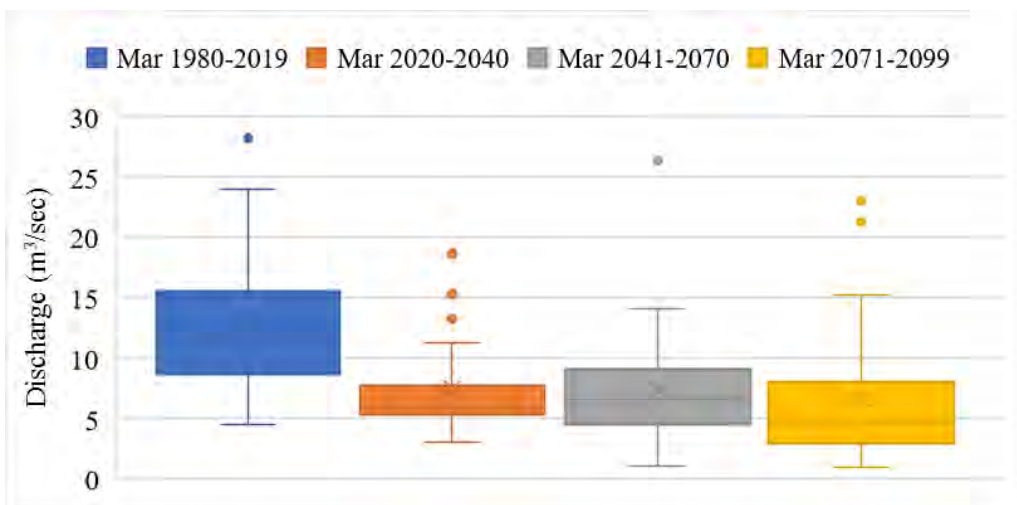
Figure 4.30: Boxplot of month-wise mean daily flow for March
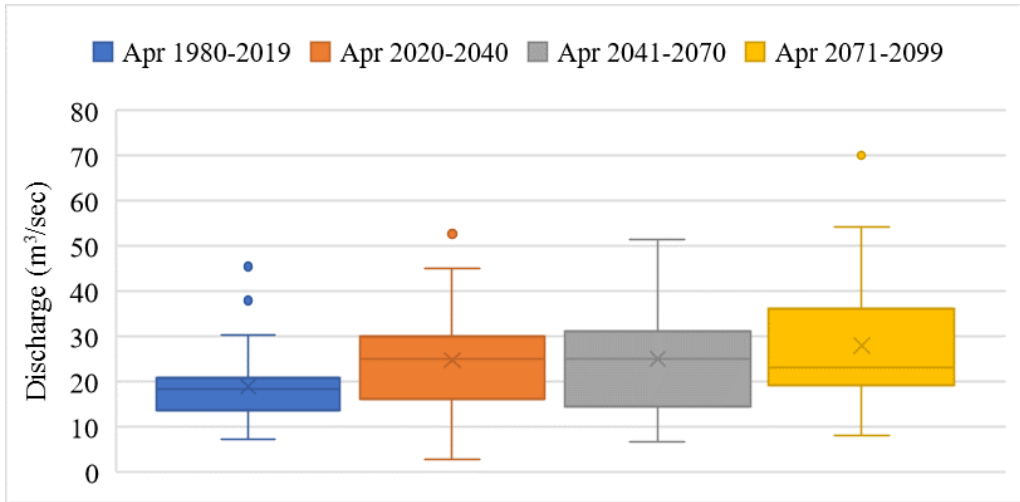
Figure 4.31: Boxplot of month-wise mean daily flow for April
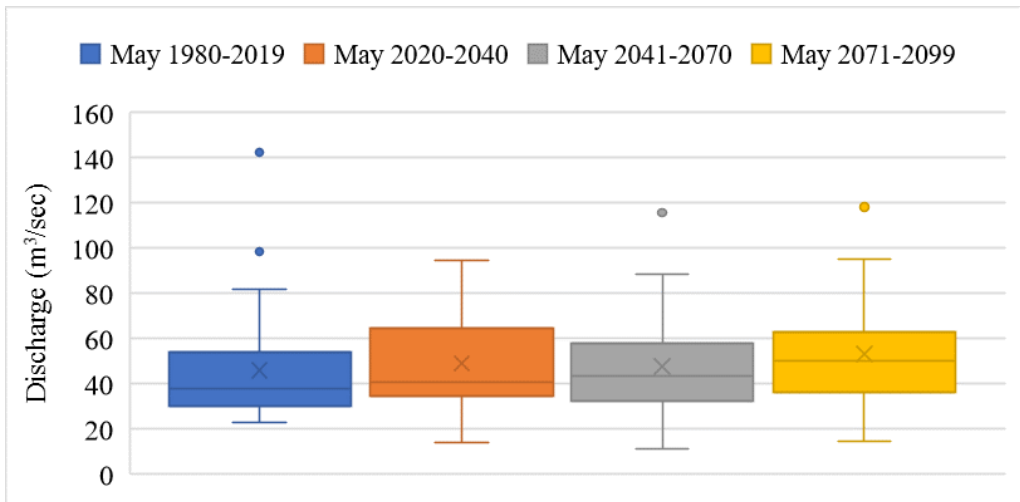
Figure 4.32: Boxplot of month-wise mean daily flow for May
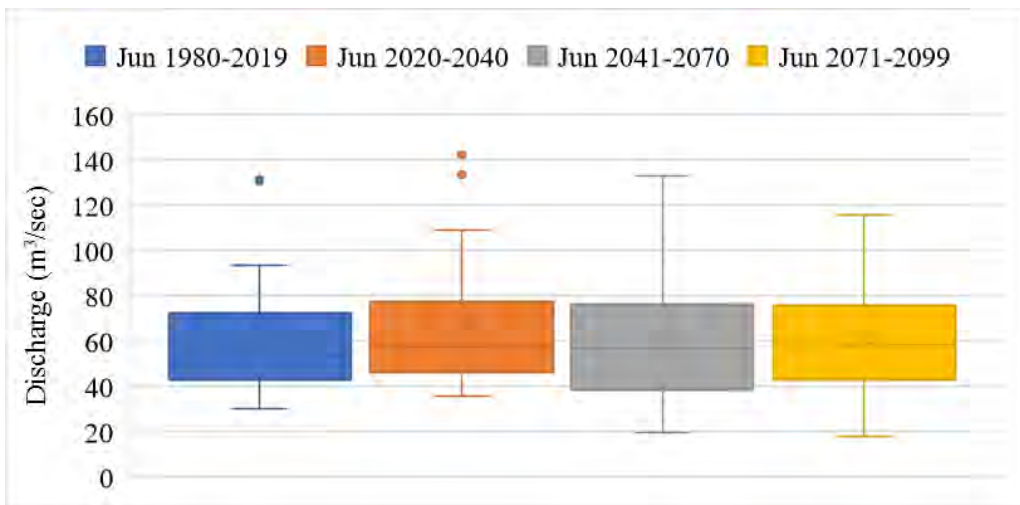
Figure 4.33: Boxplot of month-wise mean daily flow for June
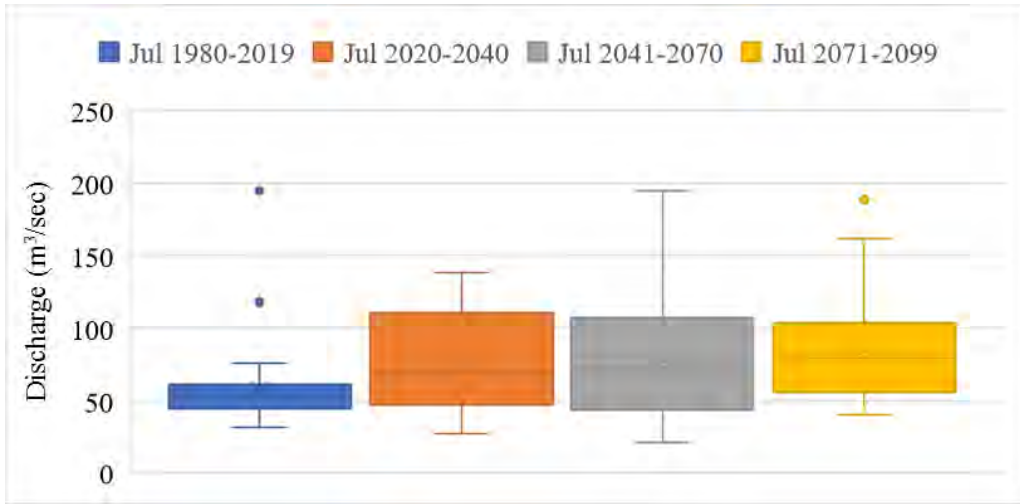
Figure 4.34: Boxplot of month-wise mean daily flow for July
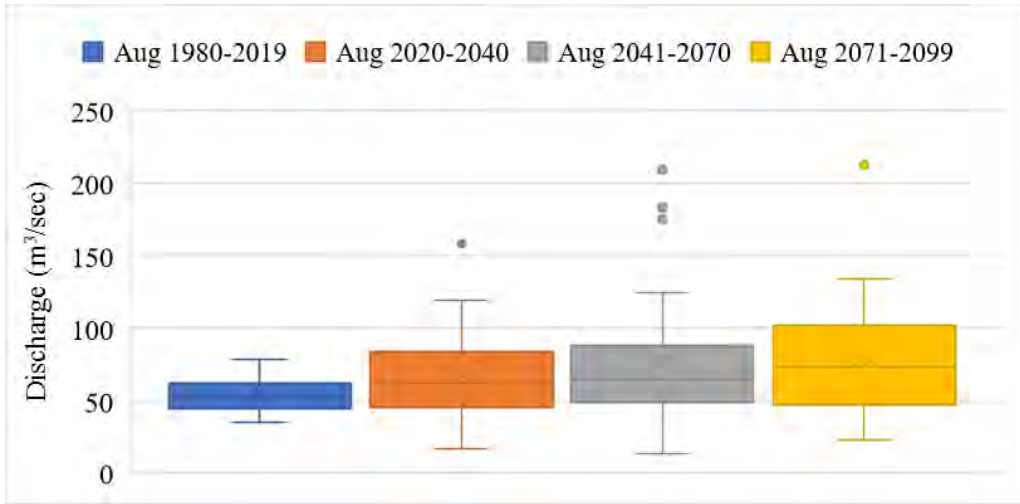
Figure 4.35: Boxplot of month-wise mean daily flow for August
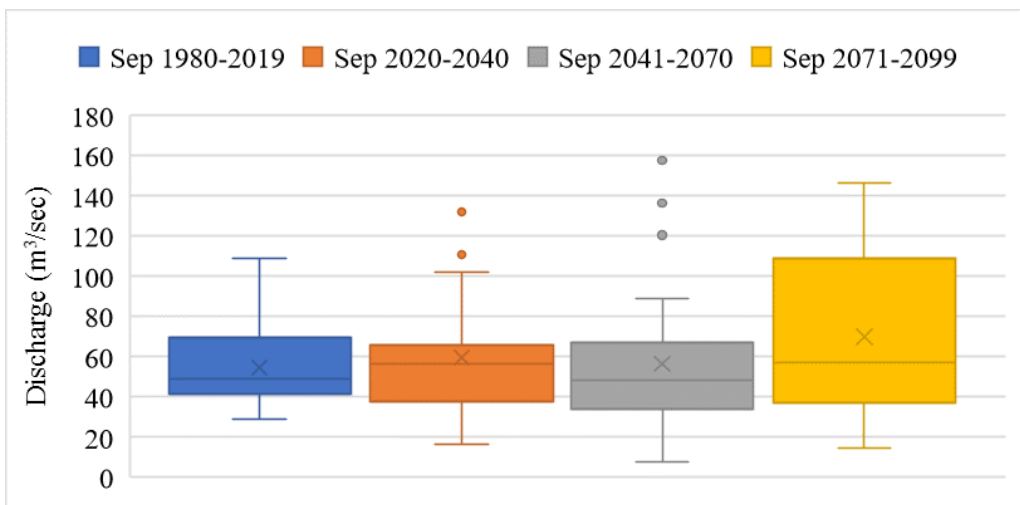
Figure 4.36: Boxplot of month-wise mean daily flow for September
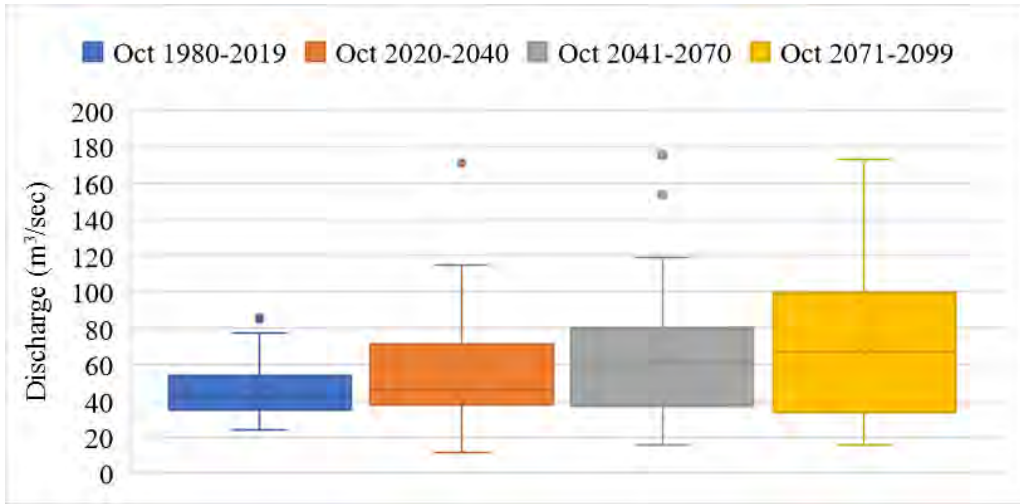
Figure 4.37: Boxplot of month-wise mean daily flow for October
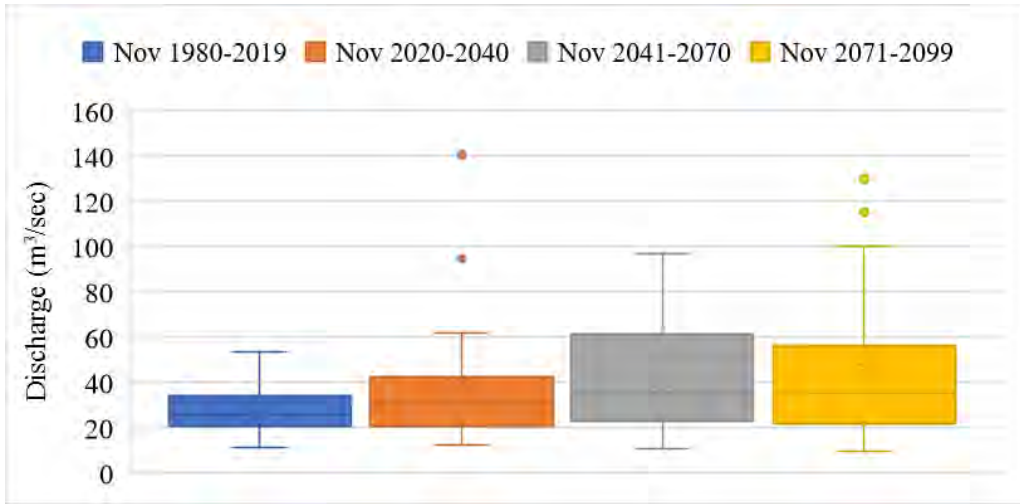
Figure 4.38: Boxplot of month-wise mean daily flow for November
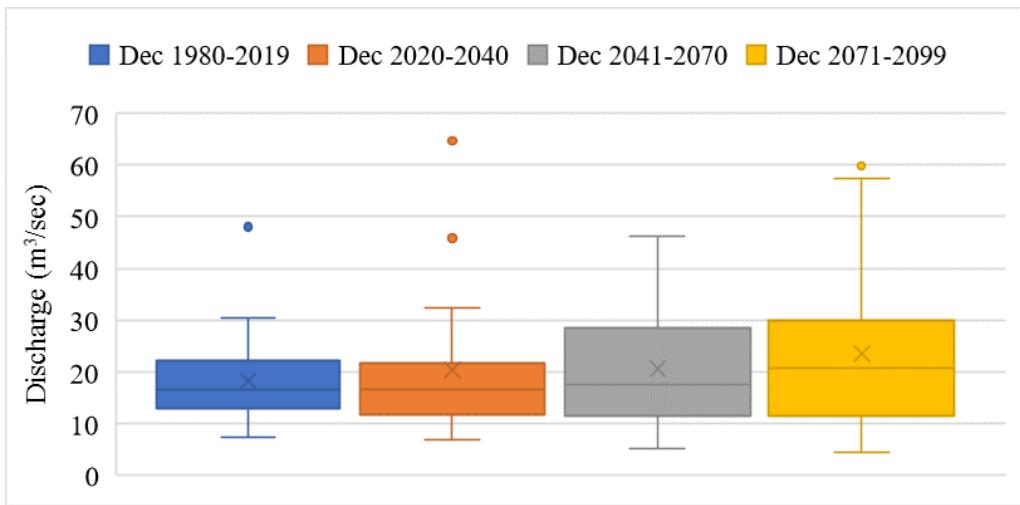
Figure 4.39: Boxplot of month-wise mean daily flow for December

Table 4.6: Statistics from daily flow analysis from 1980 to 2099

Month	Mean Flow				% Change with respect to 1980-2019		
	1980-2019	2020-2040	2041-2070	2071-2099	2020-2040	2041-2070	2071-2099
Jan	13.84	9.31	9.40	10.56	-32.76	-32.10	-23.69
Feb	12.12	4.78	4.90	5.19	-60.59	-59.55	-57.16
Mar	12.90	7.49	7.45	6.64	-41.89	-42.24	-48.51
Apr	18.94	24.85	25.04	28.06	31.23	32.24	48.19
May	46.14	49.10	47.63	53.18	6.42	3.23	15.25
Jun	57.83	67.16	60.64	61.67	16.15	4.86	6.64
Jul	57.44	73.67	78.26	85.72	28.25	36.25	49.25
Aug	53.77	68.15	76.23	80.36	26.74	41.76	49.44
Sep	54.50	59.66	56.53	69.95	9.48	3.73	28.36
Oct	44.72	59.09	64.29	70.83	32.12	43.75	58.37
Nov	27.63	39.62	41.33	46.31	43.39	49.60	67.62
Dec	18.28	20.33	20.62	23.57	11.20	12.80	28.92
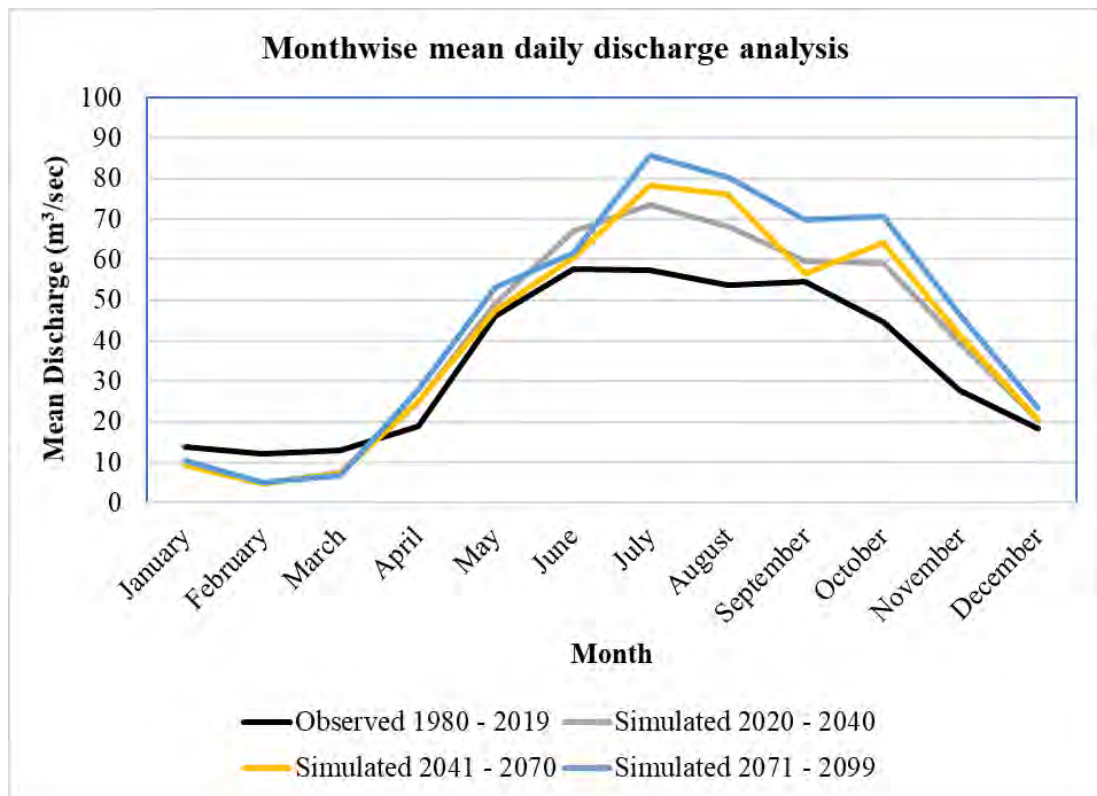
Figure 4.40: Month wise mean daily discharge (m³/sec)

82

From the boxplots Figure 4.28 to 4.39, the median value is projected to decrease in the months from January to March but the median value is projected to increase from the months of April to December in future periods compared to baseline. From Table 4.6 and Figure 4.40, it can be observed that, from 1980-2019 (base period) to the future periods 2020-2040, 2041-2070, 2071-2099 the low flow is decreasing and the high flow is increasing. So, the dry period will become drier causing water scarcity and in contrast, increasing high flow will increase the flood risk in monsoon and post monsoon periods.

4.9.4 Flow duration curve

Flow duration curve for different periods such as observed period (1980 to 2019) and, three simulated period of 2020 -2040, 2041-2070, 2071-2099 for the Khowai catchment have been plotted and shown in Figure 4.41.

From Figure 4.41, it can be mentioned that at 0.1% of time, discharge equaled or exceeded are 190, 202.3, 240.4 and 242.1 m^3/sec for 1980-2019, 2020-2040, 2041-2070 and 2071-2099, respectively. At 1%-time, discharge equaled or exceeded are 117, 163, 184 and 192 m^3/sec for 1980-2019, 2020-2040, 2041-2070 and 2071-2099, respectively. At 10%-time, discharge equaled or exceeded are 70, 94.3, 97.2 and 102.9 m^3/sec for 1980-2019, 2020-2040, 2041-2070 and 2071-2099, respectively.
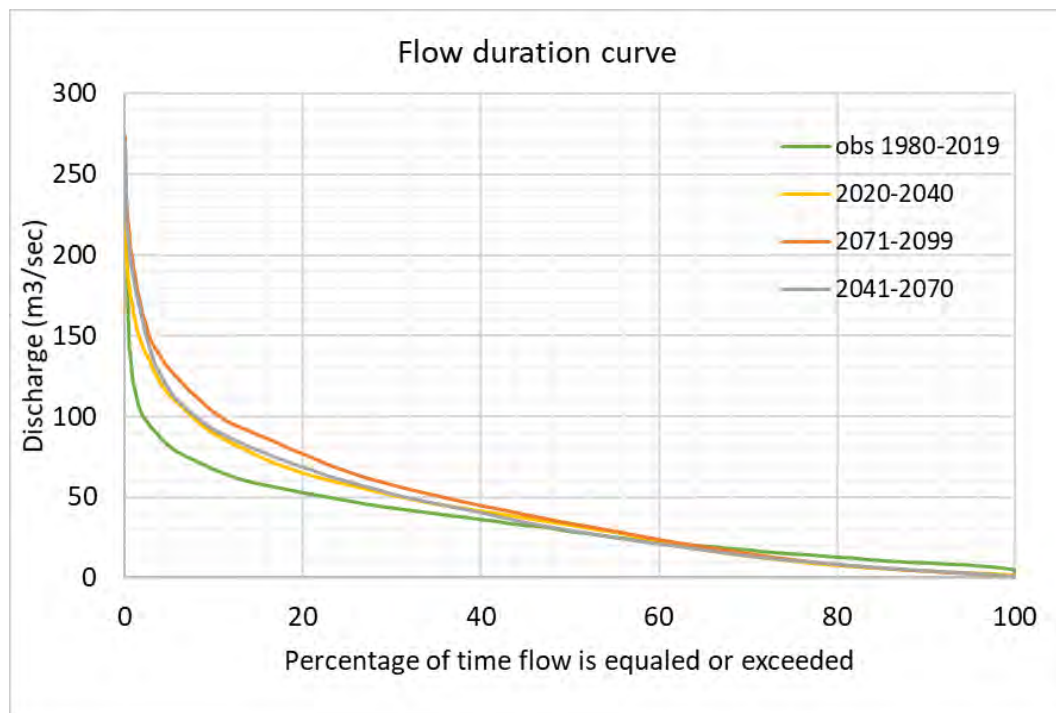
Figure 4.41: Flow duration curve

4.9.5 Frequency analysis

In order to perform frequency analysis, year wise maximum discharge from 1979-2019, 2020-2040, 2041-2070 and 2071-2099 have been computed first. The year wise maximum discharge data (Appendix- Table A 6) have been put into "EasyFit" software. It is a data analyzing program used for statistical purposes. "EasyFit" allows to automatically fit a large number of distributions to the dataset and select the best model in seconds (Easyfit, 2021).

From the Easyfit software, discharge (m^3/sec) according to the exceedance probability have been calculated. For extreme value analysis, the Generalized Extreme Value (GEV) Distribution fitted better than the other distributions.

Table 4.7: Discharge according to exceedance probability and return period calculated using Easyfit and Microsoft Excel

Return Period (T)	Discharge (m^3/sec)				% of change with respect to 1980-2010		
	1980-2010	2020-2040	2040-2070	2071-2099	2020-2040	2040-2070	2071-2099
2	107	124.56	123.7	135.49	16.41	15.61	26.63
5	144.28	171.89	176.77	193.15	19.14	22.52	33.87
10	168.53	200.2	209.99	232.47	18.79	24.60	37.94
25	198.9	232.88	249.88	283.27	17.08	25.63	42.42
50	221.37	255.07	278.05	321.85	15.22	25.60	45.39
100	243.74	275.49	304.86	361.02	13.03	25.08	48.12

4.10 Effect of Chakmaghat Barrage

Chakmaghat Barrage is situated in the upstream at Teliamura, West Tripura District, India. It is 96 m long across the river Khowai. Date of completion of the project is 31 March 2015. This barrage was mainly constructed to irrigate nearby lands in the dry season (Department of economic affairs India, 2019).

Figure 4.42: Chakmaghat Barrage (https://khowai.nic.in/bn/gallery and Google Earth)

As the Chakmaghat barrage is constructed to irrigate nearby agricultural areas in the dry season, the effect of the barrage on the dry season flow before and after 2015 is mainly analyzed in this section. For this analysis, October to April data (discharge) data have been used.

Boxplot showing the effect of Chakmaghat barrage on the flow of Shaistaganj station is presented in Figure 4.43. As the barrage tends to capture water upstream of barrage, the water level at Shaistaganj was supposed to decrease because of the barrage operation. But it is not noticed in discharge yet (Figure 4.43).
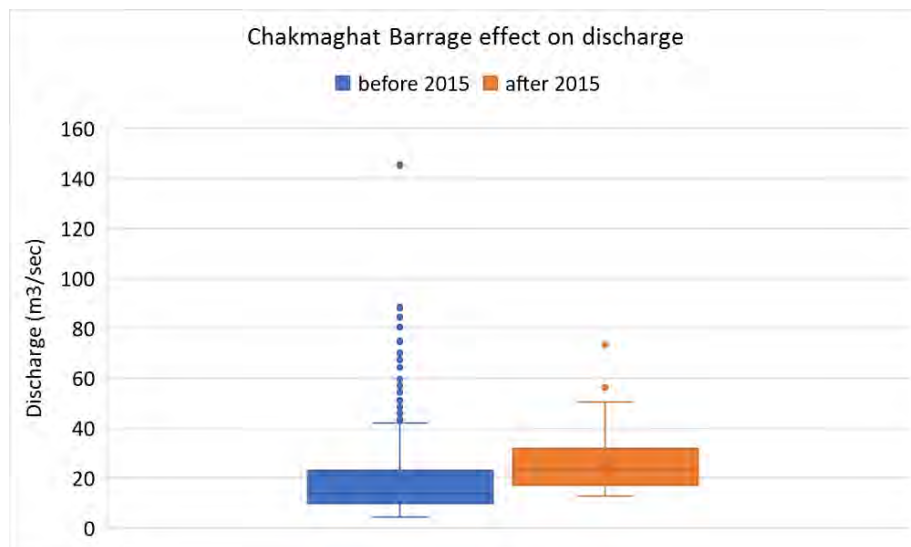
Figure 4.43: Boxplot showing the effect of Chakmaghat barrage on Khowai river, Shaistaganj station discharge (considering discharge for the dry season only – October to April)

Although the effect of the barrage is not still quite noticed in the low season flow of Shaistaganj, however in future it may affect the flow. Therefore, three different flow diversion scenarios, following a past study (Khan, 2018), have been analyzed here. Each scenario considers that a portion of upstream flow will be diverted upstream of Chakmaghat barrage and change the water availability for the Bangladesh portion of Khowai river. The changes in mean monthly flow for 2020-2040 at Shaistaganj station for different flow diversion scenarios is shown in Table 4.8.

Table 4.8: Mean monthly flow of the Khowai river at Shaistaganj due to different flow diversion scenarios for 2020-2040

Month	Mean daily flow at Shaistaganj (cumec)				
	Without Barrage	Flow after following flow diversion			
		10%	20%	30%	40%
January	9.31	8.38	7.45	6.52	5.59
February	4.78	4.30	3.82	3.35	2.87
March	7.49	6.74	5.99	5.24	4.49
April	24.85	22.37	19.88	17.40	14.91
October	59.09	53.18	47.27	41.36	35.45
November	39.62	35.66	31.70	27.73	23.77
December	20.33	18.30	16.26	14.23	12.20

Since the flow diversion activates only during lean season (October-April), the monsoon flow for all the diversion scenarios remains same. Flow of February will decrease the most. This amount of water diversion is bound to make a serious impact on the Bangladesh side. The lowest water availability will be during the month of January, February and March. The flow scenario for 2041-2070 (Table A 7, Figure A 5) and 2071-2099 (Table A 8, Figure A 6) are shown in appendix.
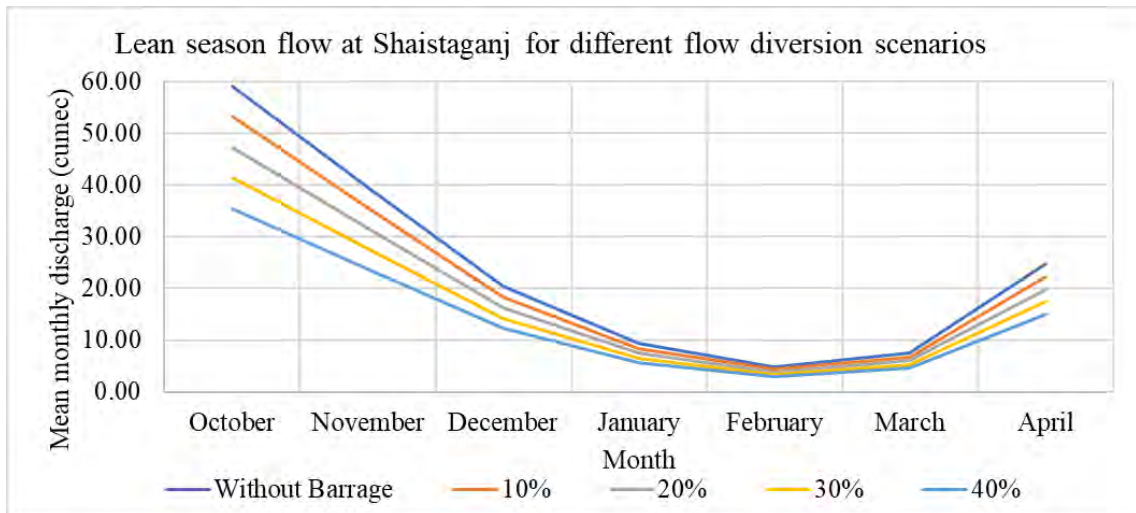
Figure 4.44: Hypothetical lean season flow at Shaistaganj for different flow diversion scenarios considering the flow period 2020-2040

4.11 Discussion and Comparison with Past Studies

The impacts of anthropogenic climate change on the water cycle are already apparent. These impacts include changes in annual river streamflow, shifts in both flood peak magnitude and timing, alterations in flow duration curves, and changes in magnitude of low-flow periods. The continued increase of global temperatures will lead to further changes in regional hydrology within the next decades through shifts in precipitation trends, melting of glaciers and permafrost, and a growing rain-to-snow ratio in cold regions. In addition, changes in natural vegetation cover, land use practices, crop water requirements, prolonged growing seasons, and soil functions may further alter the hydrological cycle. Extreme events such as river flooding pose a potential threat to human societies and are likely to occur more often. Given that these changes directly affect agriculture, forestry, energy production, drinking water supply, sanitation, and ecosystems, there are likely to be substantial consequences for societies in many regions around the world. Reliable information on potential changes to future hydrological conditions is fundamental for deciding on long-term management strategies and adaptation measures (Hakala et al., 2019).

The climate change impact assessment summary determined from this research presented in the following Table 4.9.

Table 4.9: Summary of climate change impact assessment from base period (1980-2019)

SL	Parameter	Base period	Change of mean observed future periods			
			2020 -2040	2041 - 2070	2071 - 2099	Remarks
1	Precipitation	1980 - 2019	7.69%	15.86%	21.05%	Increase
2	Temperature		0.82 ^{0}C	1.46 ^{0}C	2.41 ^{0}C	Increase
3	Evaporation		0.695%	1.755%	2.662%	Increase
4	Actual Evapotranspiration		-0.39 mm/day	-0.54 mm/day	-0.56 mm/day	Decrease
5	Annual mean Discharge		15.70%	17.985%	29.874%	Increase

According to (World Bank Climate Change Knowledge Portal, 2021), Mean temperatures across Bangladesh are projected to increase between 1.4°C and 2.4°C by 2050 and 2100, respectively. This warming is expected to be more pronounced in the winter months (December-February). In this study, temperature is projected to rise by 2.41^{0}C by the end of the century which is similar to World Bank Climate Change Knowledge Portal, 2021. Narzis (2020) has reported that the maximum temperature will increase by 4.54^{0}C in the 2080s under RCP 8.5 from the base period 1970-1999. The difference in the temperature change findings, between this research and Narzis (2020), might be due to choosing different bias correction method and different baseline period. Narzis (2020) had used linear scale bias correction method for correcting future climate datasets whereas, in this research quantile-based mapping method has been used for bias correction of the CANESM climate datasets. Rahman (2016) has shown that the magnitude of the temperature changes ranges from 1.68–2.72 °C for 2061–2080 with respect to the base period (1980-2000) for the upper Meghna basin based on Quantile Mapping (QM) bias correction method. Findings of Rahman (2016) is similar to the finding of this study.

In this study, it has been found that the precipitation will increase by 21.05% for the period of 2071-2099 from the base period. Narzis (2020) reported an increase in precipitation about 26.16% during the 2080s compared to the baseline (1970-1999)

Rahman (2016), modelled the climate change impacts on the water regimes of the river-wetland systems in the data-scarce transboundary Upper Meghna River Basin (Bangladesh and India) and has shown that precipitation will increase by 20-30% in the future (2061-2080) with respect to the base period (1981-2000) for the Tripura region where most of the Khowai basin is located. The precipitation change obtained in this study is in line with the findings of these research ((Rahman, 2016) and (Narzis, 2020)).

Murray et al. (2012) used a dynamic global vegetation model and showed that a warmer environment decreases vegetation coverage and transpiration due to water stress in the soil system which reduces overall actual ET. Alfi et al. (2014) shows that in the recent decades, the average evapotranspiration in Bangladesh has reduced in January to April. However, from July to December, ET shows slight increase in the recent decades. The south-eastern region of Bangladesh shows a notable decrease of evapotranspiration (Alfi et al., 2014). In this study we also noticed decrease in AET in some months. As for example, it has been observed that during 2071-2099, the actual evaporation decreases in the pre-monsoon to monsoon and increases in the post-monsoon period and dry period.

In this research, the discharge of Shaistaganj station is projected to increase by 15.70%, 17.985% and 29.874% during 2020-2040, 2041-2070 and 2071-2099, respectively, with respect to the base period (1980-2019). Rahman (2016) reported similar findings. He found that during 2061-2080 discharge will increase by 29% for Tripura region (Rahman, 2016) based on SWAT model output.

5   CONCLUSION AND RECOMMENDATIONS

5.1   Conclusion

Khowai is a transboundary river that plays an important role in the fields of irrigation, transportation and flood events of the north-eastern region of Bangladesh. It also contributes to the flash flood hazard in this region damaging agricultural products of large areas. Anticipated climate change may exacerbate the current situation as climate change will have a profound impact on the availability and variability of fresh water throughout the world due to the increased frequency of climatic extremes such as drought and change in rainfall pattern in response to global warming. Hence assessing the impact of climate change on the streamflow of the Khowai river basin is very important for sustainable water resources management and flood prediction in this region.

The hydrologic modeling of Khowai river produced inconclusive results in the past due to the lack of observations of rainfall in the upper catchment areas outside Bangladesh and complex hydrological response of the basin. In this study, HBV Hydrologic model has been chosen because of its flexibility, computational efficiency for data scarce regions like Khowai basin, proven effectiveness under a wide range of climatic and physiographic conditions and successful application in many previous studies.

In this study the suitability of two gridded datasets has been assessed for flow modeling in the Khowai basin. To test the datasets, a few calibrations trials have been made. Each model has been calibrated for 1980 to 2010 and validated for 2011 to 2019. In terms of Nash-Sutcliffe Efficiency (NSE) (0.336 and 0.331 for ERA5 and NOAA, respectively) and coefficient of determination (0.502 and 0.399 for ERA5 and NOAA, respectively), ERA5 data driven model shows better result than NOAA data driven model in both calibration and validation. But in the validation period (2011-2019), both ERA5 and NOAA show worse results than the calibration results. For this reason, another trial has been done using average rainfall (average of the global gridded products (NOAA, ERA5) and measured precipitation of Habiganj station) which shows better results for both calibration and validation. For the calibration and validation period R^2 has been found to be 0.67 and 0.63 and NSE has been found to be 0.65 and 0.56, respectively. On monthly

scale, R^2 have been found to be 0.78 and 0.75 while NSE have been found to be 0.75 and 0.67 for the calibration and validation period, respectively.

Future precipitation, temperature and evaporation from the CANESM2 climate model under RCP8.5 scenario has been used to simulate future flow. The datasets have been bias corrected using the quantile-mapping bias correction method. The quantile mapping method could remove the bias more efficiently than the Linear scaling method. Bias corrected precipitation has been projected to increase by 7.69, 15.86 and 21.05%, respectively in 2020-2040, 2041-2070 and 2071-2099 from the baseline period (1980-2019) whereas temperature is expected to increase by 0.82, 1.46 and 2.41ºC, respectively. Evaporation is projected to increase in all future periods while actual evapotranspiration is projected to decrease as warmer environment may reduce daily transpiration rates as reported in past studies (Kirschbaum and McMillan, 2018)

The future (2020 to 2099) flow of the Khowai basin has been simulated by the calibrated and validated model driven using bias corrected future meteorological datasets as input. Analysis of monthly flow data indicates that wet months will be further wetter while some dry months such as January, February and March will be drier. Flow may decrease up to 61% (February, 2020) while wet season flow may increase up to 50% (in July-August of 2070). Flow duration curve also indicates that at 1%-time, discharge may equal or exceed 117, 163, 184 and 192 m^3/sec during the base period (1980-2019), 2020-2040, 2041-2070 and 2071-2099, respectively while at 10%-time, discharge may equal or exceed 70, 94.3, 97.2 and 102.9 m^3/sec during 1980-2019, 2020-2040, 2041-2070 and 2071-2099, respectively. Frequency analysis shows that discharge corresponding to 100-year return period may increase by 13, 25 and 48% during 2020, 2050 and 2080s, respectively from 1980-2010.

The impact of Chakmaghat barrage at the upstream has been analyzed by considering different flow diversion scenarios which will consider flow diversion from 10% to up to 30%. Results show that flow of February will decrease the most after considering diversion. The lowest water availability will be during the month of January, February and March.

This study may play a vital role in assessing the future flow of the Khowai river basin for the proper planning and water resources management in this basin. Furthermore, as Khowai river is a transboundary river, the results of this study can also be used for the

development of an effective water sharing policy which will ensure that both countries (India and Bangladesh) can get enough water for the purpose of agriculture, livelihood, economic growth, and maintenance of ecology and biodiversity in this region in the coming decades.

5.2 Recommendation

The researcher has a few recommendations that may be considered for further study in the future.

- The rainfall data used to calibrate and validate the model in this study has been collected from the fifth generation of ECMWF (European Centre for Medium-Range Weather Forecast) atmospheric reanalysis data sets, NOAA climate prediction center and Habiganj BWDB station. As no measured rainfall data is available for this catchment, it was not possible to check the accuracy of the ECMWF ERA5 dataset and NOAA dataset. So, the average of all three datasets have been used in the model. Future studies should therefore assess the potential of other reanalysis or satellite measure dataset in obtaining more accurate runoff. Also, rainfall data from the upstream Indian catchment should be collected.

- To understand the wide range of uncertainty of the projected precipitation and temperature, future climate data from multiple RCM models and different projection scenarios can be considered in the future.

- Further studies also may assess the impact of changes in land cover in addition to the climate change scenario.

- Future study may assess the capability of this model in flash flood forecasting using weather forecast data.

- Quantile mapping method could not remove the bias in precipitation completely. Future study should test other bias correction methods in this regard.

REFERENCES

Alfi, M., Islam, S. and Bokhtiar, S.M.,. (2014). CHANGES OF REFERENCE EVAPOTRANSPIRATION (ET0) IN RECENT DECADES OVER BANGLADESH. 2nd International Conference on Advances in Civil Engineering. Chittagong: CUET.

Ali, A., Xiao, C., Zhang, X., Adnan, M., Iqbal, M. & Khan, G. (2018). Projection of future streamflow of the Hunza River Basin, Karakoram Range (Pakistan) using HBV hydrological model. Journal of Mountain Science, 2218-2235.

Ayalew, A. (2019). Rainfall - Runoff Modeling: A Comparative Analyses: Semi Distributed HBV Light and SWAT Models in Geba Catchment, Upper Tekeze Basin, Ethiopia. American Journal of Science, Engineering and Technology, Vol 4(2): 34-40.

Banglapedia. (2021, June 18). Haor. Retrieved from Baglapedia, National Encyclopedia of Bangladesh: https://en.banglapedia.org/index.php/Haor

Beck, H., Dijk, M.V., Roo, A.D., Miralles, D.G., McVicar, T.R., Schellekens, J., Bruijnzeel, A. (2016). Global-scale regionalization of hydrologic model parameters. Water Resources Research, AGU Publications,, Vol 52, pp. 3599–3622.

Bergström, S., Carlsson, B., Gardelin, M., Lindström, G., Pettersson, A. & Rummukainen, M. (2001). Climate change impacts on runoff in Sweden - Assessments by global climate models, dynamical downscaling and hydrological modelling. Climate Research, 16. 101-112.

Carlos Mendoza, Juan Adriel, Chavez Alcazar, Tamar Anaharat, and Zuñiga Medina, Sebastián Adolfo. (2021). Calibration and Uncertainty Analysis for Modelling Runoff in the Tambo River Basin, Peru, Using Sequential Uncertainty Fitting Ver-2 (SUFI-2) Algorithm. Air, Soil and Water Research, SAGE Publishing, Volume 14: 1–13.

Carbon brief. (2021). Climate modelling. Retrieved from Carbon brief: https://www.carbonbrief.org/qa-how-do-climate-models-work

CCCR. (2021, February 1). CORDEX: Coordinated Regional Climate Downscaling Experiment. Retrieved from Centre for Climate Change Research: http://cccr.tropmet.res.in/home/cordexsa_about.jsp

CEGIS. (2012). Master Plan of Haor Area. Bangladesh Haor and Wetland Development Board.

Copernicus. (2019). Copernicus Global Land Service. Retrieved from Copernicus Global Land Service: https://land.copernicus.eu/global/products/lc

Deb, R. (2015). Channel Shifting Of The River Khowai At Baganbazar, Alepsha And Kanchanghat. Department Of Geography And Disaster Management, Tripura University.

Debnath, J., Das, N., Ahmed, I. & Bhowmik, M. (2017). Channel migration and its impact on land use/land cover using RS and GIS: A study on Khowai River of Tripura, North-East India. The Egyptian Journal of Remote Sensing and Space Science, Vol 20 (197 - 210).

Department of economic affairs India. (2019). Chakmaghat project information. Retrieved from Government of India: https://www.pppinindia.gov.in/infrastructureindia/web/guest/view-project?p_p_id=viewproject_WAR_Projectportlet&p_p_lifecycle=0&p_p_col_id=column-1&p_p_col_count=1&_viewproject_WAR_Projectportlet_jspPage=%2Fhtml%2Fviewproject%2Fview.jsp&_viewproject_WAR_Pr

Easyfit. (2021). Software informer. Retrieved from Software informer: https://easyfit.informer.com/5.6/

ECMWF. (2019, August 31). ERA5. Retrieved from ECMWF: https://www.ecmwf.int/en/forecasts/datasets/reanalysis-datasets/era5

ECMWF. (2021). ERA5. Retrieved from ECMWF: https://confluence.ecmwf.int/display/CKB/ERA5%3A+data+documentation

FFWC. (2006). Consolidation and Strengthening of Flood Forecasting and Warning Services. Flood Forecasting and Warning Center, Bangladesh Water Development Board.

Gendzh, N. (2015). Statistical analysis of hydrological data using the HBV-Light Model for the Boyne catchment. Maynooth University.

Government of Canada. (2019, 12 19). CanESM2 predictors: CMIP5 experiments. Retrieved from Government of Canada,: https://climate-scenarios.canada.ca/?page=pred-canesm2

Hakala, K., Addor, N., Teutschbein, C., Vis, M., Dakhlaoui, H., Seibert, J. (2019). Hydrological Modeling of Climate Change Impacts. Encyclopedia of Water: Science, Technology, and Society.

Haque, A. (2015). Developing a Semi-Distributed Hydrological Model and Assessing Its Applicability for the Bangshi River Basin Using HEC-HMS. *Department of Water Resources Engineering, Bangladesh University of Engineering & Technology.*

Hossain, A. (2014). *Annual Flood Report 2014.* Flood Forecasting and Warning Centre (FFWC), Bangladesh Water Development Board (BWDB).

Hossain, T. (1997). *Study of aggradation and degradation of the Khowai river.* Bangladesh University of Engineering and Technology.

Intergovernmental Panel on Climate Change. (2000). *Emissions Scenarios.* Cambridge: The University of Cambridge.

International Center for theoretical physics. (2014). *Regional Model: REGCM4.* Retrieved from International Center for theoretical physics: https://www.ictp.it/research/esp/models/regcm4.aspx#close

IWFM. (2020). *Flash Flood Forecast Evaluation Report.* Bangladesh University of Engineering and Technology.

Khan, A. J., Koch, M. (2018). Selecting and Downscaling a Set of Climate Models for Projecting Climatic Change for Impact Assessment in the Upper Indus Basin (UIB). *Climate, 6, 89;* 1-24.

Khan, I. (2018). *EFFECT IN THE WATER BALANCE OF THE TEESTA RIVER BASIN DUE TO DIFFERENT CLIMATE CHANGES AND UPSTREAM DEVELOPMENT.* DEPARTMENT OF WATER RESOURCES ENGINEERING, BUET.

Khorchani, N. (2016). *Modelling the Impact of Land Use Changes on Hydrology using HBV-Light.* Pan African University.

Khorchani, N. (2016). *Modelling the Impact of Land Use Changes on Hydrology using HBV-Light.* Pan African University.

Kirchner, J. (2006). Getting the Right Answers for the Right Reasons: Linking Measurements, Analyses, and Models to Advance the Science of Hydrology. *Water Resources Research,* VOL. 42, W03S04, Page 1-5.

Kirschbaum, M.U.F. and McMillan, A.M.S. (2018). Warming and Elevated CO2 Have Opposing Influences on Transpiration. Which is more Important? *Springer (Current Forestry Reports),* Volume 4, pp. 51–71.

Knoben, W.J.M., Freer, J.E., Fowler, K.J.A., Peel, M.C. & Woods, R.A. (2019). Modular Assessment of Rainfall–Runoff Models Toolbox (MARRMoT) v1.2: an open-source, extendable framework providing implementations of 46 conceptual hydrologic models as continuous state-space formulations. Geoscientific Model Development, Vol 12. 2463-2480.

Kuo, C., Gan, T.Y. & Higuchi, K. (2017). Evaluation of Future Streamflow Patterns in Lake Simcoe Subbasins Based on Ensembles of Statistical Downscaling. Journal of Hydrologic Engineering, 22(9): 04017028-10.

Madsen, H., Wilson, G. & Ammentorp, H. (2002). Comparison of Different Automated Strategies for Calibration of Rainfall-Runoff Models. Journal of Hydrology, Vol 261. 48-59.

Majumdar, J. (1982). Morphometric analyses of the 4th order drainage watersheds of the Khowai river basin, Tripura, India -some preliminary results and observations. . Journal of the Indian Society of Remote Sensing, Vol 10. 49-53.

Majumdar, Sima and Das, Nibedita. (2014). Bank Erosion Risk: A Study on the Khowai River, Tripura. Indian Journal of Landscape Systems and Ecological Studies, Vol. 37, No. 2, pp.83- 91.

Melsen, L.A. and Guse, B. (2021). Climate change impacts model parameter sensitivity – implications for calibration strategy and model diagnostic evaluation. Hydrology and earth system sciences, Vol 25, pp. 1307–1332.

Moges, E., Demissie, Y., Larsen, L., Yassin, F. (2020). Review: Sources of Hydrological Model Uncertainties and Advances in Their Analysis. Water, 13, 28, 1-24.

Mondal, M.S., Islam, M.S., Haque, A., Islam, M. R., Biswas, S., Mohammed, K. (2018). Assessing High-End Climate Change Impacts on Floods in Major Rivers of Bangladesh Using Multi-Model Simulations. Global Science and Technology Journal, Vol 6. No. 2, pp. 1-14.

Mou, F.I. and Jahan, N. (2021). Application Of HBV Model For Runoff Simulation In Khowai River Basin. 5th International Conference on Advances in Civil Engineering (ICACE 2020) (pp. WRE-310-318). Chattogram: Chittagong University of Engineering & Technology.

Narzis, A. (2020). Impacts of Climate Change and Upstream Intervention on the Hydrology of the Meghna River Basin using SWAT. BANGLADESH UNIVERSITY OF ENGINEERING AND TECHNOLOGY.

NOAA. (2021). National Centers for Environmental Information. Retrieved from National Centers for Environmental Information: https://www.ncdc.noaa.gov/nomads/data-products

NOAA Climate Prediction Center. (2021). CPC Global Unified Gauge-Based Analysis of Daily Precipitation. Retrieved from NOAA physical sciences laboratory: https://psl.noaa.gov/data/gridded/data.cpc.globalprecip.html

Normand, S., Konz, M. & Merz, J. (2011). An application of the HBV model to the Tamor Basin in Eastern Nepal. Journal of Hydrology and Meteorology, Vol 7 (49 - 58).

NUMXL. (2021). NUMXL. Retrieved from NUMXL: https://numxl.com/

Pidwirny, M. (2009, July 05). Actual and Potential Evapotranspiration. Retrieved from PhysicalGeography: http://www.physicalgeography.net/fundamentals/8j.html

Radchenko, I., Breuer, L. & Forkutsa, I. (2014). Simulating Water Resource Availability under Data Scarcity—A Case Study for the Ferghana Valley (Central Asia). Water, Vol 6. 3270-3299.

Rahman, M. M. (2016). Modelling climate change impacts on the water regimes of the river-wetland systems in the data-scarce transboundary Upper Meghna River Basin (Bangladesh and India). University College London.

Saksena, S. (2017, January 13). Introduction to Flood Frequency Analysis. Retrieved from Data and model driven hydrology education: https://serc.carleton.edu/hydromodules/steps/168500.html

Schreur, W. (2019). Impacts of climate change on flow composition using a model tailored to runoff components. University of Twente.

Searcy, J. K. (1959). USGS. Retrieved from USGS: https://pubs.er.usgs.gov/publication/wsp1542A

Seibert, J. (2005). HBV light version 2 User's Manual. Department of Physical Geography and Quaternary Geology, Stockholm University, Sweden.

Seibert, J. and Vis, M. J. P. (2012). Teaching hydrological modeling with a user-friendly catchment-runoff-model software package. Hydrology and Earth System Sciences, Vol 16, 3315–3325.

Shiwakoti, S. (2017). Hydrological Modeling and Climate Change Impact Assessment Using HBV Light Model: A Case Study of Karnali River Basin. Iranian Journal of Energy and Environment, Vol 8(3), pp. 296-304.

te Linde, Aline & Hurkmans, Ruud & Eberle, M. (2008). Comparing model performance of two rainfall-runoff models in the Rhine basin using different atmospheric forcing data sets. Hydrol. Earth Syst. Sci., 2008.

The Daily Star. (2017, June 21). Rain triggers flash flood in Habiganj. Retrieved from The Daily Star: https://www.thedailystar.net/country/rain-triggers-flash-flood-habiganj-1423120

The Daily Star. (2018, May 9). Rain brings early flood in Habiganj. Retrieved from The Daily Star: https://www.thedailystar.net/country/rain-brings-early-flood-habiganj-1573426

The Daily Star. (2019, June 3). Dyke collapse floods areas in Habiganj. Retrieved from The Daily Star: https://www.thedailystar.net/country/news/dyke-collapse-floods-areas-habiganj-1752805

Ullah, R. (1989). Statistical Characteristics of Low Flows of Three Rivers in Bangladesh. Bangladesh University of Engineering and Technology.

University of Zurich. (2020, November 23). HBV Light download. Retrieved from Department of Geography: https://www.geo.uzh.ch/en/units/h2k/Services/HBV-Model/HBV-Download.html

USGS. (2019). USGS Earth Explorer. Retrieved from USGS Earth Explorer: https://earthexplorer.usgs.gov/

Wawrzyniak, T., Osuch, M., Nawrot, A. And Napiorkowski, J.J. (2017). Run-off modelling in an Arctic unglaciated catchment. Annals of Glaciology, pp. 1-11.

Woldemeskel, F., Sivakumar, B. & Sharma, A. (2013). Merging gauge and satellite rainfall with specification of associated uncertainty across Australia. Journal of Hydrology, Vol 499. 167-176.

World Bank. (2021). Climate Change Knowledge Portal. Retrieved from World Bank Group: https://climateknowledgeportal.worldbank.org/country/bangladesh/climate-data-projections

Xiuliang Yuan, Jie Bai. (2018). Future Projected Changes in Local Evapotranspiration Coupled with Temperature and Precipitation Variation. Sustainability, Vol 10, 3281 (1-14).

APPENDIX

Table A 1: Rating curve equations analyzing 40 years WL & Q data of Shaistaganj station of BWDB

SL	Month	Rating curve equations	Coefficient of determination (R^2) determined from observed and rating curve equation data
1	January	$y = 17.761x^2 - 313.61x + 1393.8$	0.419
2	February	$y = 17.818x^2 - 314.04x + 1391.9$	0.412
3	March	$y = 17.445x^2 - 310.31x + 1389.3$	0.5786
4	April	$y = 7.7536x^2 - 135.92x + 609.87$	0.4227
5	May	$y = 10.942x^2 - 191.79x + 862.79$	0.5746
6	June	$y = 2.252x2 - 21.03x + 34.372$	0.616
7	July	$y = 6.6655x^2 - 109.01x + 469.78$	0.6736
8	August	$y = 9.7776x^2 - 177.17x + 839.96$	0.5064
9	September	$y = 10.25x^2 - 181.2x + 832.73$	0.5808
10	October	$y = 12.063x^2 - 214.88x + 984.79$	0.4877
11	November	$y = 17.746x^2 - 320.34x + 1463.4$	0.4461
12	December	$y = 16.963x^2 - 300.19x + 1340.6$	0.3115

In the equations, x = Water Level and y = Discharge

Table A 2: Zone Distribution (elevation wise)

SL	Elevation Zone	Range (MSL)	Mean Elevation	Area (sq km)
1	Zone 1	9.33 - 33.43	21.38	137.86
2	Zone 2	33.44 - 53.82	43.63	219.60
3	Zone 3	53.83 - 74.21	64.02	224.51
4	Zone 4	74.22 - 96.45	85.335	151.77
5	Zone 5	96.46 - 118.7	107.58	180.37
6	Zone 6	118.8 - 139.1	128.95	177.30
7	Zone 7	139.2 - 159.5	149.35	99.37
8	Zone 8	159.6 - 179.9	169.75	52.45
9	Zone 9	180 - 202.1	191.05	29.71
10	Zone 10	202.2 - 226.2	214.2	19.25
11	Zone 11	226.3 - 250.3	238.3	10.62
12	Zone 12	250.4 - 274.4	262.4	9.14
13	Zone 13	274.5 - 298.5	286.5	5.41
14	Zone 14	298.6 - 322.6	310.6	3.42
15	Zone 15	322.7 - 348.5	335.6	2.04
16	Zone 16	348.6 - 374.5	361.55	1.00
17	Zone 17	374.6 - 396.7	385.65	0.77
18	Zone 18	396.8 - 420.8	408.8	0.34
19	Zone 19	420.9 - 446.8	433.85	0.27
20	Zone 20	446.9 - 482	464.45	0.21
Total area (sq. km)				**1325.41**

Table A 3: Elevation wise distribution of the land use area

Land Use	Elevation Zone	Area (sq. km)	Total Area	Ratio with respect to total area
Forest	Zone 1	16.52	1070.36	0.012
	Zone 2	124.78		0.094
	Zone 3	191.60		0.145
	Zone 4	148.84		0.112
	Zone 5	179.82		0.136
	Zone 6	176.48		0.133
	Zone 7	98.89		0.075
	Zone 8	52.19		0.039
	Zone 9	29.44		0.022
	Zone 10	19.09		0.014
	Zone 11	10.56		0.008
	Zone 12	9.06		0.007
	Zone 13	5.34		0.004
	Zone 14	3.35		0.003
	Zone 15	1.96		0.001
	Zone 16	0.97		0.001
	Zone 17	0.70		0.001
	Zone 18	0.31		0.000
	Zone 19	0.24		0.000
	Zone 20	0.20		0.000
Crop Area	Zone 1	121.53	240.49	0.092
	Zone 2	86.84		0.066
	Zone 3	29.20		0.022
	Zone 4	2.63		0.002
	Zone 5	0.19		0.000
	Zone 6	0.07		0.000
	Zone 7	0.00		0.000
	Zone 8	0.02		0.000
	Zone 9	0.00		0.000
	Zone 10	0.00		0.000

Land Use	Elevation Zone	Area (sq. km)	Total Area	Ratio with respect to total area
	Zone 11	0.00		0.000
	Zone 12	0.00		0.000
	Zone 13	0.00		0.000
	Zone 14	0.00		0.000
	Zone 15	0.00		0.000
	Zone 16	0.01		0.000
	Zone 17	0.00		0.000
	Zone 18	0.00		0.000
	Zone 19	0.00		0.000
	Zone 20	0.00		0.000
	Zone 1	3.33		0.003
	Zone 2	7.70		0.006
	Zone 3	3.46		0.003
	Zone 4	0.03		0.000
	Zone 5	0.03		0.000
	Zone 6	0.01		0.000
	Zone 7	0.00		0.000
	Zone 8	0.00		0.000
	Zone 9	0.00		0.000
Building Area	Zone 10	0.00	14.56	0.000
	Zone 11	0.00		0.000
	Zone 12	0.00		0.000
	Zone 13	0.00		0.000
	Zone 14	0.00		0.000
	Zone 15	0.00		0.000
	Zone 16	0.00		0.000
	Zone 17	0.00		0.000
	Zone 18	0.00		0.000
	Zone 19	0.00		0.000
	Zone 20	0.00		0.000
Total		**1325.41**	**1325.41**	**1.000**

Table A 4: Different optimal parameter sets used for three different trials using Monte Carlo run tools

Parameter	Trial 1	Trial 2	Trial 3
PERC	9.91	0.79	3.28
UZL	94.06	4.38	70
K0	0.17	0.05	0.05
K1	0.12	0.02	0.06
K2	0.07	0.1	0.02
MAXBAS	3.02	5.17	1
PCALT	10.62	10.29	10.41
TCALT	0.81	0.89	0.79
Pelev	343.27	381.31	477
Telev	150.96	307.54	30
TT_1	-0.92	-0.39	-0.26
CFMAX_1	6.63	7.79	9
SP_1	0.53	0.89	1
SFCF_1	0.72	0.73	0.6
CFR_1	0.1	0.02	0.1
CWH_1	0.07	0.15	0.1
LP_1	0.61	0.97	0.6
BETA_1	2.95	4.01	2.5
TT_2	-0.13	-0.66	-0.85
CFMAX_2	4.83	1.01	9
SP_2	0.92	0.98	1
SFCF_2	0.88	0.67	0.6
CFR_2	0.02	0.01	0.1
CWH_2	0.03	0.19	0.1
LP_2	0.97	0.44	0.6
BETA_2	5.88	3.94	2
TT_3	-0.38	-0.42	-0.55
CFMAX_3	5.02	7.01	9
SP_3	0.62	0.81	1

Parameter	Trial 1	Trial 2	Trial 3
SFCF_3	0.52	0.8	0.6
CFR_3	0.01	0.08	0.1
CWH_3	0.13	0.04	0.1
LP_3	0.31	0.64	0.6
BETA_3	6.58	3.24	2

Table A 5: Optimal parameter set for both calibration and validation of the final selected model

Optimized Value of Different Parameter			
Snow Routine			
TT	Threshold temperature when precipitation is simulated as snowfall (Threshold temperature for snowfall)	°C	-0.26, -0.85, -0.55
CFMAX	Melt rate of the snowpack (degree day factor)	mm/Δt °C [mm ^{0}C^{-1} d^{-1}]	9
SP	current snow storage	-	1
SFCF	Snowfall gauge under catch correction factor	-	0.6
CFR	Refreezing coefficient	-	0.1
CWH	Water holding capacity of snow	-	0.1
Soil Moisture Routine			
LP	Soil moisture value above which actual evaporation reaches potential evaporation (Wilting Point)	-	0.6
BETA	Shape coefficient of recharge function (Parameter Relating Runoff and Infiltration	-	2.5, 2, 2
Response Routine			
PERC	Maximum percolation to lower zone (Percolation)	mm/Δt [mm d^{-1}]	3.28
UZL	Threshold parameter for extra outflow from upper zone (Upper Zone Limit; Current Storage in the Upper Zone)	mm	70
K0	Additional recession coefficient of upper groundwater store	1/Δt [d^{-1}]	0.0503
K1	Recession coefficient of upper groundwater store	1/Δt [d^{-1}]	0.0649

K2	Recession coefficient of lower groundwater store	$1/\Delta t$ [d^{-1}]	0.019
Routing Routine			
MAXBAS	Length of equilateral triangular weighting function (Lag Parameter)	Δt [d]	1

Table A 6: Year wise maximum discharge data

SL	Date	Maximum observed discharge (m³/sec)
1	24/07/1979	93.70
2	25/07/1980	93.70
3	06/08/1981	65.97
4	16/09/1982	68.18
5	09/08/1983	77.97
6	23/09/1984	106.17
7	15/08/1985	78.07
8	04/09/1986	134.32
9	02/10/1987	55.09
10	07/07/1988	186.27
11	12/10/1989	107.13
12	11/10/1990	96.97
13	23/05/1991	223.38
14	16/07/1992	57.63
15	23/09/1993	107.24
16	06/10/1994	67.54
17	18/05/1995	134.85
18	26/06/1996	105.31
19	19/08/1997	94.22
20	27/05/1998	90.00
21	20/09/1999	97.41
22	27/09/2000	156.12
23	05/10/2001	126.11
24	11/09/2002	104.50
25	03/07/2003	118.53
26	**01/07/2004**	**271.35**
27	26/05/2005	119.76
28	14/06/2006	145.72
29	17/06/2007	140.54
30	09/10/2008	97.80

SL	Date	Maximum observed discharge (m³/sec)
31	02/07/2009	118.82
32	22/09/2010	121.78
33	18/08/2011	126.43
34	27/06/2012	81.03
35	11/05/2013	82.34
36	24/09/2014	89.53
37	19/08/2015	159.18
38	22/09/2016	66.63
39	20/10/2017	106.02
40	14/06/2018	120.49
41	13/07/2019	103.09
42	9/9/2020	73.75
43	7/18/2021	143.66
44	7/3/2022	93.64
45	7/27/2023	153.39
46	10/7/2024	96.65
47	10/26/2025	76.25
48	9/1/2026	117.49
49	11/1/2027	129.52
50	9/21/2028	175.61
51	5/26/2029	112.01
52	5/5/2030	110.88
53	7/16/2031	83.07
54	6/16/2032	71.03
55	8/10/2033	200.84
56	7/22/2034	182.92
57	6/16/2035	209.78
58	6/25/2036	113.58
59	10/28/2037	215.05
60	5/9/2038	51.34
61	7/19/2039	124.34

SL	Date	Maximum observed discharge (m³/sec)
62	6/8/2040	198.31
63	5/27/2041	90.34
64	7/17/2042	269.83
65	8/5/2043	73.57
66	7/29/2044	219.96
67	6/15/2045	101.14
68	10/17/2046	162.51
69	7/20/2047	118.61
70	8/11/2048	107.44
71	6/28/2049	112.66
72	10/9/2050	196.73
73	10/18/2051	141.38
74	7/14/2052	141.96
75	7/24/2053	196.68
76	7/12/2054	65.50
77	4/13/2055	37.22
78	10/5/2056	218.69
79	4/24/2057	37.83
80	8/9/2058	109.44
81	6/30/2059	130.03
82	10/16/2060	120.89
83	7/11/2061	86.45
84	4/20/2062	78.38
85	7/26/2063	142.47
86	10/27/2064	100.36
87	6/8/2065	151.85
88	7/16/2066	175.07
89	5/30/2067	75.76
90	7/13/2068	129.65
91	9/13/2069	122.96
92	8/4/2070	231.40

SL	Date	Maximum observed discharge (m³/sec)
93	10/31/2071	95.91
94	7/18/2072	143.19
95	5/22/2073	105.68
96	4/24/2074	114.93
97	7/19/2075	**273.96**
98	5/9/2076	68.07
99	7/7/2077	206.69
100	10/9/2078	204.76
101	10/8/2079	94.59
102	9/1/2080	194.90
103	7/12/2081	160.55
104	7/29/2082	105.25
105	9/12/2083	165.99
106	6/30/2084	95.10
107	10/9/2085	262.10
108	7/19/2086	226.26
109	7/17/2087	169.75
110	7/14/2088	50.75
111	9/27/2089	140.26
112	7/22/2090	100.16
113	7/16/2091	114.60
114	8/31/2092	145.43
115	8/23/2093	197.71
116	8/23/2094	202.48
117	7/5/2095	108.44
118	6/27/2096	131.61
119	5/13/2097	176.54
120	7/3/2098	54.99
121	10/21/2099	155.89

Table A 7: Mean monthly flow of the Khowai river at Shaistaganj due to different flow diversion scenarios for 2041-2070

Month	Mean daily flow at Shaistaganj (cumec)				
	Without Barrage	Flow after following flow diversion			
		10%	20%	30%	40%
January	9.40	8.46	7.52	6.58	5.64
February	4.90	4.41	3.92	3.43	2.94
March	7.45	6.71	5.96	5.22	4.47
April	25.04	22.54	20.03	17.53	15.02
October	64.29	57.86	51.43	45.00	38.57
November	41.33	37.20	33.06	28.93	24.80
December	20.62	18.56	16.50	14.43	12.37

Table A 8: Mean monthly flow of the Khowai river at Shaistaganj due to different flow diversion scenarios for 2071-2099

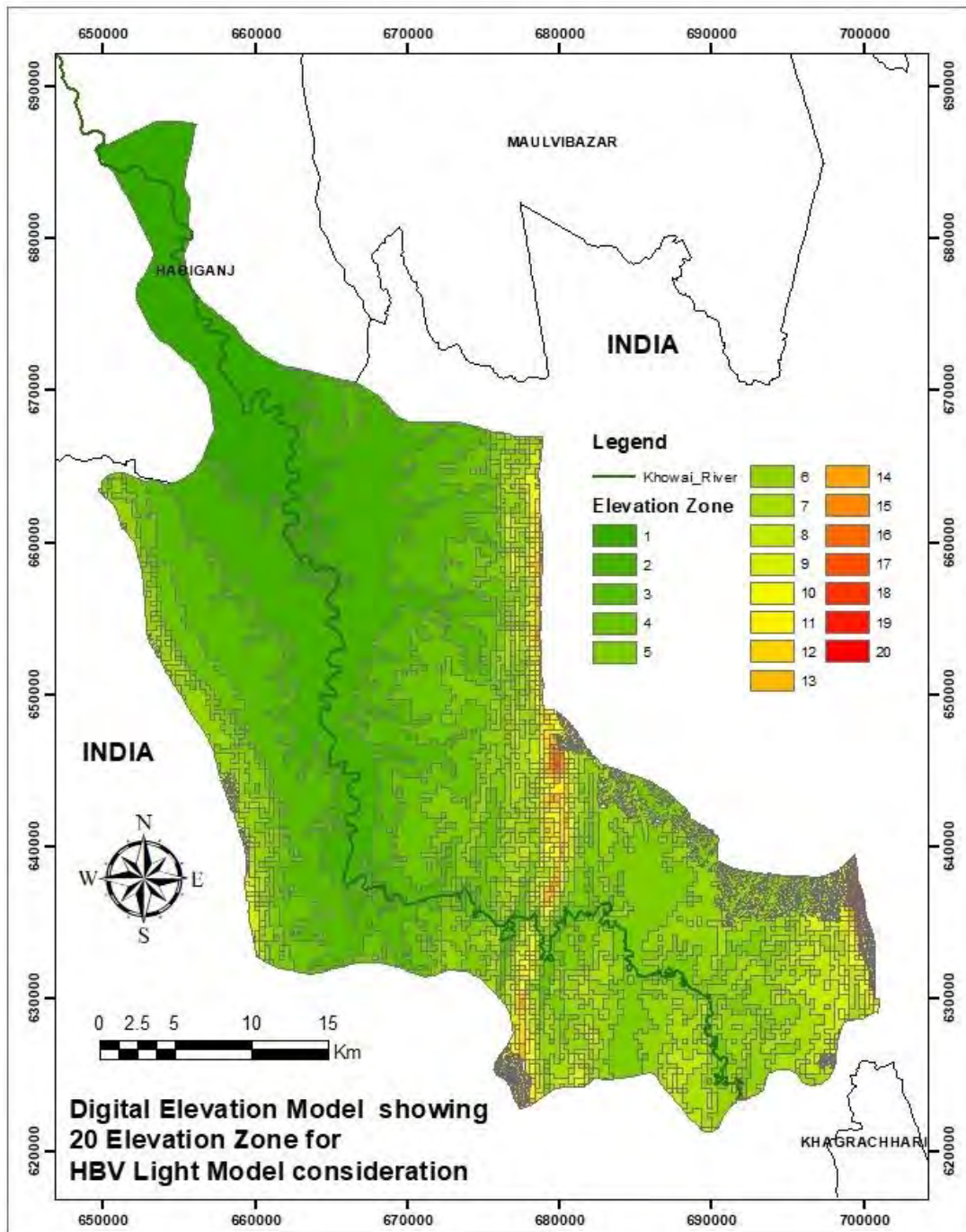| Month	Mean daily flow at Shaistaganj (cumec)				
	Without Barrage	Flow after following flow diversion			
		10%	20%	30%	40%
January	10.56	9.50	8.45	7.39	6.34
February	5.19	4.67	4.15	3.63	3.11
March	6.64	5.98	5.31	4.65	3.98
April	28.06	25.25	22.45	19.64	16.84
October	70.83	63.75	56.66	49.58	42.50
November	46.31	41.68	37.05	32.42	27.79
December	23.57	21.21	18.86	16.50	14.14

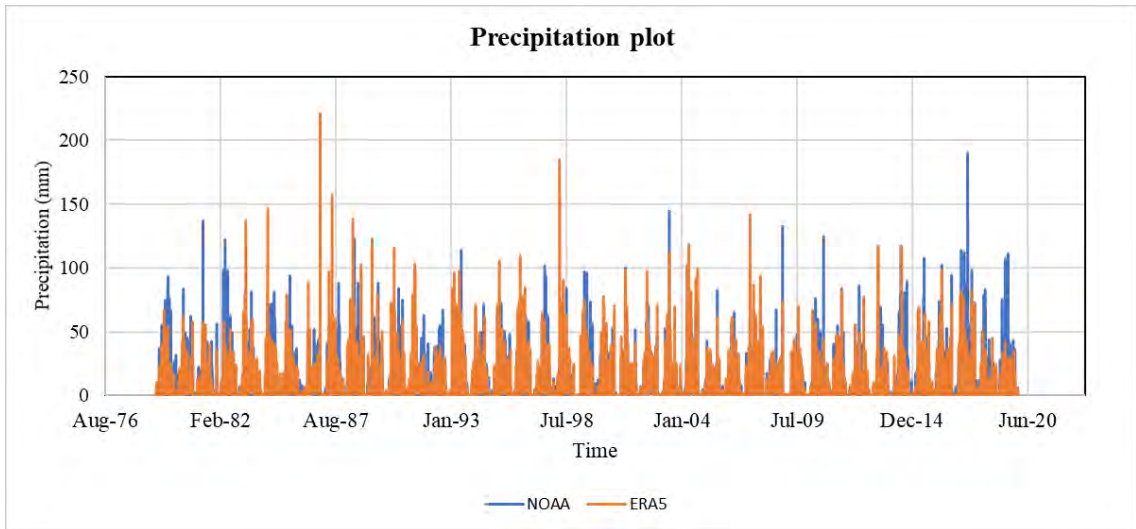Figure A 1: Zone distribution (Elevation wise)

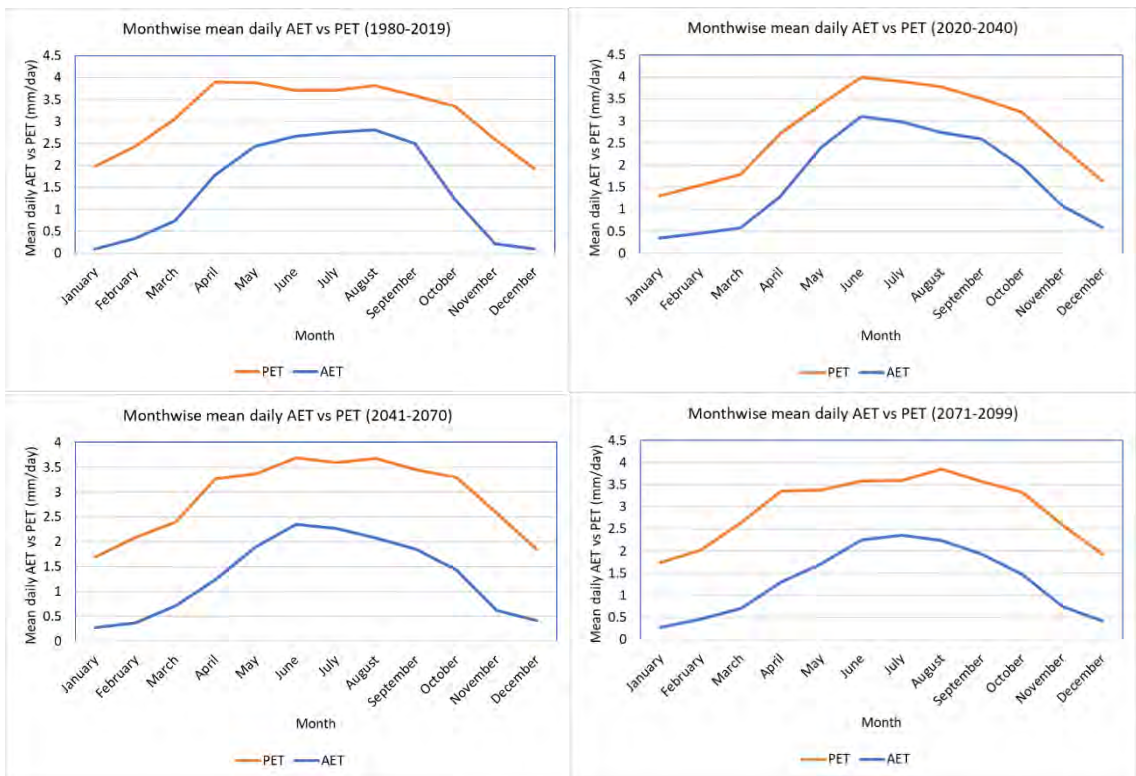Figure A 2: Precipitation plot – NOAA vs ERA5

Figure A 3: Month wise mean daily AET vs PET (1980-2099)
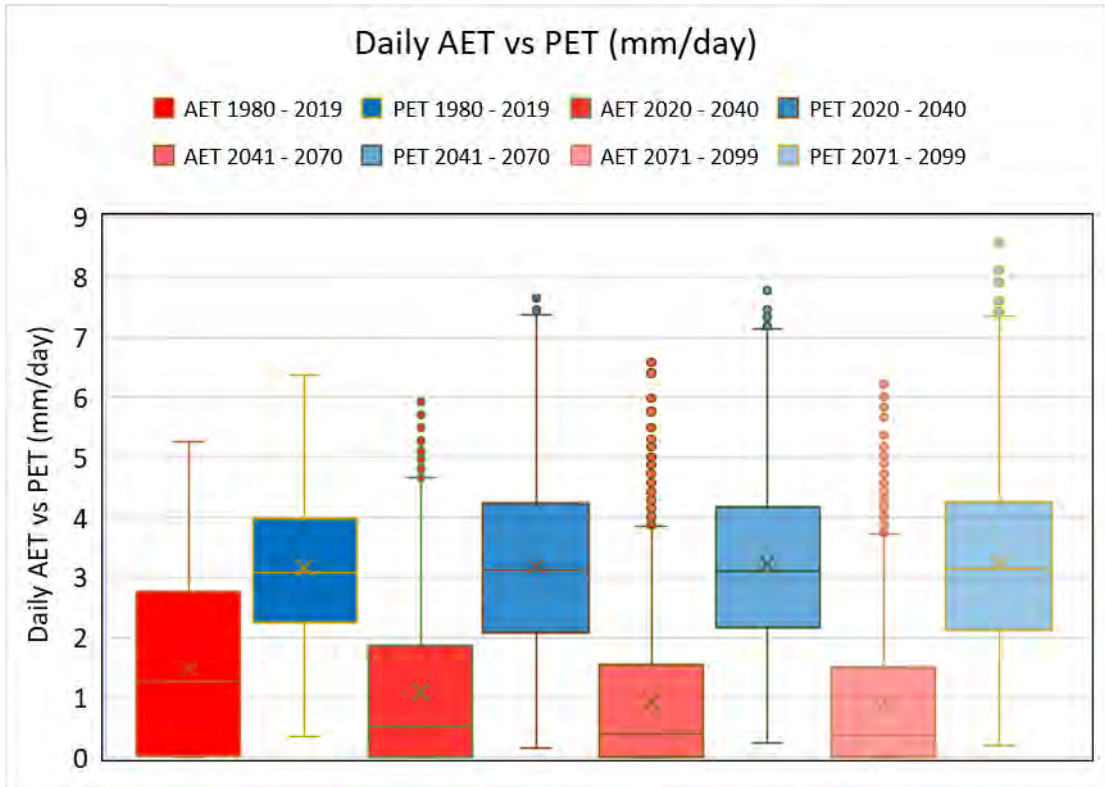
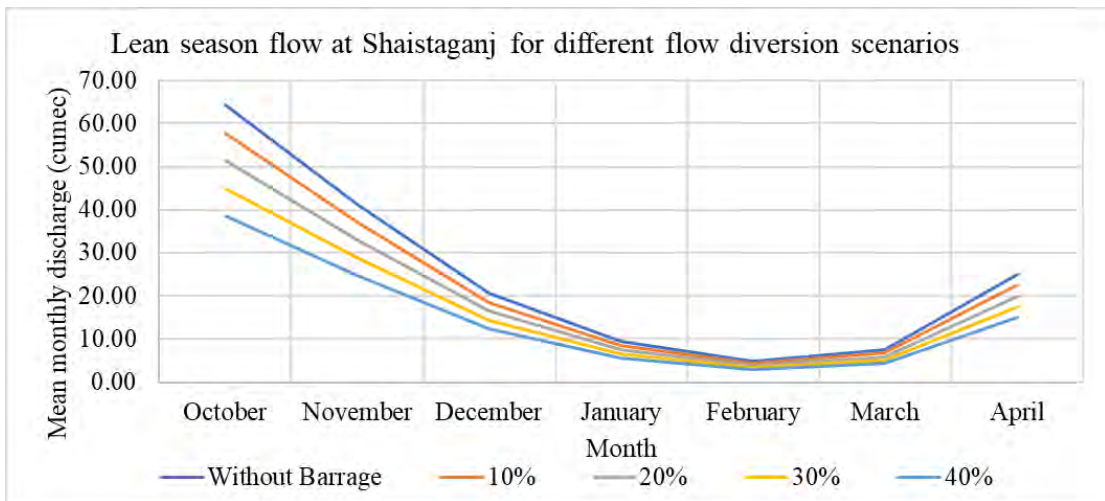Figure A 4: Daily AET vs PET analysis

Figure A 5: Lean season flow at Shaistaganj for different flow diversion scenarios considering the flow period 2041-2070
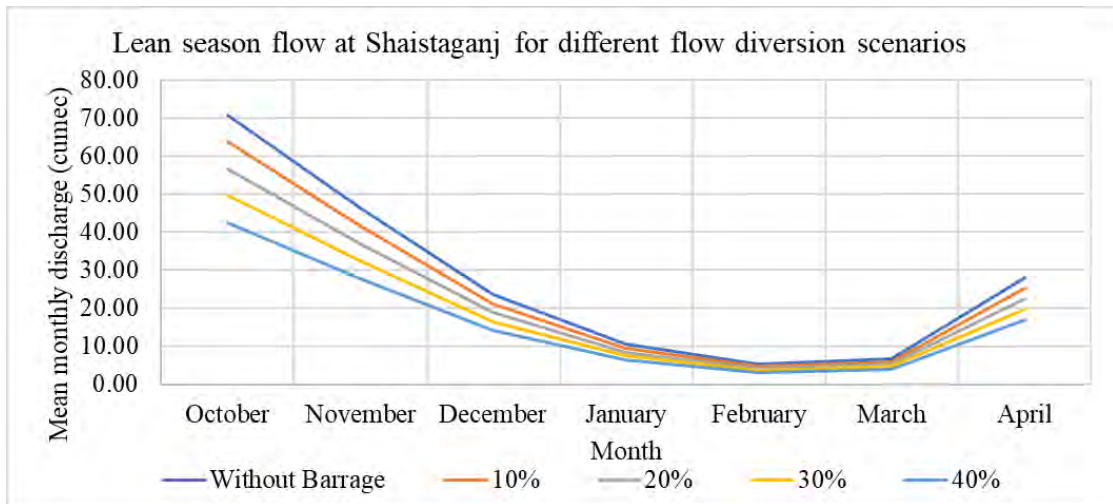
Figure A 6: Lean season flow at Shaistaganj for different flow diversion scenarios considering the flow period 2071-2099